The University of Nottingham
UNITED KINGDOM • CHINA • MALAYSIA

Development of novel fibre reinforcement architectures

Dimitrios Karanatsis

Thesis submitted for:

Engineering Doctorate in Composites Manufacture

2019

Abstract

This research focuses on the development of novel carbon fibre reinforcements and the effect of the support structure on the physical properties of the produced fabric. Scrim is the selected support structure for the focus of this work. The scrim is the support structure for the carbon fibres and it is used for the manufacture of non-crimp fabrics (NCFs). The scrim is an open mesh grid construction comprising of individual threads and can be placed at different orientations. The carbon fibre tows are bonded onto the substrate by means of pressure and heat. The manufactured fabric can potentially improve the physical and mechanical properties of a fibre-reinforced composite component when compared with a conventional stitched fabric, as it does not interfere to a large degree with the fibre arrangement and alignment. By systematically varying different parameters of the scrim, the effect on the physical properties of the fabrics was examined.

The selection of an appropriate non-crimp fabric for a specific application requires an extensive knowledge and a deep understanding of all the process parameters involved during composite manufacture. This selection is a complex process as it requires a high number of different adjustable factors in manufacturing that can affect a structural fabric's behaviour during processing. Knowing the exact relation between the manufacturing parameters and the processing parameters will lead to improved methods and reduced manufacturing time, cost and even weight of the composite components. The goal of this study is to understand how the support structure in newly developed non-crimp fabrics affects the manufacturing process of carbon fibre composite materials. Moreover, a newly developed automated dry fibre placement process was developed which utilizes the newly developed substrates and non-crimps fabrics manufacture. Net shape manufacture is presented as an important cost reduction step in the evolution of composite materials within the automotive industry, particularly as their use extends from low to high volume applications. The new process aims to minimize waste associated with the production of composites as well as improve the performance of the manufactured composite parts.

Experimental observations show that the in-plane permeability of the scrim-backed fabrics is affected by the scrim architecture. As the permeability of unidirectional carbon fibre bundles is inherently high parallel to the fibre direction and low in the transverse direction, when a scrim is added, flow is locally enhanced parallel to the fibre bundles, since the geometry of flow channels formed in the fabric is affected. In particular, new flow channels can form along transverse scrims threads which can increase the transverse bundle permeability. Moreover, experimental observations show that shear behaviour of the fabrics is not affected to a high degree on biaxial scrim supported fabrics. Formability of the fabrics remains almost the same for every scrim architecture and this can lead to further weight savings as the additional scrim yarns do not contribute to a significant degree to the processing characteristics of the fabrics.

A secondary study, before discussing the development of the new materials, was focused on modifying existing NCF products and examining their physical properties in order to understand the significance of the support structure on the processing of NCFs. Although there is a significant amount of research focused on examining the effect of the stitch thread of non-crimp fabrics, the number of studies using bespoke materials is limited as samples are only available from specific and widely used materials. The cost of ordering for example materials with specific stitch thread lengths would be prohibitive due to the fabric manufacturer requiring minimum orders that would exceed a typical research budget. The need to explore a systematic approach on changing the stitch thread parameters, and more specifically for this study the stitch thread tension, on NCFs was important for the development of the new structural fabrics. As the author had access to the manufacturing equipment at Hexcel Leicester, he could systematically change parameters in the NCFs, designing and manufacturing specific materials. Moreover, the stitch thread parameters were strictly controlled during the production stages, in order to be confident that the results would reflect changes in the support structure.

Constraining the bundle mobility by increasing the stitch tension was found to result in decreasing levels of fibre bundle waviness. The stitch thread tension

affects the size and geometry of fibre bundles and inter-bundle gaps in the fabric. Experimental observations suggest that this has an effect on the in-plane permeability, particularly transverse to the fibre bundles. Variations of the stitch thread tension will translate into rearrangements in the fibre structure and thus affect the permeability of the reinforcement. The higher the stitch tension, the tighter and closer packed the arrangement of the fibre filaments that can lead into alterations of the flow during liquid resin injection for composite manufacture. Moreover, experimental observations show that shear behaviour of the fabrics is affect by the stitch tension and there is a linear effect to the degree of shear they experience. High stitch tension results in reduced formability of the fabric on a complex geometry. As the stitch thread rearranges the fibre filaments, these are packed in a tight formation where the bundles tend to have constricted movement.

Contents

1.Introduction……...…...14
1.1.Overview……..14
1.2.Composites manufacture……..17
1.3.Fibre reinforcements…….19
1.4.Non-crimp fabrics (NCFs)……...….20
1.5.Thesis outline……....25

2.Review of Literature Related to the Manufacture and Processing of Novel Fibre Reinforcement Architectures……..27
2.1.Overview of Preforming and Liquid Moulding Technologies……. 27
2.2.Permeability of Reinforcement Fibre Architectures……..28
2.3.In-plane shear…….34
2.4.Diaphragm Forming of Fibre Reinforcements……...42
2.5.Scrim based fibre reinforcement architectures…….……..46

3.Experimental methodology……....49
3.1.Materials characterization……..49
3.2.Forming……..62

4.Effect of stitch tension on the processing parameters of non-crimp fabrics..67
4.1.Unidirectional non-crimp fabrics……...67
4.2. Biaxial non-crimp fabrics……..81

5.Development of Novel Scrim-based non-crimp fabrics……....98
5.1.Scrim architecture……..98
5.2.Scrim-based fabric manufacture: early development……..103
5.3.Scrim-based fabric development…….108
5.3.1.Permeability of scrim-based unidirectional fabrics:Part1……...115
5.3.2.Scrim-based Unidirectional fabrics…….124
5.3.2.1.Permeability of scrim-based unidirectional fabrics:Part2……...124

5.3.3.Scrim-based Biaxial fabrics……127
5.3.3.1.Permeability of scrim-based biaxial fabrics……..……..127
5.3.3.2.Forming of scrim-based biaxial fabrics……..131

6.Direct Dry Fibre Placement (DDFP)……..144

7.Conclusions…….152

8.References……...156

List of figures

Figure 1 a) Manufacturing of non-crimp fabrics at Hexcel Leicester , b) close up of a non-crimp fabric (ncf) 12
Figure 2: a) Degrees of crimp in different fabrics, b)Scrim architecture and manufactured fabric with scrim as the support structure 14
Figure 3 A production process for composite materials- Liquid Composite Moulding process (LCM) [1] 17
Figure 4 Crimp degree comparison between a a)stitched (a) and a woven fabric (b) [1] 18
Figure 5 Schematic of a woven fabric and description of crimp [2] 18
Figure 6 Non-crimp fabric with pillar stitch (shape of a straight line), top and bottom surfaces [3] 19
Figure 7 Non-crimp fabric manufacture – overview of the stitching process (movement of stitch head) [3] 20
Figure 8 Non-crimp fabric production machine schematic (the width of the conveyor belt is approximately 2m): a)side view, b)top view, where different possible layer orientation can be seen [3] 21
Figure 9 Different stitch styles of NCFs and Stitch parameters: stitch gauge and stitch length description for a ncf with tricot stitching [3] 22
Figure 10 Close-up view of a conventional biaxial stitched fabric [3] 25
Figure 11 The different scales in permeability [1] 27
Figure 12 Comparison of permeability results between different methods used by different companies and institutes [17] 30
Figure 13 Influence of the stitching length on a NCFs permeability [16] 31
Figure 14 Micrographs of dry carbon fibre fabrics showing the gaps that can be created during fabric production [19] 31
Figure 15 Macroscale deformations: a)shear, b)extension, c)ply-ply friction, d)bending , e)compaction [21] 33
Figure 16 Sample size used in this study for picture frame testing and direction of test and picture frame geometry [23] 35

Figure 17 Shear force vs shear angle of a biaxial -45°/+45° ncf - experiment conducted by different companies and institutes showing the different results obtained by them using different process parameters [31] 39
Figure 18 Shear deformation stages of biaxial stitched fabrics [28] 39
Figure 19 Cross-section through four harness satin weave at shear angles from 0° (top image) to 55° (bottom image) - the line is the assumed tow path [37] . 40
Figure 20 Different shear behaviour of different stitched fabric (GR-T: tricot style, GR-C: cord style, GR-P: pillar style): the higher stitch thread density the higher the shift in the plane of the fabric [33] 40
Figure 21 Diaphragm forming process (double diaphragm process) [39] 42
Figure 22 Permeability measurement rig at Hexcel Leicester 48
Figure 23: Dimensions of permeability measurement plates and location of pressure sensors 49
Figure 24 New picture frame rig (left) and previous iteration (right) 52
Figure 25 New picture frame rig (mounted on mechanical test equipment – top row) and overview when placing the fabric sample (bottom row) 53
Figure 26 Recesses in the new picture frame rig design 54
Figure 27 Aluminium base for supporting the fabric sample 54
Figure 28 Clamps/grips on picturef frame rig 55
Figure 29 Centreline location in the new picture frame rig 55
Figure 30 Centreline location in the old picture frame rig 55
Figure 31 New picture frame design during testing (positive shear – left, and negative shear – right) 56
Figure 32: Load vs extension of fabrics during testing using the new frame (top graph: stitch thread direction parallel to direction of test, bottom image: stitch thread direction perpendicular to direction of test) 57
Figure 33: Load vs extension of fabrics during testing using the old frame (top graph: stitch thread direction parallel to direction of test, bottom image: stitch thread direction perpendicular to direction of test) 58
Figure 34 Forming tool: a)top view, b)side view 59
Figure 35 Forming of preforms 61
Figure 36 Heating set-up with Infra red lamps (rig above tool/preform) 62
Figure 37 Removal of the preform from the tool 63
Figure 38 Overview of fabric 64

Figure 39 Stitch architecture in the fabric 65
Figure 40 Overview of the fabric: top surface of the fabric shown at a 30° angle to emphasize the stitch and weft thread geometry 66
Figure 41 Weft support thread spacing occurrence of L1, L2, R1 and R2 68
Figure 42 Defect analysis of the fabrics: a) image of an in-plane wave b) number of in-plane waves of fibre bundles at a specimen length of one metre. 69
Figure 43: Number of in-plane tow waves 71
Figure 44 Experimentally determined data for principal permeability values, K_1 and K_2, as a function of the fibre volume fraction, V_f 73
Figure 45 Experimentally determined data for ratio of anisotropy, K_1/K_2, and angle of flow (describing the orientation of the main flow direction) as a function of the fibre volume fraction, V_f 74
Figure 46 Vacuum bag set-up of a 4 layer dry stack: Top image permeability K_1, a) low stitch tension, b)high stitch tension. Bottom image permeability K_2, a) low stitch tension, b)high stitch tension 76
Figure 47 Top image (warp direction): images taken using an optical microscope (a)high stitch tension, b)low stitch tension), Bottom image (warp direction): images taken using SEM (a)high stitch tension, b)low stitch tension) 79
Figure 48 Closeup of the fabric: stitch thread in the warp direction 80
Figure 49 Top side of fabrics: a)high stitch tension, b)low stitch tension 81
Figure 50 Back (loop) side of fabrics: a)high stitch tension, b)low stitch tension 81
Figure 51 Experimentally determined data for principal permeability values, K_1 and K_2, as a function of the fibre volume fraction, V_f 83
Figure 52 Experimentally determined data for ratio of anisotropy, K_1/K_2, and angle of flow (describing the orientation of the main flow direction) as a function of the fibre volume fraction, V_f 84
Figure 53 K_1 permeability a)low stitch thread tension, b)high stitch thread tension 85
Figure 54 K_2permeability a)low stitch thread tension, b)high stitch thread tension 85
Figure 55 shear force vs shear angle of the different fabrics 86
Figure 56 Apodius system 88

Figure 57 Preform analysis 89
Figure 58 Mesh generation 89
Figure 59 Manufactured preform with the high stitch thread tension 90
Figure 60 Scanning of preform with the high stitch thread tension using the Apodious system 90
Figure 61 Analysis of the preform with the high stitch thread tension using the Apodious software 91
Figure 62 Fibre orientation destribution of the preform with the high stitch thread tension 91
Figure 63 Manufactured preform with the low stitch thread tension 92
Figure 64 Scanning of the preform with the low stitch thread tension using the Apodious system 92
Figure 65 Analysis of the preform with the low stitch thread tension using the Apodious system 93
Figure 66 Fibre orientation distribution of the preform with the low stitch thread tension 93
Figure 67 Comparison between the fabric preform parts with the high (a) and the low stitch thread tension (b) 95
Figure 68 Scrim parameters 97
Figure 69 : Scrim construction schematics: On the left a conventional readily available scrim (Bafa 300/8) and a bespoke manufactured for Hexcel scrim (Bafa 40/8) a construction with a reduced number of 0^{o} oriented yarns 98
Figure 70 Manufacturing of the scrim material 99
Figure 71 Laminating equipment for scrim-supported fabric manufacture and schematic (side view) of set-up 108
Figure 72 Laminator equipment and manufactured fabric 109
Figure 73 4x2 , 4x3, 4x4 scrim architectures overview 110
Figure 74 Scrim materials , 4x2, 4x3, 4x4 111
Figure 75 Top view: a)4x4 scrim, b)4x2 scrim 112
Figure 76 Side view (fabric titled at 85^{o} relative to the microscope set-up): a)4x4 scrim, b)4x2 scrim 112
Figure 77: Manufactured fabric - top (left) and bottom (right) view 113
Figure 78: Measuring the distance between two adjacent scrim yarns for the three types of scrim material 114

Figure 79 Experimentally determined data for principal permeability values, K_1 and K_2, as a function of the fibre volume fraction, V_f 116
Figure 80 Experimentally determined data for ratio of anisotropy, K_1/K_2, and angle of flow (describing the orientation of the main flow direction) as a function of the fibre volume fraction, V_f 117
Figure 81 Top image: a) 4x4 scrim warp direction (direction of the fibre), b)4x4 scrim weft direction. Bottom image: same image with notations 119
Figure 82: Calculated mean permeability 121
Figure 83 Predicted and calculated permeability 123
Figure 84: Correlation between the K2 permeability and the distance between the two weft scrim yarns at 55% fibre volume fraction (typical target FVF for composite parts) 124
Figure 85 Experimentally determined data for principal permeability values, K_1 and K_2, as a function of the fibre volume fraction, V_f 126
Figure 86 Experimentally determined data for ratio of anisotropy, K_1/K_2, and angle of flow (describing the orientation of the main flow direction) as a function of the fibre volume fraction, V_f 127
Figure 87 Experimentally determined data for principal permeability values, K_1 and K_2, as a function of the fibre volume fraction, V_f 129
Figure 88 Experimentally determined data for ratio of anisotropy, K_1/K_2, and angle of flow (describing the orientation of the main flow direction) as a function of the fibre volume fraction, V_f 130
Figure 89 Shear force vs shear angle comparison between the 4x4 and the 4x2 types of scrim materials 131
Figure 90 Manufactured preform 4x2 132
Figure 91 Scanning of preform 4x2 using the Apodious system 132
Figure 92 Analysis of the preform 4x2 using the Apodious software 133
Figure 93 Fibre orientation distribution of the preform 4x2 133
Figure 94 Manufactured preform 4x4 134
Figure 95 Scanning of preform 4x4 using the Apodious system 134
Figure 96 Analysis of the preform 4x4 using the Apodious software 135
Figure 97 Fibre orientation destribution of the preform 4x4 135
Figure 98 Preform manufacture using scrim material 137

Figure 99: Experimentally determined data for principal permeability values, K1 and K2, as a function of the fibre volume fraction, Vf 139
Figure 100: Calculated mean permeability 140
Figure 101: Predicted and calculated permeability 142
Figure 102: Correlation between scrim yarn dtex and permeability at 55% fibre volume fraction (typical target FVF for composite parts) 142
Figure 103: Experimentally determined data for principal permeability values, K1 and K2, as a function of the fibre volume fraction, Vf 144
Figure 104 Direct Fibre Placement (DDFP) concept drawing 147
Figure 105 DDFP comparison with conventional fabric manufacture 148
Figure 106 Manufacture of a fabric on the DDFP 149
Figure 107 Scrim material used as substrate for fibre deposition 149
Figure 108 Double diaphragm forming cell 150
Figure 109 Net shape manufacture a)top view of fabric stack, b)bottom view of fabric stack, c)close up of fibre deposition capabilities on anticipated composite part loads 151
Figure 110 Placement of scrim at different orientations: Orientation of scrim at -45°/+45 ° relative to the carbon fibre tows 151
Figure 111 Comparison between conventional ncf and fabric manufactured by the newly developed DDFP process 152
Figure 112 a)AFP head design and b)L-shaped part that can potentially be replaced in order to reduce overall parts weight 154

List of tables

Table 1. List of trialled membranes and their properties/attributes……..55
Table 2. Stitch parameters…….59
Table 3. Material parameters……....60
Table 4. Combinations of numbers of fabric layers and cavity height to obtain target fibre volume fractions…….62
Table 5. Material parameters……69
Table 6. Architecture parameters for the different fabric versions……..75
Table 7. Scrims trialled…….91
Table 8. Scrim trialled – continuation……...92
Table 9.Yarns trialled……...92
Table 10. List of trialled yarns for scrim manufacture…….....98
Table 11. Combinations of numbers of fabric layers and cavity height to obtain target fibre volume fractions……...111
Table 12. Combinations of numbers of fabric layers and cavity height to obtain target fibre volume fractions……..123
Table 13. Material parameters……...150
Table 14. Material parameters……...154

Acknowledgements

The author would like to thank the academic supervisors Professor Andy Long and Dr Andreas Endruweit and industrial supervisor Thomas James, for their help, guidance and support throughout the project as well as the University of Nottingham and Hexcel Leicester for providing the equipment, materials and support necessary to complete the research and work. This Engineering Doctorate was sponsored by the University of Nottingham and Hexcel. The author would also like to acknowledge the support of the Engineering and Physical Research Council and all its members as well as all the colleagues at Hexcel for all their support and help throughout the duration of the project.

1. Introduction

1.1. Overview

The focus of this work is the understanding of fibre-reinforced materials with bonded support structures, where the manufactured fabrics can potentially offer improved physical and mechanical properties when compared with conventional stitched fabrics (non-crimp fabrics: NCFs) as well as the development of a new automated fibre placement method that can manufacture these types of materials. The bulk of the work focuses on characterizing these materials and by varying different parameters in the support structure to examine how these affect the physical properties of the fibre reinforcement. In figure 1, the production as well as an image of a non-crimp fabric are shown.

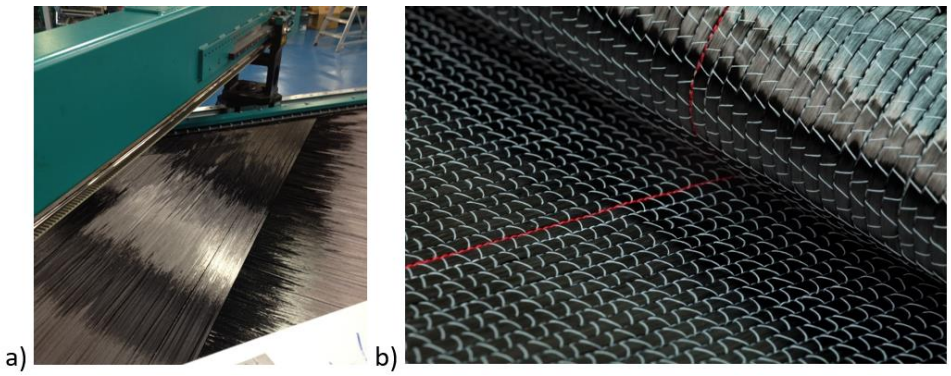


Figure 1 a) Manufacturing of non-crimp fabrics at Hexcel Leicester ,
b) close up of a non-crimp fabric (ncf)

In conventional NCFs, the fibres are not aligned perfectly parallel to each other where defects such as tow and fibre waviness as well as crimp that are often not taken into account when researching or designing a composite component can affect its performance. In addition, during forming of a stitched fibre reinforced fabric, the material undergoes large deformations where the stitch allows more easily for the carbon fibre tows to move to other regions (adjacent tows) and thus change the local fibre volume fraction of the composite part. By using an adhesively bonded support grid (scrim), the tows can also be spread more uniformly and “maintain” the shape on the scrim and can consequently allow for a more “controlled” change in thickness and fibre volume fraction of the resulted manufactured composite. The irregularity of the fibre structure in

conventional stitched fabrics deters from using for example permeability values for flow simulation as these vary to a large degree between trials. As the fibres in the scrim supported fabric are aligned to a higher degree, changing parameters in the support structure can be the main influence for any type of modification to the fabric architecture.

Stitching can introduce waviness in the carbon fibre tow, both in the in-plane and out-of plane directions. During the stitching process, the stitch head in the stitch equipment "separates" the warp direction tows from the adjacent tows inducing crimp in these areas. In this study, a scrim-fixated carbon fibre fabric is used, where the tows are joined together by a thermoplastic bond between the reinforcement tows and the scrim. The scrim consists of thermoplastic yarns laid in an open mesh construction. The bond between scrim and tow is created through heat and pressure (the process is described in a subsequent chapter). There are no mechanical interlocks, links or loops as seen in conventional woven, knitted or stitched fabrics.

The parameters available for optimisation of this material format relate to the design of the scrim and the positioning of the tows on the scrim. Conceptually (ignoring availability) the scrim can be designed with a range of yarn spacings and orientations, and the scrim yarns can be specified with a range of materials, sizes and coatings. Moreover, the handleability and drapeability of the stitched fabrics during the manufacturing of the composite part is mainly affected by the stitching parameters. The mechanical properties of the composite part are defined by the orientation of the fibres, the position of the fibres, and the targeted fibre volume fraction. Defects in the fabrics such as gaps and the shape of gaps, tow waviness, the stitch piercing through the tow, folds, undulations and different stitch patterns will affect the mechanical performance of the composite part. Most of these defects will alter the load bearing capabilities of the fibres, disrupt the resin flow and create resin rich areas that can lead to initiations of micro-cracks in the manufactured composite. A scrim as a support structure for the fibres can potentially eliminate to a large degree these occurrences. In figure 2, an assumption of the

reduction of the crimp level of different categories of structural fabrics as well as a schematic of the scrim material and the manufactured fabric.

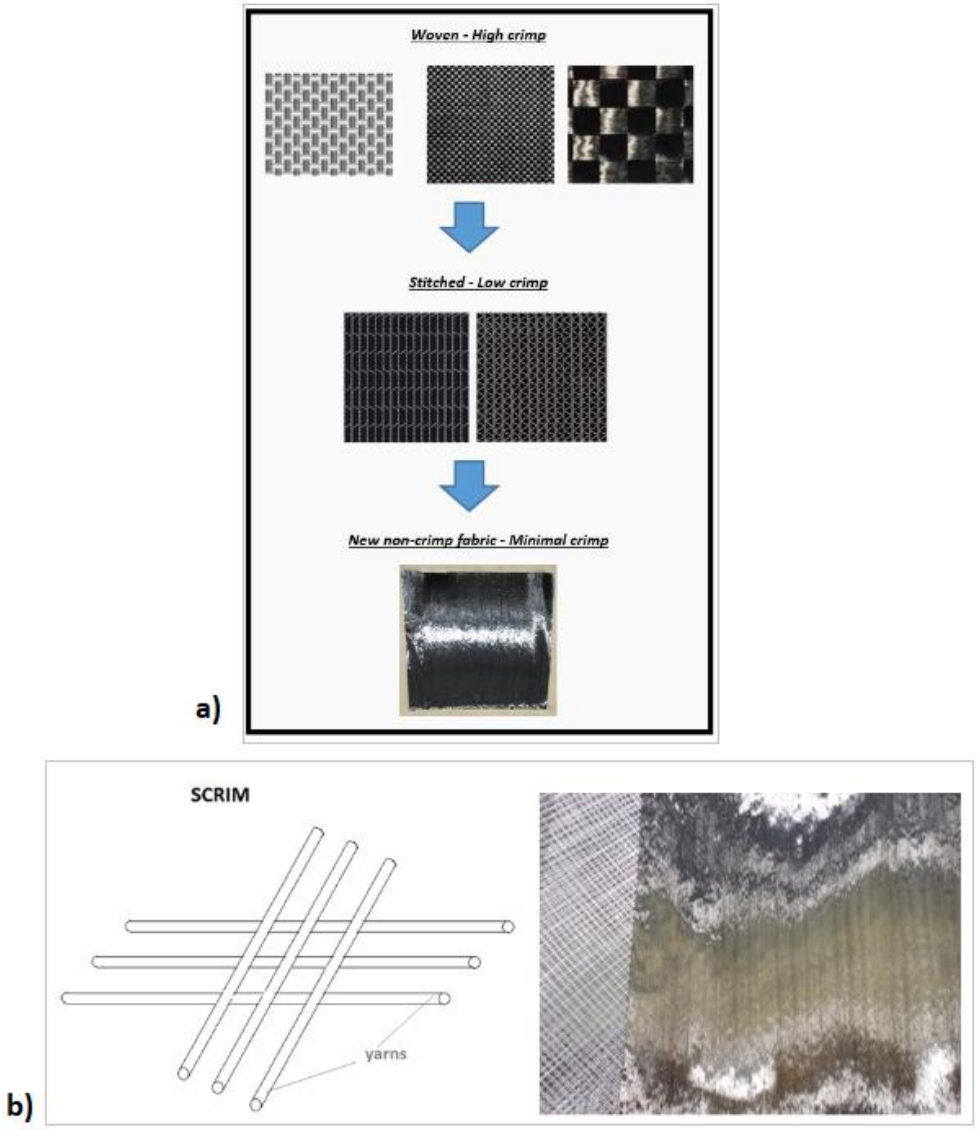


Figure 2: a) Degrees of crimp in different fabrics, b)Scrim architecture and manufactured fabric with scrim as the support structure

Most attempts to define even basic models for the prediction of permeability of textile reinforcements have low accuracy due to the difficulty in measuring the permeability of the reinforcements as the high variation between trials under the same conditions prevents that. Possible variations can be from equipment and operation variations and the inherent material variability. However, the main source will always be the material variability and inherent instability due to the effect of the stitch thread. Variations in the internal structure of the

fabric at a small scale will cause the experimental scatter during testing. The interaction between shear deformation and permeability is linked as the forming of textiles will affect the flow during composite manufacture. The material properties and the deformation mechanisms of the textile preforms are interrelated. Distortion induced by the stitch thread in non-crimp fabrics will affect the physical properties of the structural fabric and ultimately the mechanical performance of a manufactured composite part.

A second study on the influence on varying the stitch tension in conventional non-crimp fabrics is discussed. This was important to focus on as studies include a relatively low number of trials and only focus on a specific stitch thread pattern. Moreover, this study could inform how by methodically changing parameters in a stitched fabric can be used and examined when changing parameters in the scrim supported fabric. Also, the values chosen for the manufacture of the stitched fabrics corresponds to the upper and lower limits of the stitch thread tension values before the stability of the fabrics would be reduced significantly (high and low stitch thread tension).

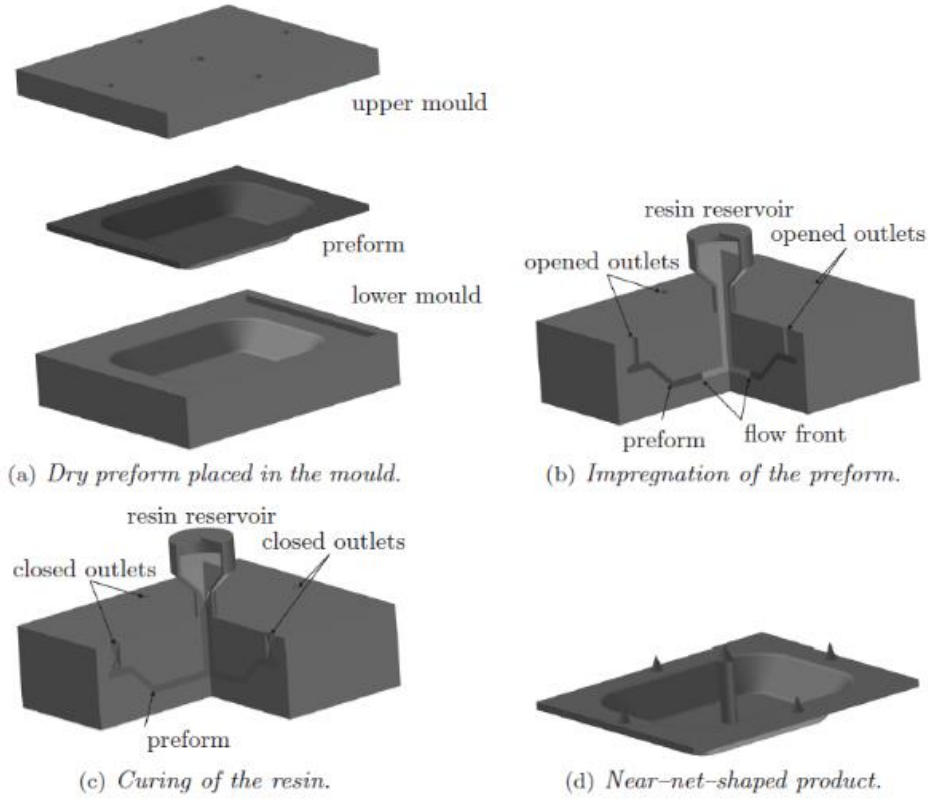
1.2. Composites manufacture

Fibre reinforcements (usually carbon or glass fibre) constitute one of the two constitutes that are required for composites. Fibre filaments are bundled (tows) and are used to create the fabric for subsequent processing. These textile reinforcements can have different forms such as multiaxials with the fibre tows stitched together or woven with the tows interlacing in order to create the fabric. The architecture of the fabric leads to dual-scale porosities. Gaps are created between the tows as well as between the individual filaments that allow for the resin to flow.

The second part of a composite is the resin/hardener system. A polymer (frequently epoxy for high performance applications) impregnates the fibre reinforcement and then is cured to create the composite. The resin is the component that will transfer the load between the fibres. Different types of

resin used for composite manufacture will result in different mechanical and thermal properties of the component. During the resin infusion process, where a fabric stack is infused with resin, the gaps in the fabric have to be saturated in order to produce a composite without any dry areas that could potentially lead to defects which can compromise the final properties and the load transfer in service of the composite.

The increasing application of complex components with these types of materials accompanied by an increasing demand to reduce costs and increase efficiency has led to an increasing number of investments in the research and development of new manufacturing technologies. Knowledge and expertise in this sector plays an important role in the production process to achieve high quality in a cost effective manner. Optimization on all levels of production, and more importantly the material development, will allow for a more reproducible product. An integral process approach should be employed in order for the engineers to be aware of all the relations between all the manufacturing process steps. The quality of a manufactured composite component depends on a number of factors, a main parameter being the successful impregnation of the fibre reinforcement with the resin. A common method of composite manufacture is by resin transfer moulding (RTM – figure 3). In RTM, a preformed fibre reinforced fabric is placed inside a tool held in a press, where resin is injected into the material usually at high pressures.



(a) *Dry preform placed in the mould.* (b) *Impregnation of the preform.*

(c) *Curing of the resin.* (d) *Near–net–shaped product.*

Figure 3 A production process for composite materials- Liquid Composite Moulding process (LCM) [1]

1.3. Fibre reinforcements

Dry structural fabrics are reinforcements for structural composites. The architecture of the structural fabric has to provide the required processability characteristics as well as the required performance as a finished composite material. This trade-off of processability and performance must be weighted appropriately: the dry fabric will exist as such only during manufacturing - the resulting composite must subsequently perform for the lifetime of the part. The two main types of structural fabrics are woven and non-crimp fabrics. The woven fabrics have two fibre directions ($0^o/90^o$) interlaced together. The waviness introduced at the interlacing point of the fibre bundles refers to as crimp. A comparison of the degree of crimp between a woven and a non-crimp fabric can be seen in figure 4.

The frequency of the interlacing fibre directions can be controlled, resulting in different weave patterns. Weave geometries include twill (more common), satin and plain weave. Lower crimp translates to higher mechanical performance due to a straighter fibre (as the fibre will carry the load). The lowest crimp is found in the satin weave pattern. A description of crimp is shown in figure 5.

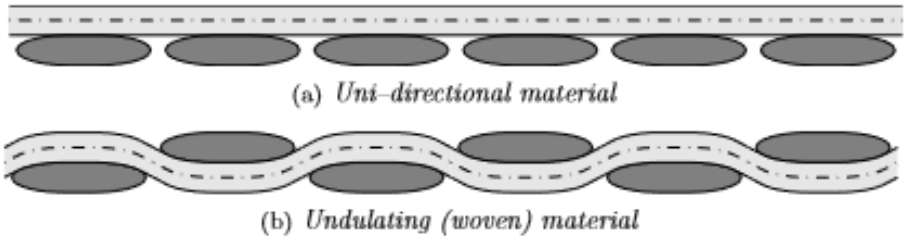


Figure 4 Crimp degree comparison between a a)stitched (a) and a woven fabric (b) [1]

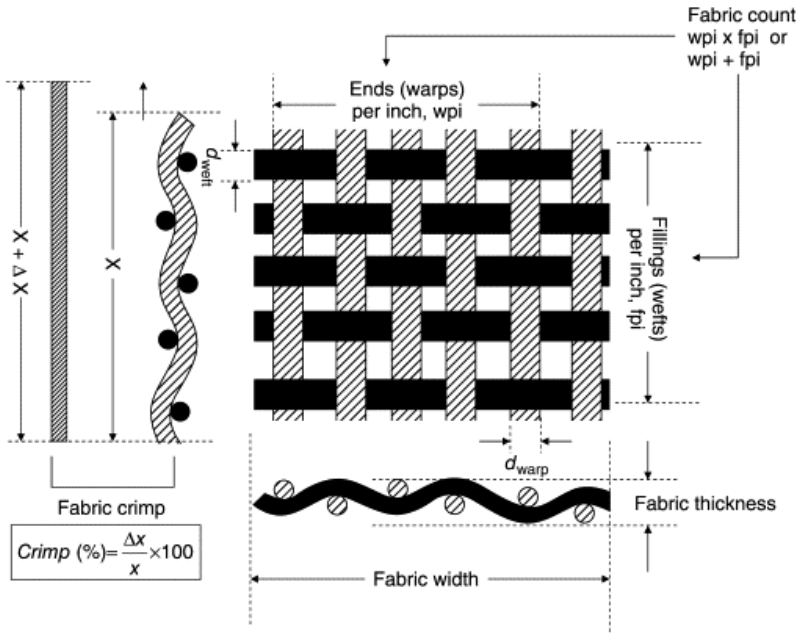


Figure 5 Schematic of a woven fabric and description of crimp [2]

1.4 Non-crimp fabrics (NCFs)

The focus of this study is on non-crimp fabrics. Non-crimp fabrics consist of tows of fibre that when stitched together create the fabric layer. During production, a bar with needles feeds a thread that penetrates the fibres to create

the fabric. Usually, the stitching process creates gaps between the tows and through the z-direction where the thread penetrates the layers leaving the thread in its place, as seen in figure 6 where for a -45 º/+45 º carbon fibre stitched fabric the stitch is in the 0º direction. The stitch thread type is pillar, where the stitch resembles lines running across the length of the produced fabric at specific distances between them.

Different types of carbon fibre tow can be processed for non-crimp fabric manufacture. Each tow exhibits different processability characteristics. The primary characteristics that affect the textile manufacturing process are filament waviness, filament continuity, sizing, tow width, tow width consistency, tow folding and tow twist. Typical fibre filaments number (filament count) range from 1000 (1K) to 50000 (50K). Some carbon fibres benefit from a period of preconditioning at a given temperature, humidity and time prior to manufacture.

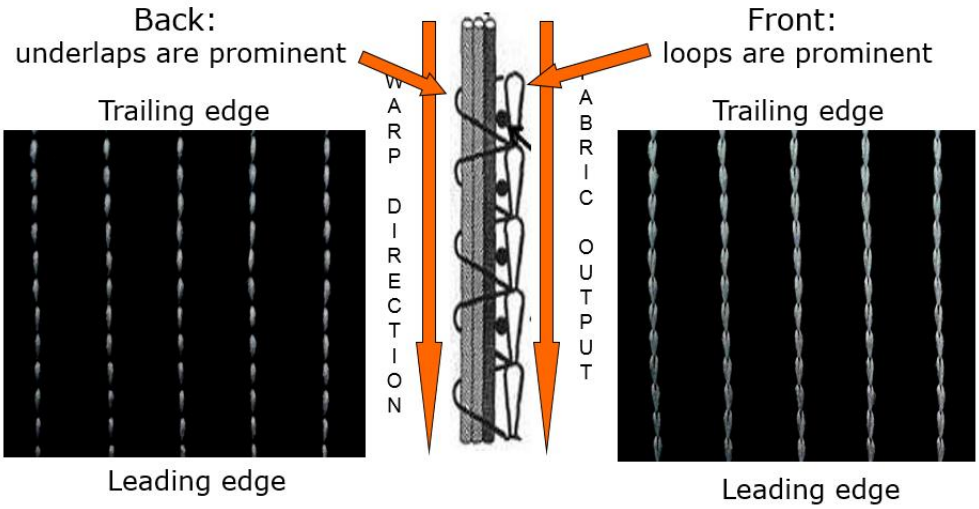


Figure 6 Non-crimp fabric with pillar stitch (shape of a straight line), top and bottom surfaces [3]

The needle in the stitch head penetrates the fibre bed and the fibres are separated into different bundles. When the needle retreats, the stitch thread is pulled back through the fibre bed and a loop of the stitch thread is left at the bottom surface on the fibre bed as shown in figure 7. The stitch thread passes through the loop during the next machine action. Although the needle in the

stitch head might not damage the fibres to a significant degree, the tow paths are distorted by the stitch thread during the stitching process. Moreover, the distortions are different for the top and bottom surface of the fabric.

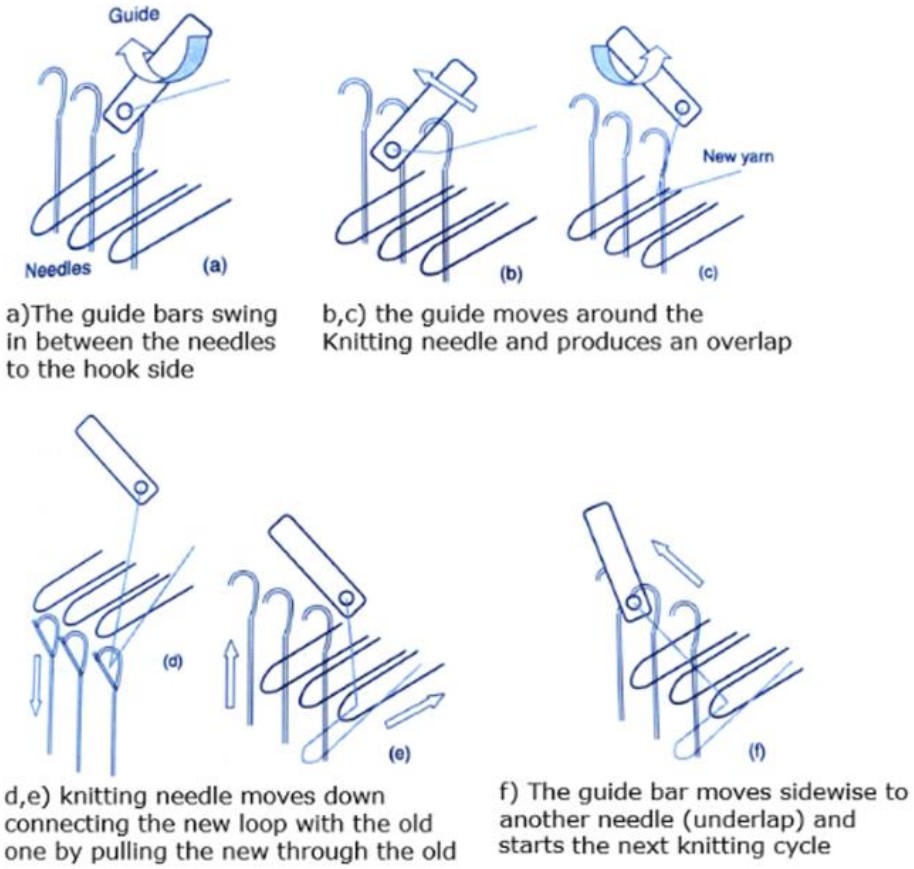


Figure 7 Non-crimp fabric manufacture – overview of the stitching process (movement of stitch head) [3]

The stitch style ranges from pillar (straight stitch lines) to tricot (zig-zag pattern). The stitch gauge is the number of stitches per 25.4mm across the width of the fabric and usually ranges from 2 to 6 stitches per 25.4mm. The stitch length usually ranges from 2mm to 5mm. Conventional stitched fabrics are groups of tows held together and aligned parallel to each other within a layer. Unidirectional fabrics consist of a single layer. Multiaxial fabrics consist of multiple layers. A schematic of the machine that manufactures the non-crimp fabrics is shown in figure 8. Although stitching is known to adversely affect the mechanical performance of the finished composite, the method has inherent versatility. The prevalence of stitched fabrics over other types of non-

crimp fabrics has led to a greater understanding of the former, and parameters such as stitch length, stitch type and stitch spacing can be adjusted to create different fabric versions. However, there is a large degree of variation in stitched fabrics due to the nature of the fabric: variability during manufacture and issues created when handling and processing of the material.

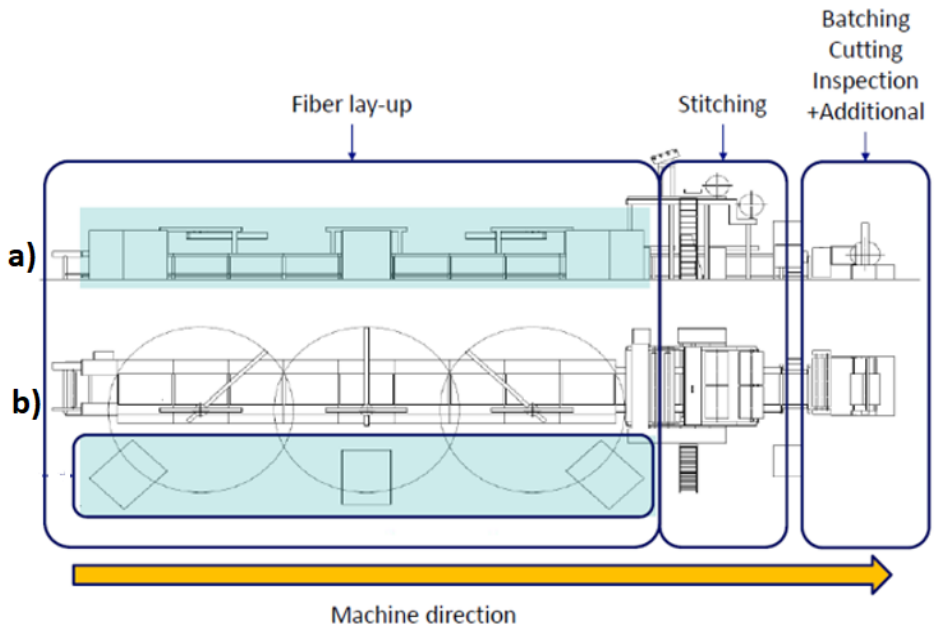


Figure 8 Non-crimp fabric production machine schematic (the width of the conveyor belt is approximately 2m): a)side view, b)top view, where different possible layer orientation can be seen [3]

The types of fabrics that can be manufactured range from unidirectional to quadriaxial. After the fibres are layed in their specified angles on the machine bed, they pass through the stitch head where they are stitched together. The basic stitch types are (and can also be seen in figure 9 along with a description of the stitch length and the stitch gauge):

- Pillar (chain stitch)
- Tricot (zig zag stitch)
- Half pillar tricot (1x zig zag stitch followed by a 1x chain stich and this is repeated)
- Full pillar tricot (1x zig zag stitch followed by a 3x chain stitch and this is repeated)

There are five parameters that can be changed:

- Stitch length
- Stitch gauge
- Stitch thread dtex
- Stitch thread type
- Stitch style

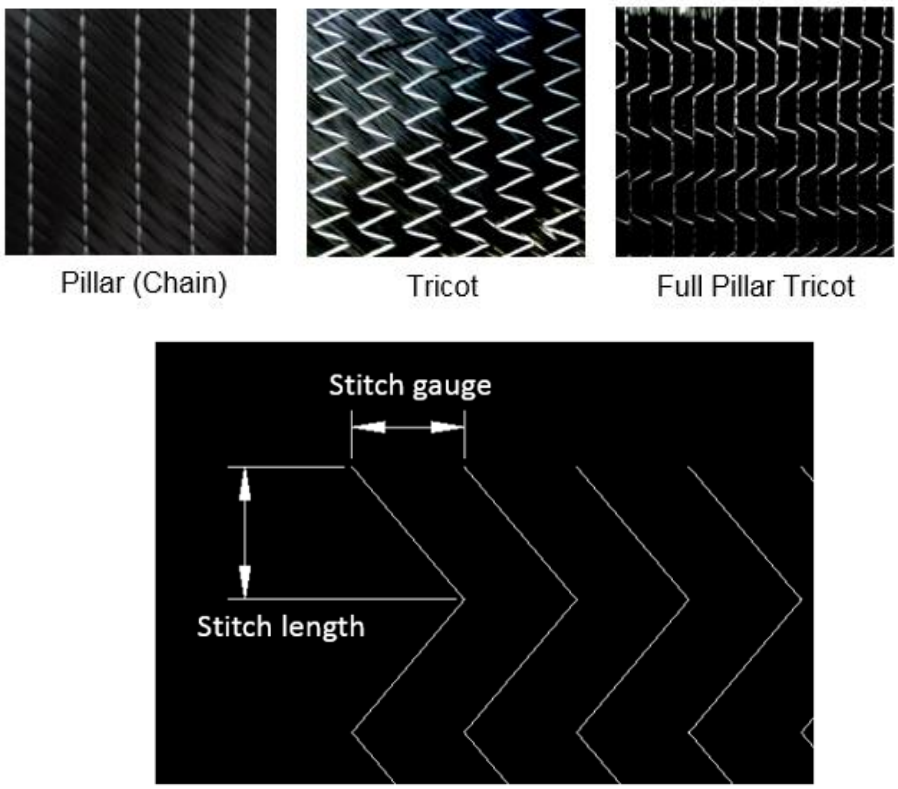


Figure 9 Different stitch styles of NCFs and Stitch parameters: stitch gauge and stitch length description for a ncf with tricot stitching [3]

The stitch gauge length can be calculated as:

$$l = \frac{25.4mm}{E} \qquad (1)$$

Where:

E: stitch gauge number

Other parameters of NCFs that can be changed:

- The fabrics can be manufactured with a range of different fibres
- Support threads: glass fibres that can act as support threads in the fabrics to enhance stability that is usually required during processing
- Different weights of fabrics range from 100gsm to 1000gsm
- Thermoplastic powder can be applied to the surface of the fabric for preform manufacture and subsequent processing: this step is eliminated when using scrim materials and is discussed in a subsequent chapter, where cost savings can be significant
- Chopped fibres can be added in a form of a mat on the surface of the fabric to enhance permeability

1.5 Thesis Outline

Chapter 2: Reviews previous research on non-crimp fabrics and how the support structure parameters affect the fabric's behaviour in the stages of characterization and in processing and more specifically in the pre-forming process.

Chapter 3: In this chapter, the experimental methodology is discussed as well as a novel method for shear testing that was developed and implemented for the first time and specifically for this research is illustrated.

Chapter 4: The further development of existing non-crimp fabric versions are discussed in chapter 4. By altering parameters, the stitch thread tension, the effect on processing is examined. Mainly, the permeability and shear behaviour is the focus of this research.

Chapter 5: In chapter 5, the development of the new materials, scrim based non-crimp fabrics, is outlined. From early stages of development with existing technologies, up to the manufacture of bespoke materials utilizing novel methods.

Chapter 6: A novel non-crimp fabric manufacturing process is discussed that utilizes fibre placement technologies. The resulting research was published in a patent and it is available in the references section.

Chapter 7: This chapter discusses the results and conclusions from the previous chapters, findings and outcomes as well as possible future studies resulting from all the research.

Chapter 8: References

2. Review Of literature Related to the Manufacture and Processing of Novel Fibre Reinforcement Architectures

2.1. Overview of Preforming and Liquid Moulding Technologies

Fabric deformation alters its local permeability characteristics which will result in influencing the resin infusion process. The permeability of the fabric depends on its geometry which in turn is affected by deformations during the draping process. The main deformation mode is shear. Fibre reorientation and an increases of local fibre content can affect the permeability of the fabric reinforcement. This might not be an issue for simple parts where the porosity is expected to remain somewhat uniform throughout the fabric. However, dry spots or voids are more likely to occur in complex parts where changes in local porosity and shear angle are significant.

Variations in the structure of the fabric such as the stitch material, stitch length, distance between the stitches and stitch pattern can affect processing. In figure 10, the top and bottom side of a non-crimp fabric is shown. Although the stitching is essentially a parasitic element within the finished composite, it performs two primary functions within a structural fabric. Firstly, it must be tough enough to be formed into the loops of a warp knit using the stitchhead. Secondly, it must have enough elongation and strength to maintain the fabric structure during handling, forming and resin injection. Moreover, the stitch type will affect the permeability and consequently processing of the fabric reinforcement.

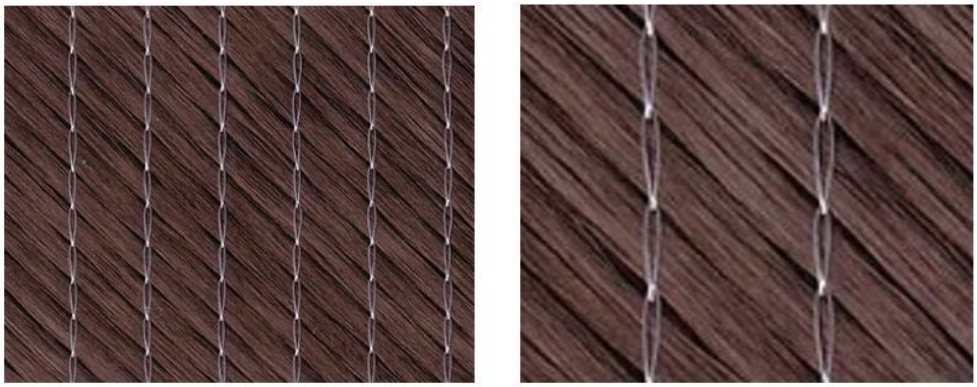


Figure 10 Close-up view of a conventional biaxial stitched fabric [3]

2.2. Permeability of Reinforcement Fibre Architectures

2.2.1. Definition of Permeability

Flow of a liquid through a fibre reinforcement follows Darcy's law [1]. The relationship between the pressure gradient and the flow rate is linear and can be expressed as:

$$v = \frac{-K}{\mu} \nabla p \qquad (2)$$

Where

K: permeability tensor

∇P: pressure gradient

μ: viscosity

v: phase-averaged flow velocity

Behaviour of the flow of a fluid through the fibre reinforcement is assumed to be uniform in terms of permeability at the macroscopic level in the principal directions. However, the dual-scale porosity that exists leads to different types of flow. The different scales in permeability can be seen in figure 11. The permeability of the fibre reinforcement describes the ability of the resin (viscous liquid) to impregnate the fibre fabric (porous medium). The level of impregnation depends on the physical properties of the fabric. Dry fabric is infused with the fluid, where capillary forces may also affect the flow. The capillary forces depend on the surface tension of the fluid and the contact angle

on the fibres surface. These are frequently considered negligible as they are typically small compared to the applied pressure field in the tool and are consequently neglected. The velocity of the fluid is proportional to the pressure gradient. The constant of proportionality is the permeability of the fibre reinforcement. Permeability is a symmetric second order tensor, where it can vary with orientation.

Deformation of the fabrics during handling can result in permeability values exhibiting large scatter. A recent benchmark exercise that involved a high number of participants showed large scatter of results. The level of material variability as well as the material history (handling and processing of the material) shows the difficulty in predicting the in-plane permeability and consequently the reinforcement impregnation process outcome during resin flow [4]. Measured permeability is reported to vary significantly according to different studies [5 – 8]. Material quality is the main factor for reproducibility. Inhomogeneous areas in the fibre reinforcement are the main cause of high standard deviations of permeability values.

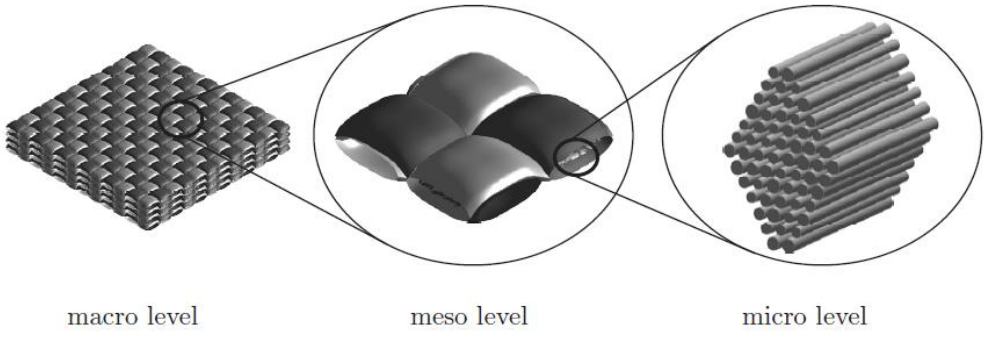


Figure 11 The different scales in permeability [1]

The two types of flow are: microscale flow (within the fibre bundle) and mesoscale flow (between the fibre bundles). The overall flow rate through the fibre reinforcement is set by the mesoscale flow. Therefore, the permeability of a textile can be estimated by the analysis of the fluid flow through the gaps created by the arrangement of the fibres.

The two most employed experimental testing set-ups for measuring the in-plane permeability of a textile are (the out-of-plane permeability can be ignored due to the relative low thickness of the material):

a)One dimensional: linear flow tests

b)Two dimensional: this test can measure the two in-plane principal permeability values and their orientation

Researchers have characterized the permeability of a structural fabric using radial flow equipment, where the flow front is detected and recorded in real time using image digitation method [9]. The elliptic contour of the flow front is used to calculate the principal axes. The in-plane permeability was then calculated from the characteristic lengths and the orientation of the ellipse. Other researchers have used different methods in order to calculate the principal permeability and orientations [10]. In radial flow experiments, the dry fabric is wetted by the flow front (displacing of air). A circular flow front pattern is observed for isotropic materials whereas an elliptic flow front is seen for anisotropic materials.

The orthotropic (anisotropic) reinforcement in-plane permeability consists of two principal permeability values (K_1 and K_2). An elliptic flow front is observed during the radial injection. In order to understand and characterize the in-plane permeability, the orientation (angle) of the in-plane tensor needs to be determined and thus provide the principal directions of the principal axes. It is acknowledged that the permeability values variability source can be the testing equipment [11] and/or be attributed to the variation in the fabric's structure [12].

The equations used and the methods used to compute the material permeabilities are listed in the literature [13 – 15]. Moreover, it is important to aim for the same fibre volume fraction for each trial, as any deviation can affect the results significantly. For example, in one study it was found that the permeability of a woven carbon fibre fabric was reduced by half when the fibre volume fraction was increased from 56% to 62% and shows to what degree the permeability can be affected by small fibre volume fraction deviations [16].

The parameters that can affect the permeability of a fabric are:

- Fibre type
- Number of fibre filaments in the tow
- Fibre diameter
- Fibre orientation
- Target fibre volume fraction: fibre volume fraction relation to permeability is non-linear
- Tow size
- Cross sectional area of the carbon fibre
- Distance between the carbon fibre tows
- Stitch type in the fabric (stitch pattern, stitch diameter, stitch gauge and length)

2.2.2. Influence of the support structure on permeability

No standard for measuring the permeability values of a fibre reinforcement exists. A benchmark study compared different processes (as seen in figure 12) and strategies to obtain permeability values [17]. An up to 50% difference in values was observed during trials from the same company as well as a significant difference between different companies and institutes. However in this and other benchmark studies, the materials used were woven fabrics which have low stability where the results can significantly be affected (fabric distortions during cutting, handling and tool placement). Another main factor causing the difference in the results is that the trials were performed by different operators and with different conditions (mainly the equipment used to calculate the permeability). A significant error between the studies might also be the specific fibre volume fraction that was used/targeted. Equipment such as shims to adjust the cavity height of the mould in order to achieve the desired fibre volume fraction have tolerances that can influence the permeability values. The tighter the tolerances the more accurate the results will be. A method for accurately measuring the permeability values needs also to be established.

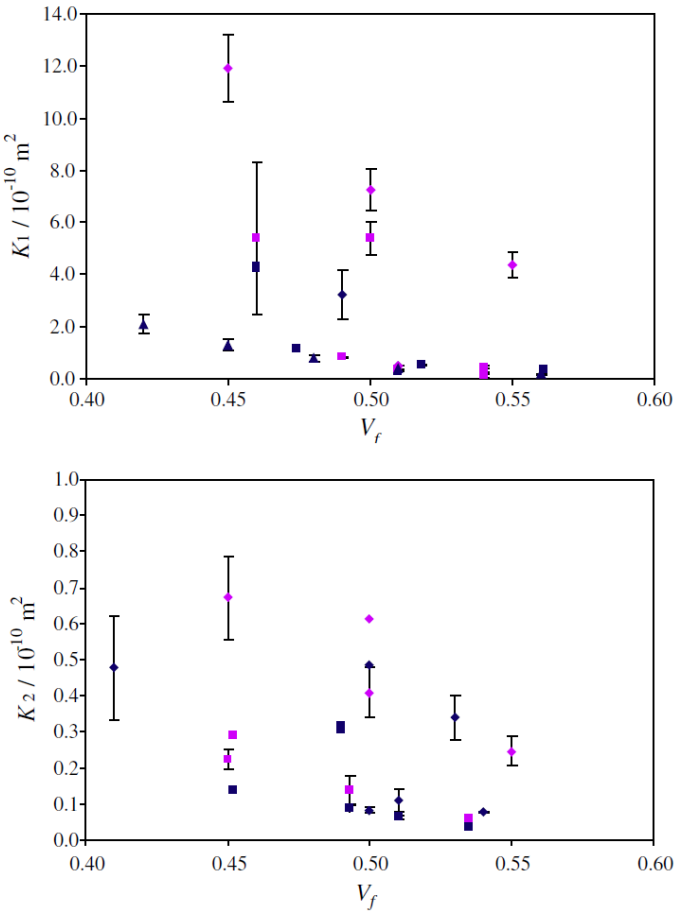


Figure 12 Comparison of permeability results between different methods used by different companies and institutes [17]

Changing the stitching parameters in a fibre reinforcement, the in-plane permeability can be affected to a significant degree. In one study, by changing the stitch length from 2mm to 5mm in a carbon fibre biaxial fabric, the permeability was increased significantly [18]. This is shown in figure 13, where a comparison of the effect of the different stitch lengths on the permeability of the fabrics used is shown. The strong influence of the stitch thread shows clearly that the permeability is strongly affected by the stitch thread of the fibre reinforcement. Any form of modification to the stitch pattern will have an effect on the fabric geometry and consequently will affect the flow behaviour. In figure 14, the separation of the fibre bundle can be seen in a stitched fabric and the gaps that are created, their shape and location can potentially affect the resin flow. Although the gaps are created to a large

degree by the stitch, gaps can be created during placement of the tows during production as well.

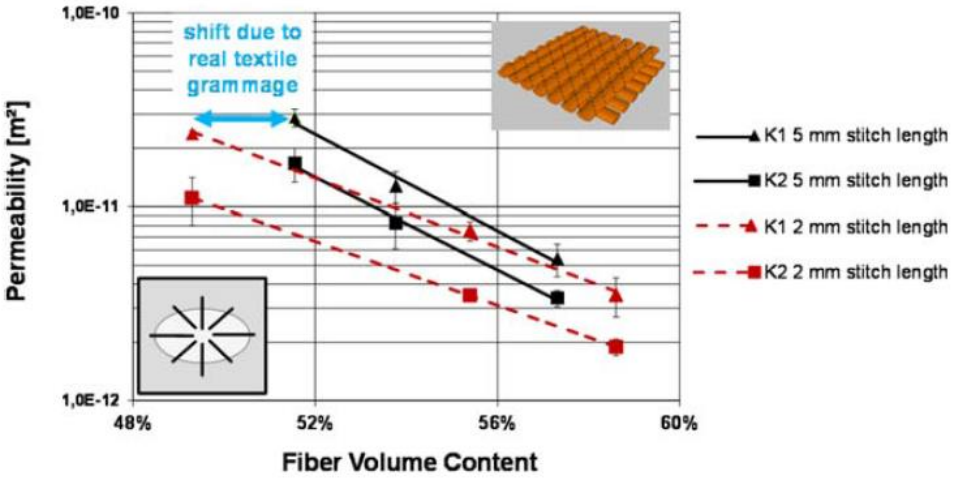


Figure 13 Influence of the stitching length on a NCFs permeability [16]

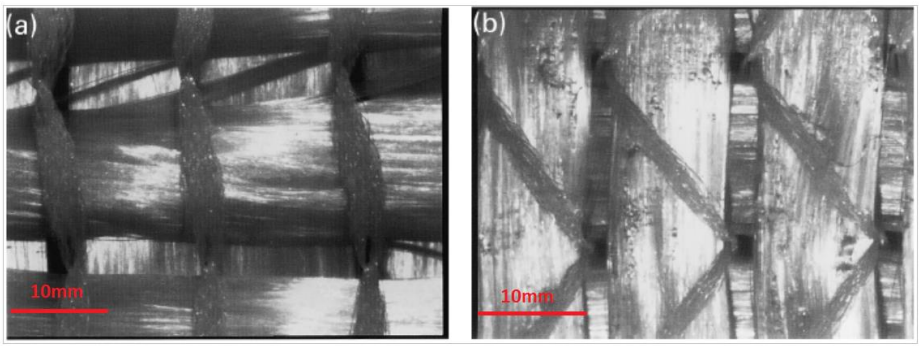


Figure 14 Micrographs of dry carbon fibre fabrics showing the gaps that can be created during fabric production [19]

When comparing different stitch densities, it was found that at a higher stitch density the permeability of the fibre reinforcement is increased. The permeability of fabrics with the same fibre structure and same fibre type but with different stitch gauge values was compared. Although the stitching exists to provide stability to the fabric during manufacturing and subsequent processing, a number of different studies have focused on confirming the

influence of the stitch thread on the permeability of the non-crimp fabric and how varying its parameters (mainly stitch length and gauge) affects the physical properties of the fabric (permeability and drape). It was also shown that the stitch pattern has a strong influence on permeability. A higher number of stitches can increase the fabric's permeability [20]. Although a specific stitch parameter is not stated, it can be determined that the stitch gauge is higher in order to create a higher number of fibre bundles. When comparing the different fabrics (with the same surface density), it is stated that the permeability is reduced with a lower number of stitches. Changes in the shape of the gaps between the fibre bundles can also affect the flow paths during resin infusion. The permeability in the warp direction, direction of the stitch thread, tends to be higher than the permeability in the weft direction due to the creation of channels that allow the resin to flow at a faster rate.

2.3. In-plane shear

2.3.1. Picture frame testing

During the forming process of a textile on a three dimensional tool, local deformations such as changes in fibre directions, the fibre volume fraction and the ply thicknesses occur for the fabric to be able to conform onto the tool's shape. The major deformation mechanism is considered to be in-plane shear where the fibres rotate at the crossover points. Different deformation mechanisms such as shear and ply to ply friction occur during forming and these are shown in figure 15 (mesoscale (inter-yarn shear and cross-over shear) and microscale (transverse shear deformations)). For the in-plane shear behaviour, two types of tests are predominately used: picture frame testing and bias extension test.

Forming of fibre reinforcements is a significant step in the manufacture of composite components where defects such as wrinkles can occur that need to be understood well in order to optimize the fabric's architecture for optimized proccessing. Deformation mechanisms occur during the forming of a composite material. When the fibre reinforcement is formed to obtain the

desired shape/geometry on a tool, mechanisms such as intra-ply shear (the rotation of the tows at their crossovers in the fabric layer) and slip, occur during the process. Moreover, the interaction between the tool and the fabric as well as the forming of the different materials and number of layers in the fabric stack must be taken into account during the design as well as the manufacturing stage. Maximum shear angle is observed when the fibres "lock" and deformations such as bridging, wrinkling and fibre bundling can occur at which point the fabric cannot conform onto the tool's shape/geometry or create severe defects that will cause part rejection during manufacturing.

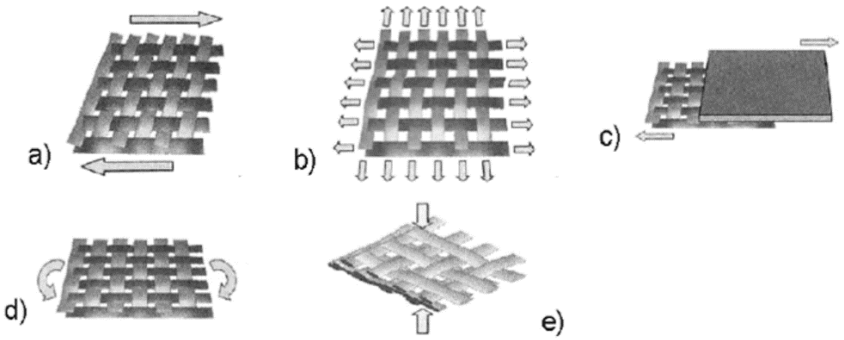


Figure 15 Macroscale deformations: a)shear, b)extension, c)ply-ply friction, d)bending , e)compaction [21]

The two main types of shear testing is picture frame testing and bias extension testing:

Bias extension test:

A tensile test, where a rectangle shaped specimen of a biaxial fabric is tested in the 0^o direction (direction of the stitch line for NCFs) with the warp and weft directions of the fabric at -45^o and $+45^o$ angle of the test. When the fabric specimen is stretched from L to L+d, the motion/rotation of the yarns leads to the deformation of the specimen. There is no deformation in the areas where the yarns have a clamped end. The "active" zone of the test is where the yarns are free to rotate (where the yarns have free ends – middle section of the fabric) [22]. The rotation at the crossover point leads to pure shear deformation. The global stretching of the fabric sample leads to shear strain.

Disadvantages of this method: The deformation area in the sample is non-uniform, with a combination of shear and inter-tow slip in the clamped areas of the fabric sample. Moreover, deformation is measured only by visual methods which can be time consuming and a complicated procedure to obtain accurate results.

Picture frame testing (this method is used for this study):

The picture frame testing is performed for shear testing of the fabric using the method stated in the literature [23]. Picture frame testing results in homogenous deformation of the fabric sample throughout the entire test. The picture frame geometry and sample dimension can be seen in figure 16. Moreover, the shear rate is controlled and the shear angle can be calculated from the displacement of the mechanical testing equipment. The material is clamped within an articulated frame which is subjected to tension within a mechanical testing machine. The specimen is loaded onto the frame and subjected to tension.

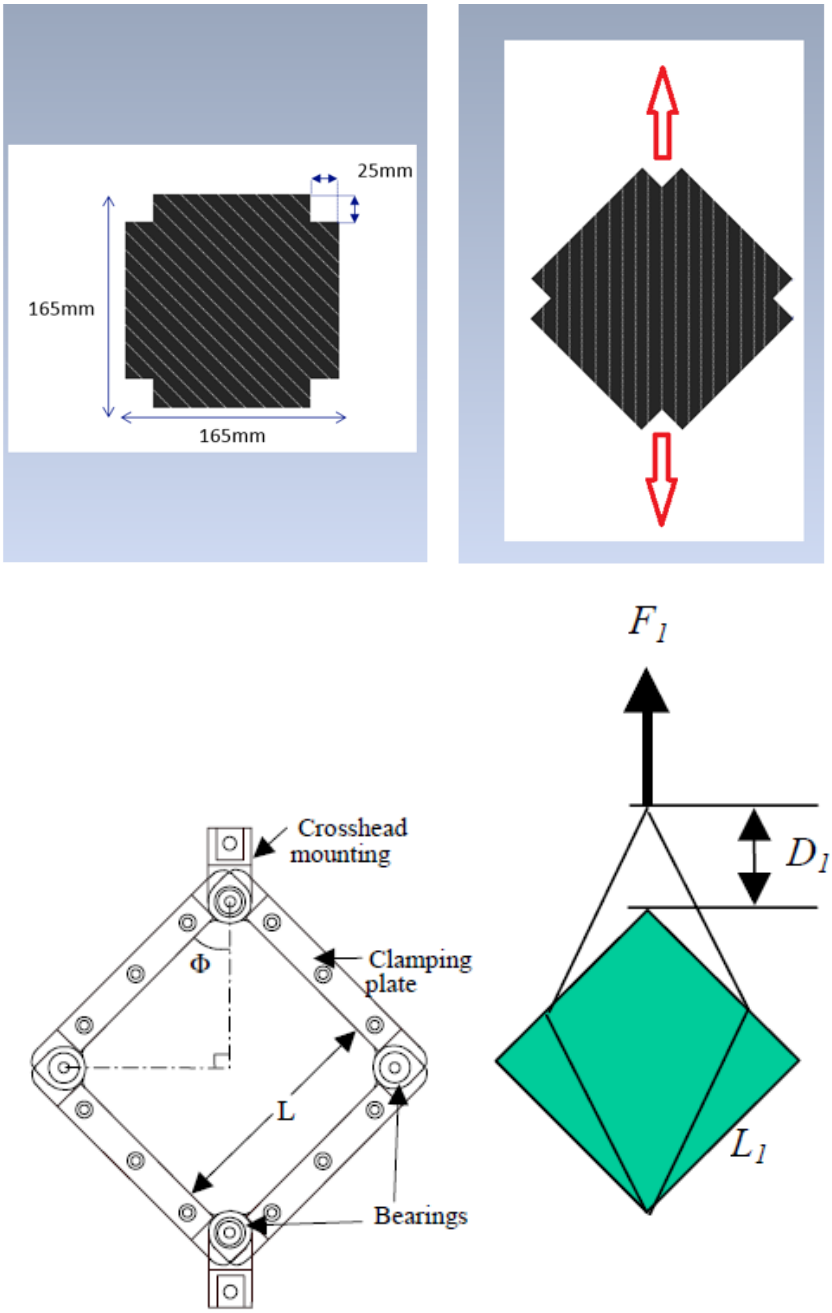


Figure 16 Sample size used in this study for picture frame testing and direction of test and picture frame geometry [23]

The method is intended to indicate the resistance of a material to shear deformation. If fibres are aligned with the tensile direction of the test, the results are typically dominated by the tensile performance of these fibres. The drapeability (how the fabric drapes onto a geometry) of the fabrics is affected mainly by the stitch thread.

During the picture frame testing, three stages can be distinguished:

1. Low shear resistance during the start of the test, where frictional rotation of the tows at the crossover point occurs, where the parallel tows shear (inter-yarn)
2. During the test, the different fibre tows begin to come into contact with each other and lateral yarn compression starts to occur
3. Locking angle: increase in shear, defects such as wrinkling and fibre bundling will occur

For a typical NCF, during the test the load reaches a maximum peak where at that point the stitch starts to break and the load drops rapidly and then rises until the fibres reach the locking angle. In comparison, a woven fabric does not exhibit this behaviour as only the fibres in the two directions shear until they reach the locking angle. As shear loading is applied, the shear angle increases where the gaps between the yarns start to close and lateral compaction occurs. Depending on the architecture of the fabric this usually occurs for shear angles between 20^{o} and 65^{o}. Out-of plane buckling occurs after this stage (onset of wrinkles) [24 - 26].

As the picture frame deforms into a rhomboid during the test, the fabric reinforcement will exhibit pure shear. Moreover, the force that is required to pull the empty frame is measured (no fabric sample mounted) and then subtracted from any subsequent tests in order to produce results occurring only from the fabric sample. The shear angle during the picture frame test is calculated by the displacement of the mechanical testing equipment.

The shear force is calculated by the force that is applied by the mechanical testing equipment and is given by the equation:

$$l = \frac{25.4\,mm}{E} \qquad (3)$$

The shear angle is then calculated by:

$$\gamma = \frac{\pi}{2} - 2\Phi \qquad (4)$$

Where:

F_s: shear force

F: force applied from the mechanical testing equipment

γ: shear angle

Φ: frame angle

The shear angle can be linked with the displacement of the cross-head D:

$$v = \frac{-K}{\mu} \nabla p \quad (5)$$

Where:

L: length between the frame arms

Tests can be used to characterize the drape behaviour of textiles and can be related to the forming of a material. These tests focus mainly on the in-plane characteristics of the fabric reinforcement. The resistance of the fabric during the test can be used to measure the shear resistance of biaxial reinforcements. These tests do not follow a standard, however they have been proved useful. In this study, forming experiments are carried out to examine and determine the effect of the fabric structure on the formed fibre pattern. Other occurrences during the forming process include inter-tow slip which is a significant deformation mechanism when forming structural fabrics to complex geometries where the shear angles can vary significantly [24]. The picture frame test might be sensitive to fibre misalignment. However, it produces uniform shear deformation if carefully performed. Studies show that uniform shear is observed during the picture frame test using surface analysis equipment [27]. Additional comparison studies between the picture frame test and bias extension are discussed extensively in the literature, where the majority of the studies show that the picture frame testing produces more accurately results compared to other tests [28 - 30].

Disadvantages of this method: The forces in the tow directions are not possible to calculate. Ideally, there are no forces acting in the tow directions. If there are tensile forces in the tows, the test will not be accurate. Any pre-tension in the material (in the two tow directions) that can result in changes in the geometry and architecture of the fabric sample are dependant on these forces.

2.3.2. Influence of stitch on shear behaviour

In a benchmark study where different institutes and companies have taken part in order to examine the shear behaviour of a specific woven fabric, showed a significant difference in their results [31]. In figure 17 the results of the picture frame testing are shown. Different picture frame test rigs as well as fabric dimensions were used for the tests (depending on companies/institutes capabilities and set-up). As with the permeability testing, experimental conditions and set-up are two of the major sources of variation. Moreover, some of the institutes used different methods for the calculations such as optical methods to determine the shear angle or to calculate the displacement from the crosshead movement of the mechanical testing equipment. In addition, the effect of the clamping forces needs to be taken account as the fabric sample placement on the rig can affect the accuracy of the results. Shear behaviour of textiles is also discussed extensively in the literature [32 – 38]. It is speculated that a major source in variations is fibre misalignment. This is also addressed in a subsequent chapter, where efforts have been made in order to improve the picture frame test and the accuracy during testing.

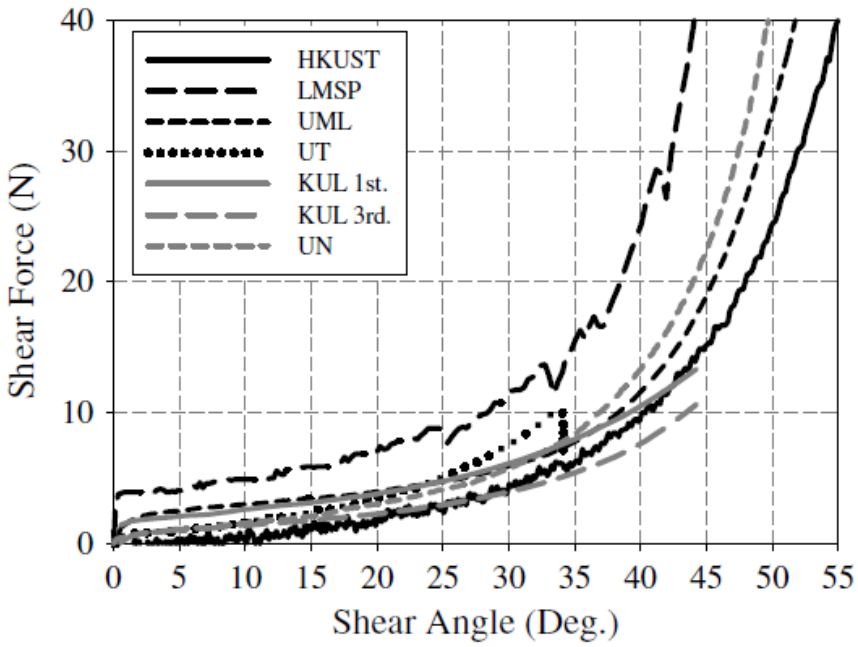


Figure 17 Shear force vs shear angle of a biaxial -45°/+45° ncf - experiment conducted by different companies and institutes showing the different results obtained by them using different process parameters [31]

The locking angle occurs at around 35° angle shear. The locking angle can be used as a characteristic value for describing the level of conformity of a structural fabric to a geometry/tool and a schematic of the process is shown in figure 18 and also in figure 19 where cross-sections from a typical four harness satin weave fabric at different shear angles. Fabric deformation can be distinguished into two categories: Before and after the lock-up stage. Inter-yarn spacing: The larger the gap width between adjacent tows, the movement of the tows becomes greater.

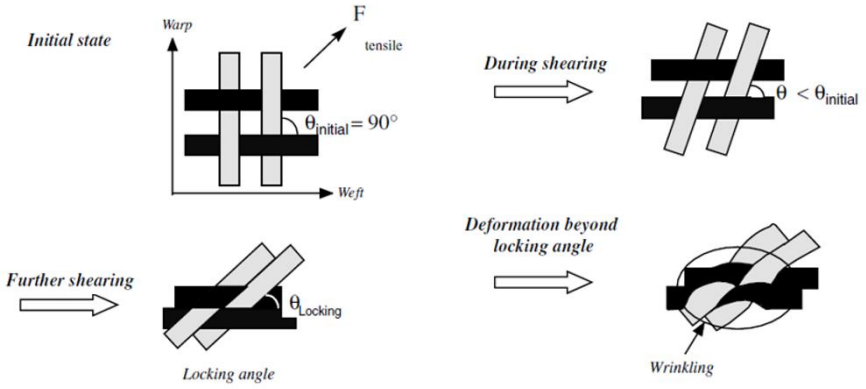


Figure 18 Shear deformation stages of biaxial stitched fabrics [28]

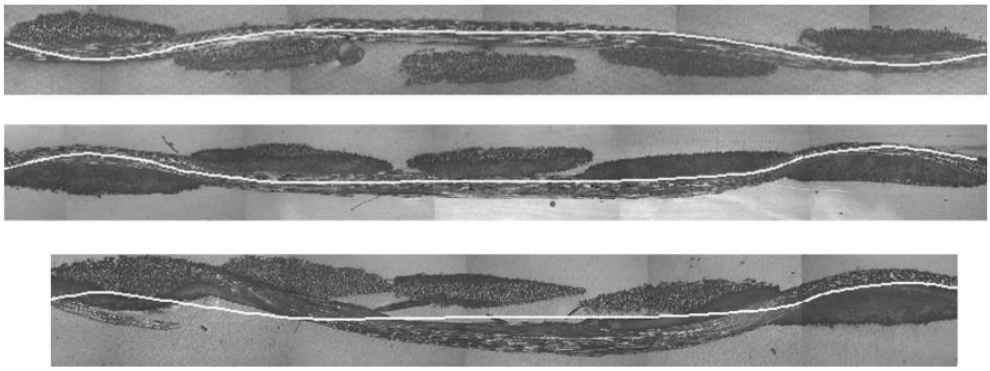


Figure 19 Cross-section through four harness satin weave at shear angles from 0º (top image) to 55º (bottom image) - the line is the assumed tow path [37]

The connection between the stitch thread yarn and the carbon fibre tows can significantly affect the properties of the fabric. Differences in the stitch type of the fabric can cause differences in the shear behaviour (figure 20). Higher stitch thread density will increase the load required to shear the fabric [30]. However, easy shift of tows can create unequal size cells throughout the fabric, which can lead to defects during composite manufacture.

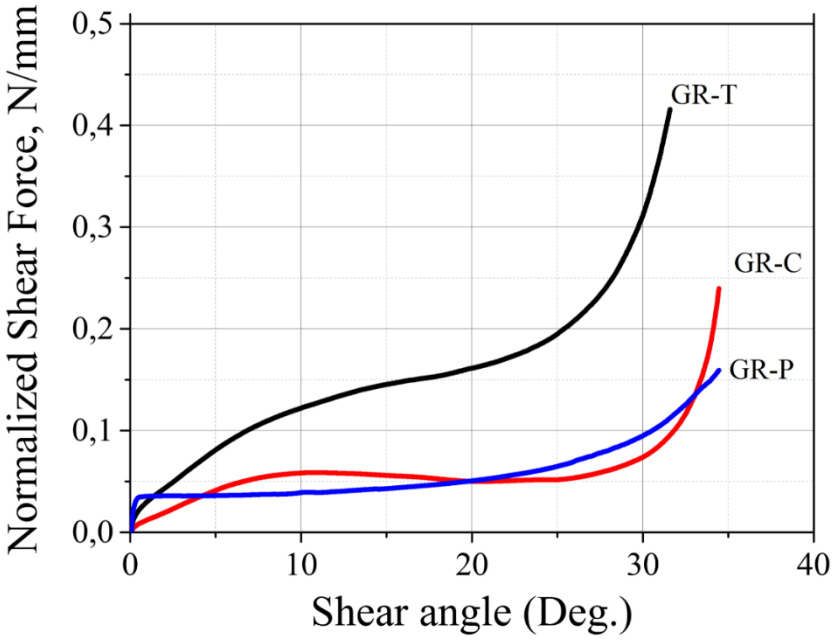


Figure 20 Different shear behaviour of different stitched fabric (GR-T: tricot style, GR-C: cord style, GR-P: pillar style): the higher stitch thread density the higher the shift in the plane of the fabric [33]

2.4. Diaphragm Forming of Fibre Reinforcements

A major step in the composites manufacture for high volume applications is the preforming stage, where the fabric stack (usually with the application of a binder) is preformed to a semisolid state in order to prepare the material for the resin infusion process [39 - 44]. A method for automated production of preforms for high volume applications is the diaphragm forming method. It is a relatively low cost solution for this type of application. The process is shown in figure 21. The rig consists of the top and bottom frame where diaphragms/membranes are mounted. The fabric stack is placed between the frames and the set-up is formed onto a tool's surface. This process is called double diaphragm forming.

The concept of the diaphragm process originated from the processing of thermoplastic composites, it is agreed that it is a process that can create high quality and parts with double curvatures and complex geometries. However, depending of the laminate set-up problems that car arise from the diaphragm forming process include fibre wrinkling and fibre bridging, out-of plane fibre buckling, as well as unwanted thickness variation. More severe out of this issue if fibre buckling, and early detection of these issues is needed before progressing to subsequent manufacturing process stages.

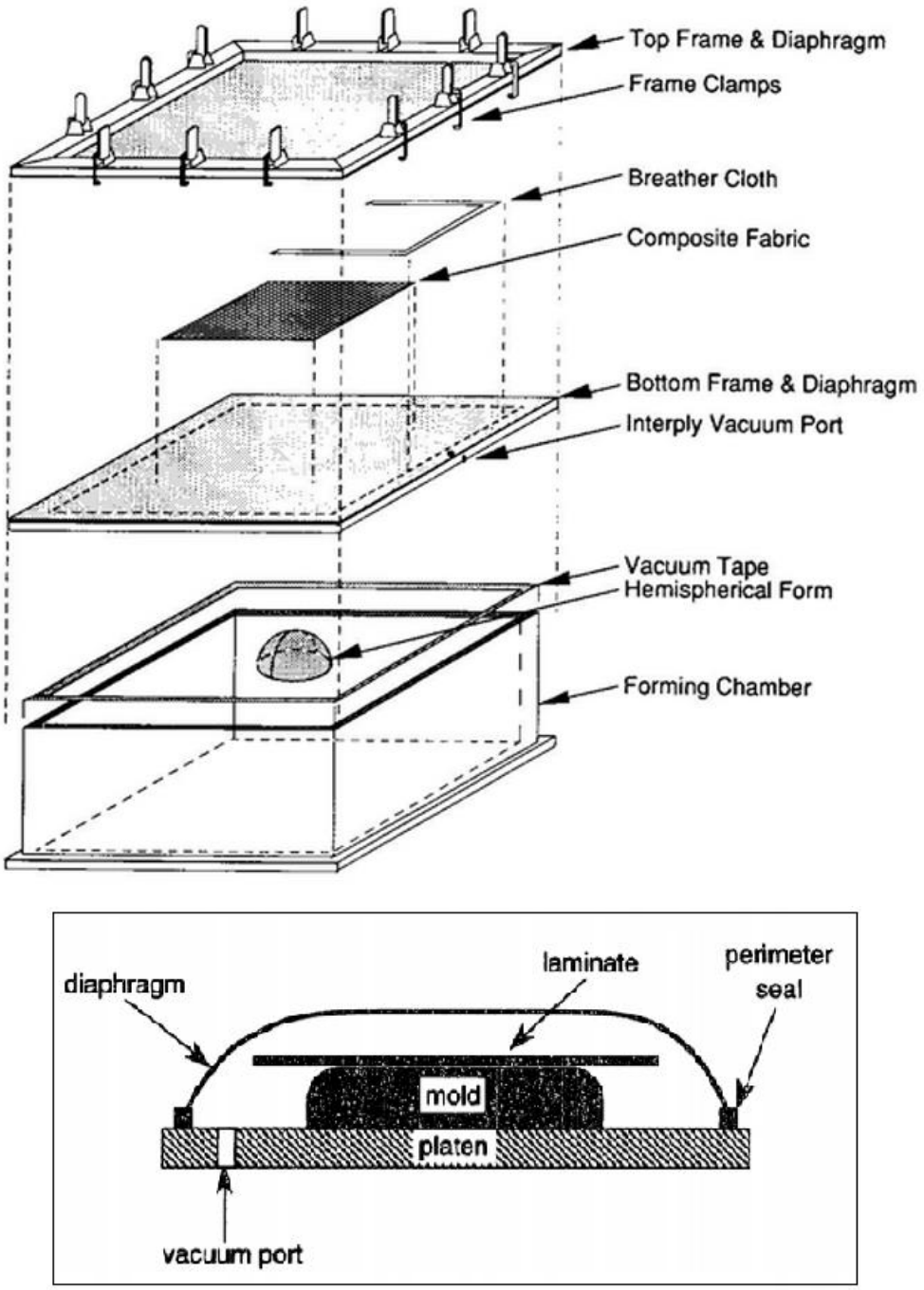


Figure 21 Diaphragm forming process (double diaphragm process) [39]

The laminate is placed between two diaphragms, where these are clamped onto a mould. Vacuum is applied between the two diaphragms and the tool. The set-up is usually placed in an autoclave and heated to the process temperature. After a specific process temperature is reached, a hydrostatic pressure difference is created [39]. This pressure force the diaphragms on the tools

surface. With this process, high quality can be realised. This process usually takes between one and two hours.

When a laminate is deformed on a three dimensional part, that might have double curvatures, in order to offset the compressive stress caused by the deformation, the application of tension is required [42]. However, because of the nature of the carbon fibres (inextensible), the fabric stack cannot be clamped around the edges during the pre-forming process. The diaphragm forming process allows for the application of tension to the stack, confining between two deformable membranes whose edges are clamped on a rig. Moreover, relative slippage between the fabric stack and the diaphragms is created.

Different types of membranes exist, ranging from low to high stiffness and low to high elongation. However, low stiffness membranes can cause thickness variation during forming as well as resulting in weaker applied tension causing failure modes such as fibre buckling and fibre wrinkling. The problem can be accentuated when is the tool is of high complexity and has areas with double curvature. Problematic parts resulting from the process are then discarded, causing delays in the overall manufacturing process.

In single diaphragm forming, a single membrane is sealed around the mould and the fabric stack and air is evacuated from the bag. The membranes stretches in onto the mould geometry and at the same time pressure onto the fabric's surface. The fabric stack and mould are brought to the desired temperature. The single diaphragm is highly operator dependant process but if done correctly can have the same high quality results as the diaphragm forming process.

The forming step is crucial to the success of the manufacture of the component. Parameters that have to be taken into account and influence the forming process are: the contact between the tool and the membrane, the deformation mechanisms such as intraply and interply slip and the contact between the membrane and the fabric.

Types of membranes

-Polymer diaphragms

-Polyimide films for high temperatures: The main drawback, apart from the high costs, is that they remain plastically deformed after one production cycle

-Silicone rubber diaphragms: much more expensive, but can be re-used many times which reduces costs in the long term. This makes them suitable for manufacturing smaller preforms at higher manufacturing rates

Two are the main types of diaphragm forming: single diaphragm forming and double diaphragm forming:

In the single diaphragm forming the fabric stack is placed on the surface of the tool and with the use of one membrane, and vacuum drawn from the setup, the preform is manufactured. It is a faster process than the double diaphragm forming and it used mostly for simple shapes. However, it is a highly operator dependant process where the risk of fibre layer misalignment is a risk to consider. In the double diaphragm forming the fabric stack is placed between two membranes and the process is similar to the single diaphragm process with the advantage of having the fibre layer stack is completed flat, thus reducing the risk for fibre misalignment. Complex shapes are possible with this process, however the costs associated with the procedure are higher for limited production components. Producing a higher number of parts, the cost can be lowered as the production cycle is decreased due to the automated set-up of the process.

2.5. Scrim-based fibre reinforcement architectures

To the knowledge of the author, no research has been performed on the development of scrim materials and their effects on permeability and formability and specifically no previous work on comparing different scrim architectures in terms of permeability and drapeability and their influence on a fibre reinforcement apart from a study stating that a significant influence on permeability of the reinforcement with the scrim when using the LCM process exists [45]. Also, most research focuses is on woven fabrics or non-crimp

stitched fabrics, and how to optimize their structures for permeability as these materials occupy the majority of the production for composites manufacture [46]. Moreover, a published conference paper states that the scrim can increase permeability of the fabric by up to 300%, however no information or analysis is included [47]. It has to be noted that to the knowledge of the author no other fibre reinforcement fabric manufacturing company is using any other type of scrim other than the $-30^{o}/0^{o}/+30^{o}$ 7gsm polyester fibre type construction. Moreover, this type of fabric is mostly used in low production volumes as the materials is expensive compared to other types of support structures.

3. Experimental Methodology

3.1. Materials Characterization

3.1.1. Permeability

The permeability values were calculated using the Hexcel Leicester in-house permeability measurement rig (figure 22). Figure 23 shows the location of the pressure sensors. The rig comprises of sensors that detect the arrival time of the flow front of a fluid (low viscosity oil – Silmid Xiameter 200 100cs used in this study) in a fabric stack, with calculations based on Darcy's Law. Data acquisition software (Labview) produces the permeability values in the two directions as well as the fibre volume fraction and the angle of flow. The permeability in the 2 directions (K_1 and K_2: unsaturated in-plane permeability) is determined by determining the function of the flow front ellipse as a function of time.

The Radial injection at constant pressure of liquids in planar porous media has been extensively discussed [48-53]. Permeability for an isotropic material can be obtained by the equation:

$$K = \frac{\Phi \mu {R_o}^2}{4\Delta P t}\left(\left(\frac{R}{R_o}\right)^2\left(2ln\left(\frac{R}{R_o}\right)-1\right)+1\right) \qquad (6)$$

Where

t: time of the flow front to reach the radial position

R: radial position

R_o: radius of the circular injection

ΔP: pressure difference between the injection and the vent

μ: viscosity of the resin

ϕ: porosity of the fibre reinforcement stack

K: permeability

The permeability rig consists of two horizontally oriented aluminium plates. The thickness of each plate is 25mm. The fabric samples are placed on the bottom plate during the experiments, and when the plates are closed, the cavity height between the plates is adjusted by inserting shims (depending on the target fibre volume fraction their thickness will change). The fabric samples are homogeneously compacted after the tool is closed. The shims are flat, always ensuring that the plates stay parallel to each other. A circular injection gate exists on the bottom plate, where the oil is injected. For all fabric layers, the same size hole is stamped at their centre. The pressure is set at 2 bar for all experimental trials.

Along the edge of the specimens, a channel inside the bottom plate is engraved in order to vent the tool and obtain a constant pressure boundary condition. A threshold of 0.05×10^5 Pa triggers the pressure sensors and any recorded data below this value are discarded as noise. The flow front arrival times are measured in the sensors at different distances between the central positioned sensor. The software run is completed when all seven sensors are triggered.



Figure 22 Permeability measurement rig at Hexcel Leicester

During handling and subsequent processing of non-crimp fabrics, for example cutting the required shapes and then placing them in a tool for composite manufacture, low stability NCFs tend to result in the carbon tows changing their position within the fabric. Low stability for an NCF, during fabric manufacture, denotes the weft stability and is mainly affected by the stitch thread parameters as well as any additional support threads along the edge of the fabric. The inter-yarn gaps will change from parallel to random and this can affect the permeability of the fabric. Thus the preparation and handling of the samples/specimens is crucial to the results of the tests.

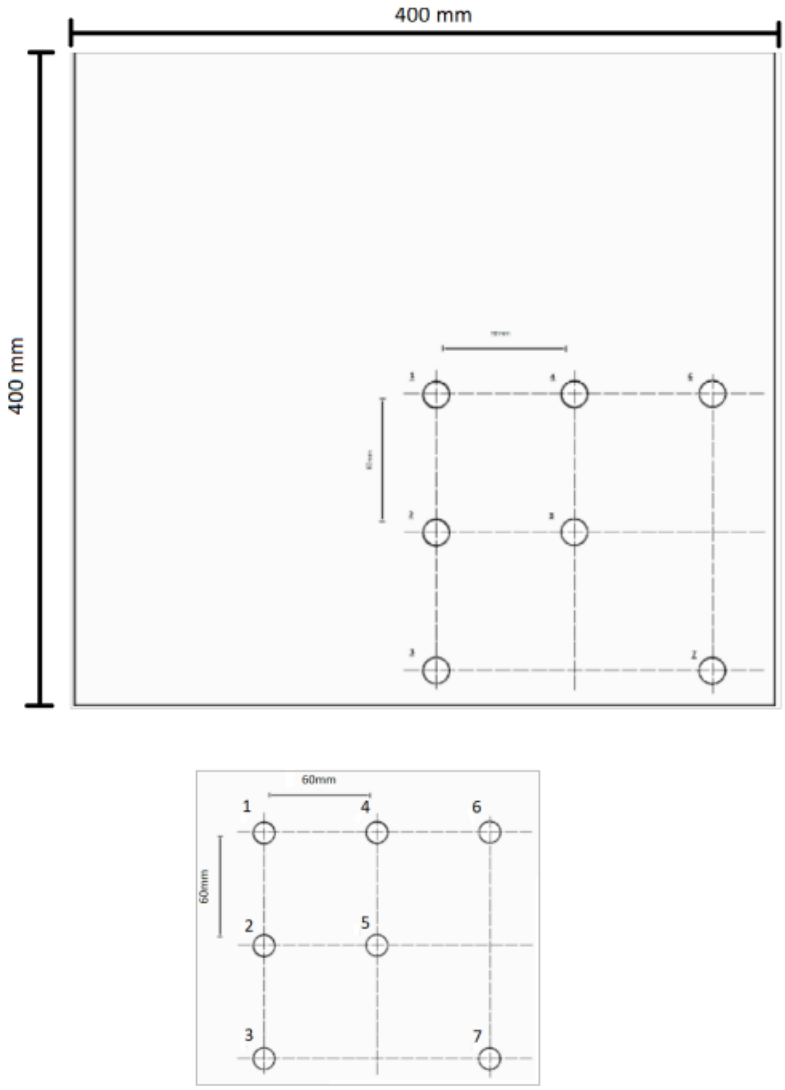


Figure 23: Dimensions of permeability measurement plates and location of pressure sensors

The input parameters are:

- Density of fibre
- Fluid viscosity
- Number of fabric layers
- Weight of fabric layer stack
- Cavity height

Scatter of values – possible causes from material aspect:

- Deformation (shearing and creation of gaps as the fibres are pulled) of the fabric during handling (prior to cutting and placement of the fabric stack in the tool)
- Correct angle placement of each layer in the stack: every fabric layer should be placed at the same orientation with the one below it: any angle deviation will affect the flow front and consequently affect the K_1 and K_2 permeability values
- Nesting of the fibre filaments during stacking (and subsequent nesting during stacking and compaction in the mould) of the fabric/tows. Nesting will result in different thicknesses in different areas of the fabric stack. This will can ultimately cause layers and tows to shift during the trials thus creating channels with different sizes and at different locations and orientations where the oil/resin flows.
- Loose fibres, broken stitches and defects in the fabric layers can affect permeability: the fabric should be cleaned thoroughly prior to placement in the tool

3.1.2. In-plane Shear

It was observed during testing (early trials performed with several stitched fabrics) that the existing rig used for characterizing the shear behaviour of biaxial non-crimp fabrics did not produce consistent results. This also can be seen in different studies, where a large scatter of values exist in most cases. A decision was made to improve the fixture by redesign it and implementing changes that could produce more consistent and accurate results before performing any additional tests. Fibre misalignment can cause progressive extension or compression onto the fibres which can result in fibre tension or wrinkling. Without any measures to prevent that, it would lead to inaccuracies during materials characterization. The new rig can be seen in figure 24 and figure 25.

Requirements;

1. A more accurate method of placing the fabric sample to avoid fibre misalignment
2. A more accurate method of placing the fabric sample and avoid any "slack" or distortions in the fabric
3. A different clamping method to reduce the procedure time
4. To redesign fabric sample positioning set-up so that the centreline of the mechanical test equipment passes through the centreline of the sample as the previous version of the rig had an offset (8mm) where metal on metal contact and bending could give false readings. Although this would be considered a negligible influence to the results, since the load required to shear the fabric is low, this has to be taken into consideration for improving the rig
5. Use of bearings in place of the screws to improve quality of rig and eliminate any sources of variation

The main sources of possible imperfections in the existing picture frame testing fixture arise from sample position and orientation, where these are mainly operator, and therefore highly susceptible to error, dependant. Even with small deviation from missallignment will contaminate the results from the testing significantly. The new picture frame rig aims to eliminate these inconsistencies by incorporating a design where the sample mounting operation is exempt from human interaction.

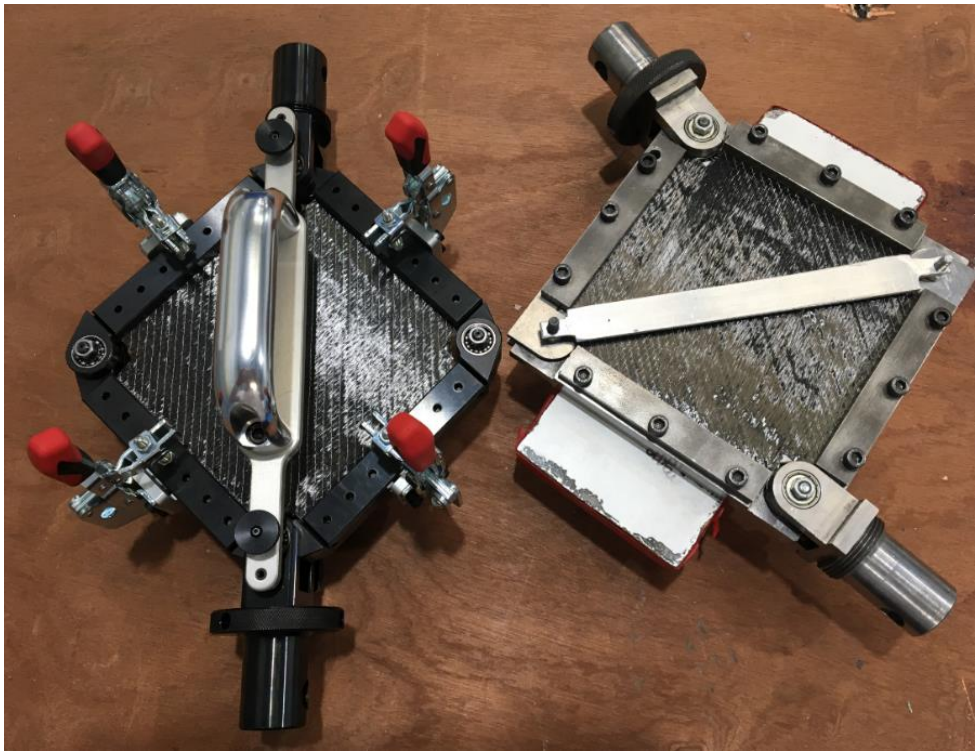


Figure 24 New picture frame rig (left) and previous iteration (right)

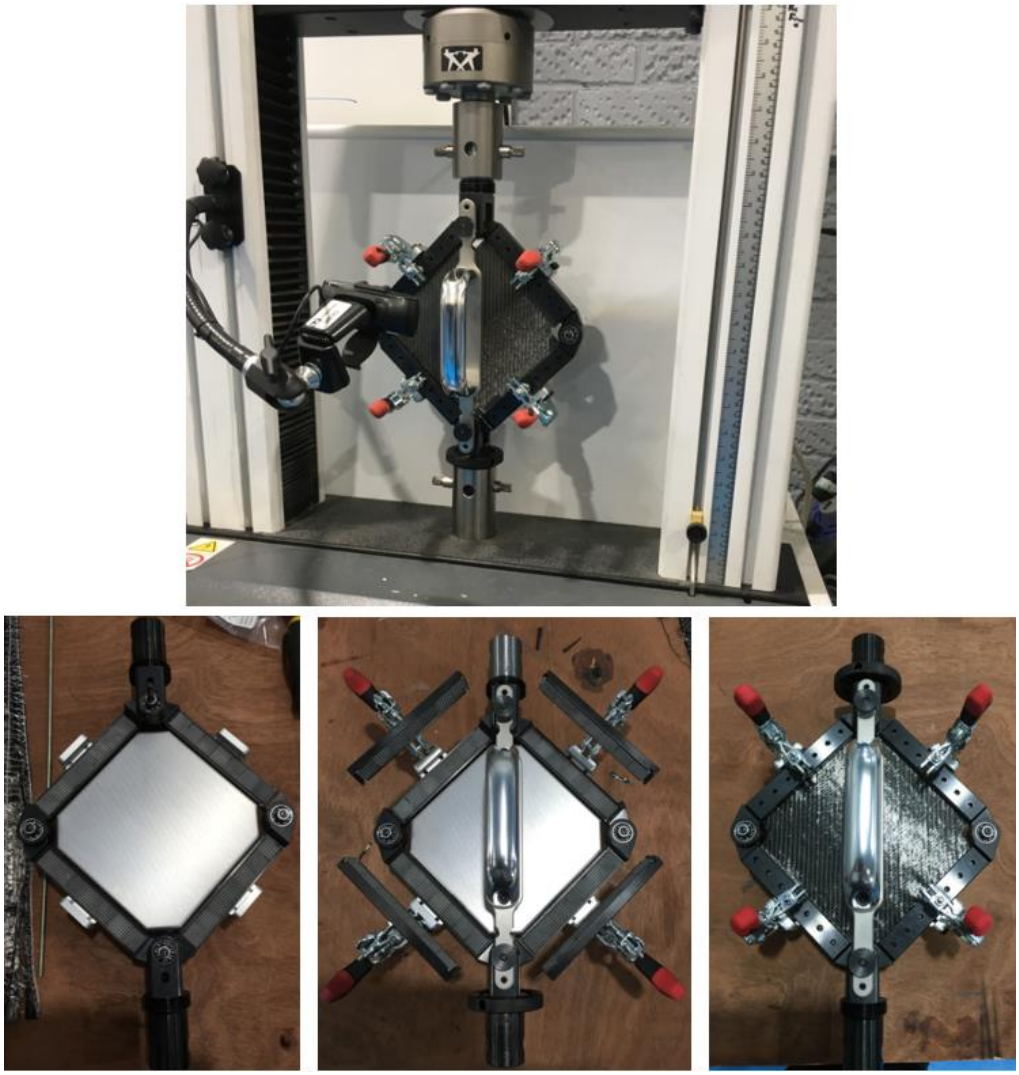


Figure 25 New picture frame rig (mounted on mechanical test equipment – top row) and overview when placing the fabric sample (bottom row)

Improvements;

1. The bars in the frame have recess so that the fabric sample can be mounted so that to minimize any angle deviation (figure 26). The bars have recess so that the fabric sample can be mounted without any angle deviation. Slots were incorporate into the design so that the fabric "falls" into place and can't move (so as to not have any angle deviation).

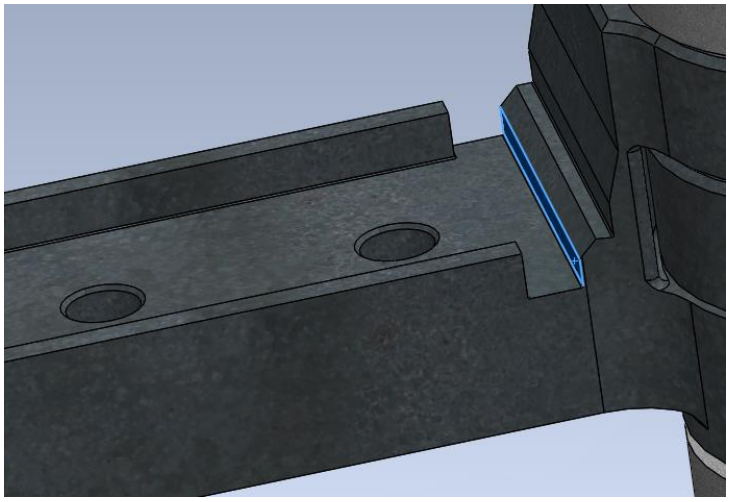


Figure 26 Recesses in the new picture frame rig design

2. Placement of sample:

   An aluminium base was manufactured (figure 27) to place and secure the sample flat without any distortions and any resulting “slack”

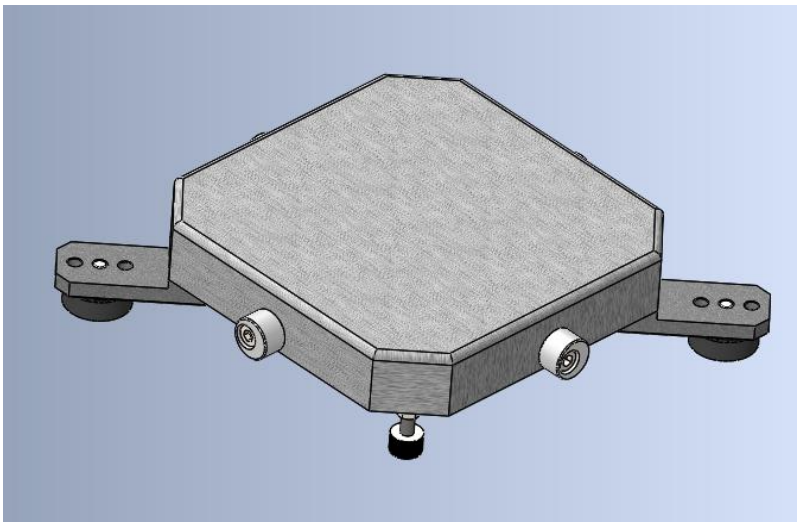


Figure 27 Aluminium base for supporting the fabric sample

3. Use of clamps (figure 28) in order to avoid the use of screws: 12 screws had to be secured in place for each trial when using the old picture frame rig



Figure 28 Clamps/grips on picturef frame rig

4. Centreline (figure 29):
   In the previous iteration of the picture frame rig used, the centreline of the mechanical testing equipment did not pass through the centreline of the fabric sample and the frame. This lead to higher load / friction (metal on metal contact) and bending of the frames to result in inaccurate data (figure 30). In the original picture frame design the fabric sample was placed at an offset of 8 mm.

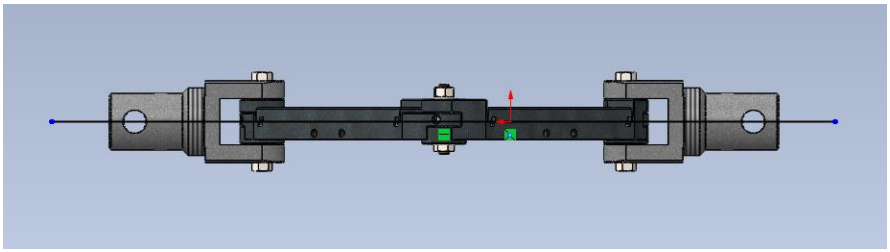


Figure 29 Centreline location in the new picture frame rig

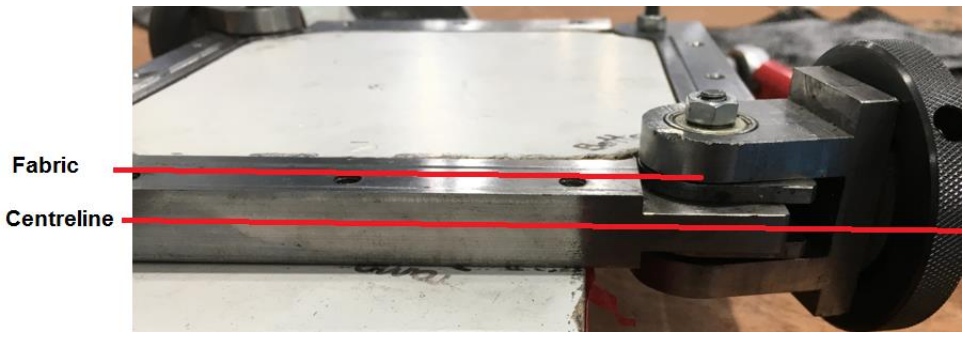


Figure 30 Centreline location in the old picture frame rig

No fabric slack is observed in the new frame; this can be seen from the graphs when compared with the old frame where in the old frame some small drops in the load can be seen. Moreover, the same gradient/slope is observed for all experimental trials. In the previous rig iteration, although it could be argued that the mean from the trials could potentially be used, due to the samples curves not being the same this could not be achieved. The new picture frame rig in operation can be seen in figure 31.

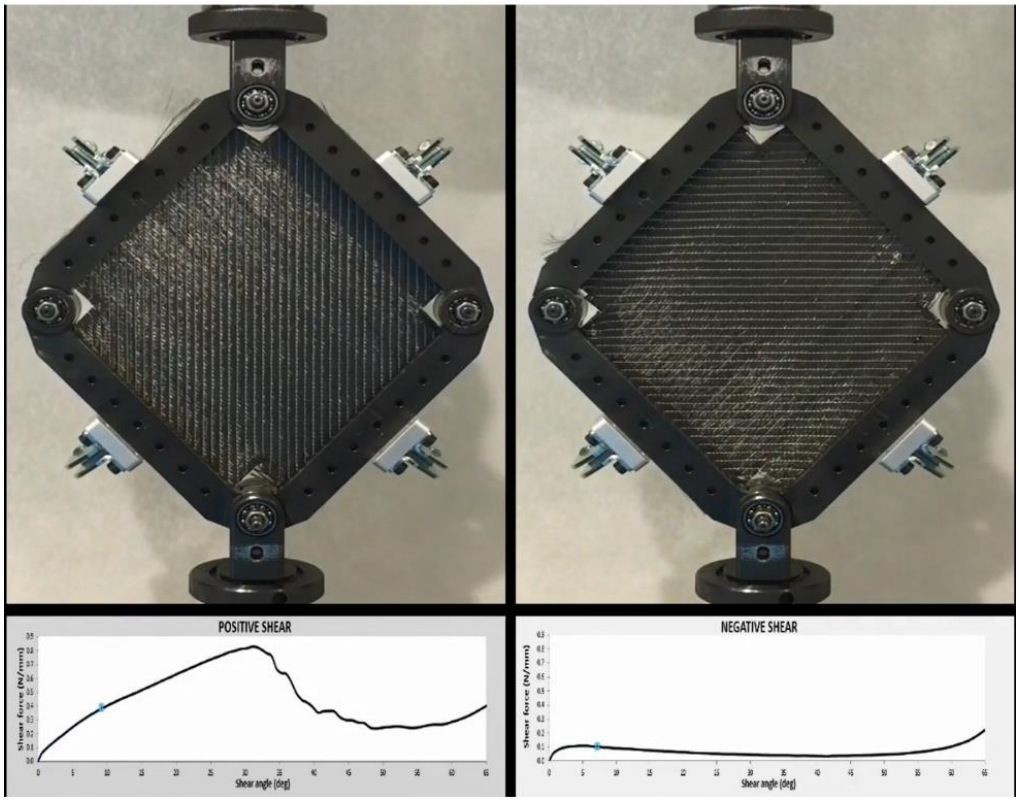


Figure 31 New picture frame design during testing (positive shear – left, and negative shear – right)

No fabric slack is observed in the new frame during testing. This can be seen from the graphs (figures 32 and figure 33) when compared with the old frame where in the old frame the load is very low. The fabric was a 440gsm -45º/+45º biaxial carbon fibre fabric. Moreover, the results are more consistent with the new frame. In addition, the gradient is similar during sample run testing for all samples for the new frame as well as the time required for the tests (compared when using the old picture frame) is significantly reduced (no

need for screws fastening, faster sample placement, safer rig placement on the Instron with the use of an incorporated handle into the design).

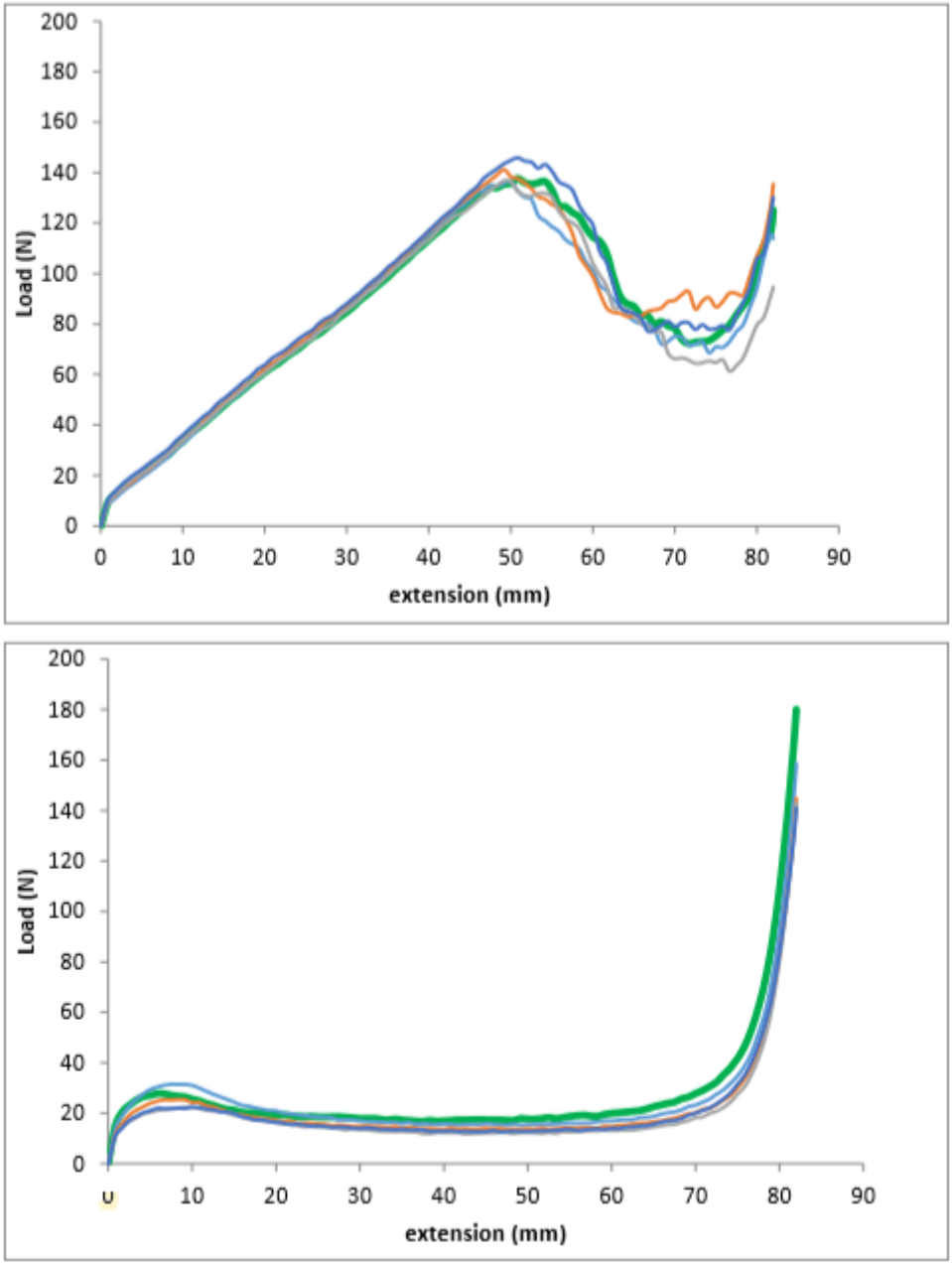


Figure 32: Load vs extension of fabrics during testing using the new frame (top graph: stitch thread direction parallel to direction of test, bottom image: stitch thread direction perpendicular to direction of test)

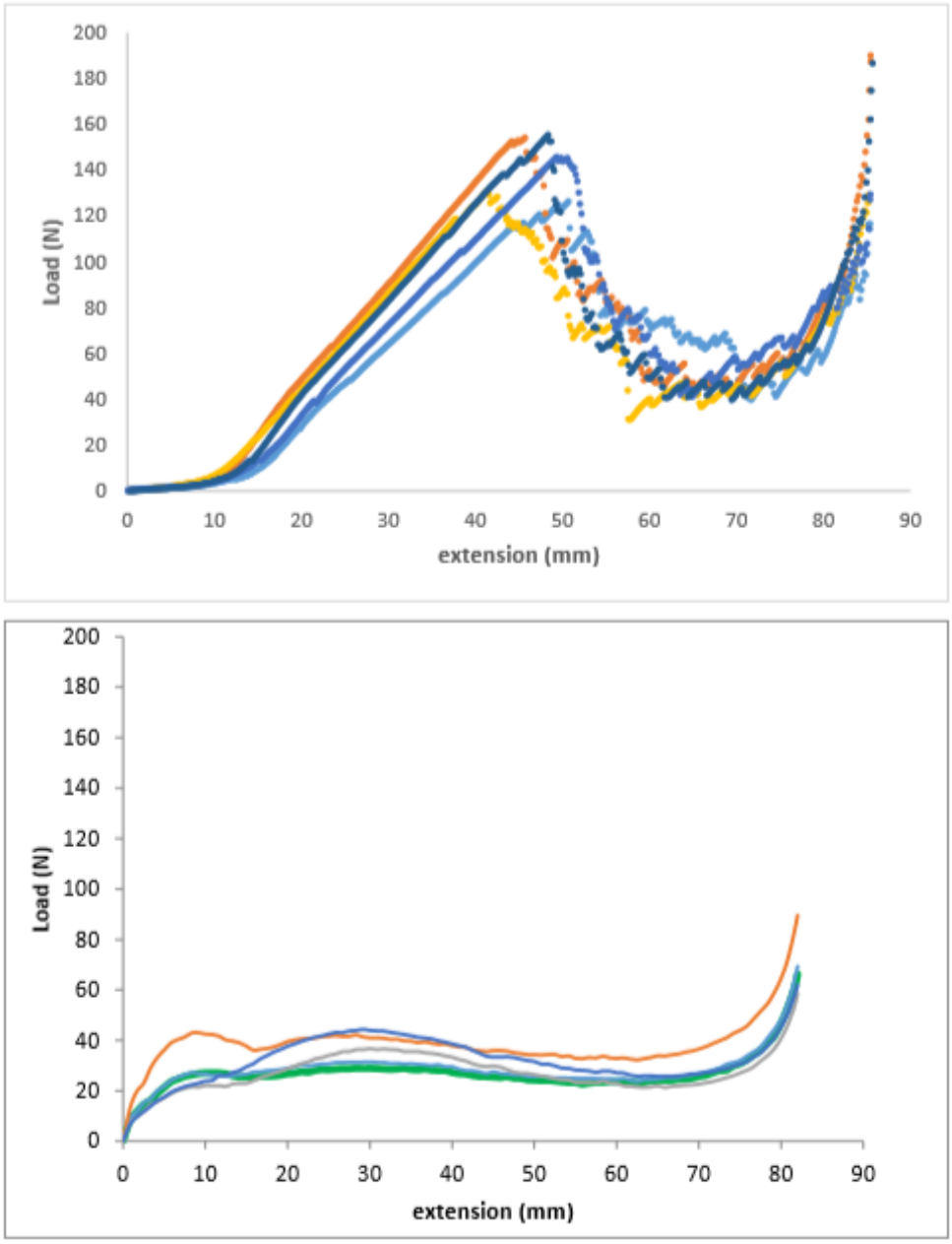


Figure 33: Load vs extension of fabrics during testing using the old frame (top graph: stitch thread direction parallel to direction of test, bottom image: stitch thread direction perpendicular to direction of test)

3.2. Forming

During the forming process, deformable membranes (diaphragms) are heated (with the fabric stack on top if single and sandwiched between 2 membranes for double diaphragm forming) and formed on a tool. Vacuum drawn beneath the membranes forms the desired shape. The membranes are clamped on the edges of a 1sqm aluminium frame, where only the fabric stack can slide within the membranes. The tool selected for the forming trials is a bespoke tool made for the specific trials (figure 34). Complex enough, with double curvatures, to characterize the materials.

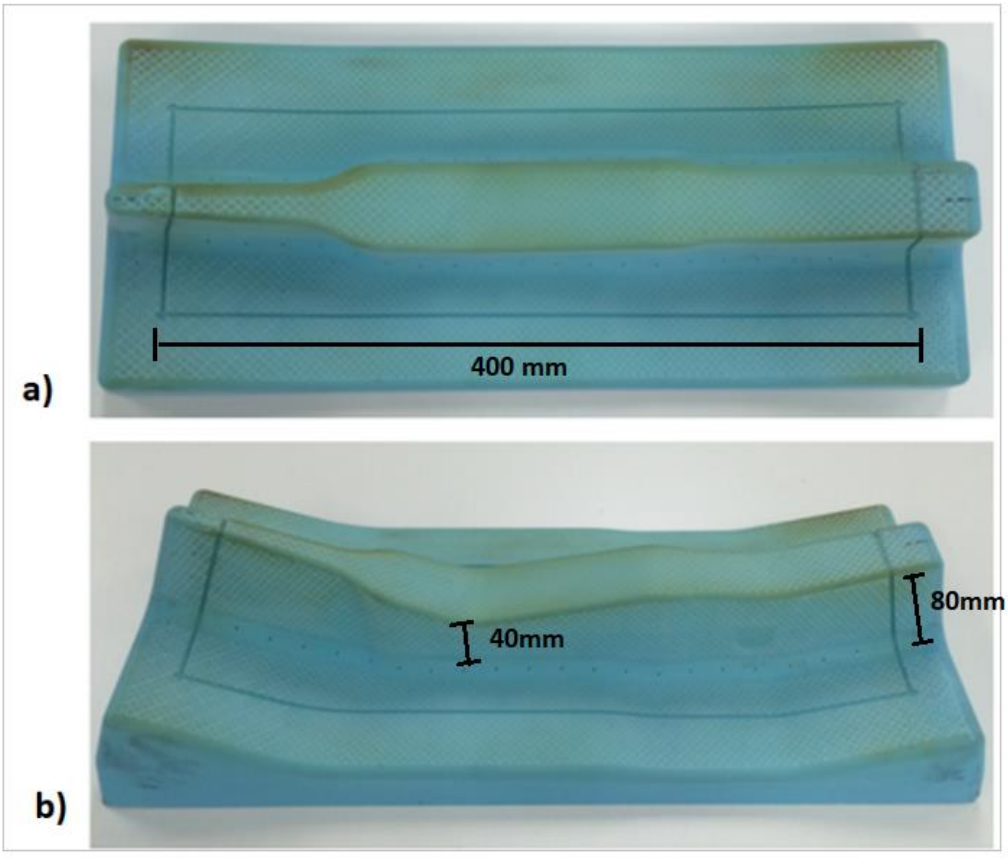


Figure 34 Forming tool: a)top view, b)side view

During forming, as the membranes stretch they consequently suppress defects occurring such as wrinkling. The membranes can withstand the processing temperatures and deformation during forming. During deformation of the plies the membranes accommodate most of the deformation of the materials. For all experimental trials, single diaphragm forming method was used. A co-polymer membrane (Airtech MR1) was used, with a thickness of 25 microns. Although the membrane is usually used as a release film, the high elongation of the membrane was deemed suitable for the trials. The fabric is heated between 150^{o}C and 200^{o}C in order to melt the epoxy powder that will result in the manufacture of the preform. A dwell time of 5 minutes allows for full consolidation of the epoxy powder and the preform is then removed from the tool. All the membranes that were trialled before choosing the airtech MR1 are listed in table 1 [54 – 62]. Most of the membranes were used during early trials, however for all trials listed in this study the MR1 was used.

Company	Product	Material Type	Thickness	Elongation at break
			µm	%
Tygavac	Stretchlon 700	Thermoplastic elastomer	75	500
Tygavac	Stretchlon 350	Thermoplastic elastomer	75	550
Tygavac	Stretchlon 200	Thermoplastic elastomer	35	500
Tygavac	WL7400	Nylon	50	375
Tygavac	Thermalimide E	Polyimide	50	85
Fenner precision	Fenform 50	Silicone (uncured)	N/A	600
Ube	Upilex 50RN (Ube)	Polyimide	50	136
Upilex	Upilex 25S	Polyimide	25	42
Upilex	Upilex 50S	Polyimide	50	50
Upilex	Upilex R	Polyimide	50	42
J-flex	VAC-SIL PRO	High elongation silicone sheet	300	700
Mosites	Mosites 1453	silicone rubber	150	650
Cytek	Vacfilm430	co-polymer	50	640
Cytek	Stretchvac350	co-polymer	75	800
Airtech	MR1	co-polymer	25	400
Airtech	MR2	co-polymer	50	400
Steinbach	Silicone GP60T - Shore 60	Silicone	500	280

Table 1 List of trialled membranes and their properties/attributes

The forming of the preforms (figure 35) the heating set-up (figure 36) an example of when a preform is removed from the tool (figure 37) are illustrated in the following pages.

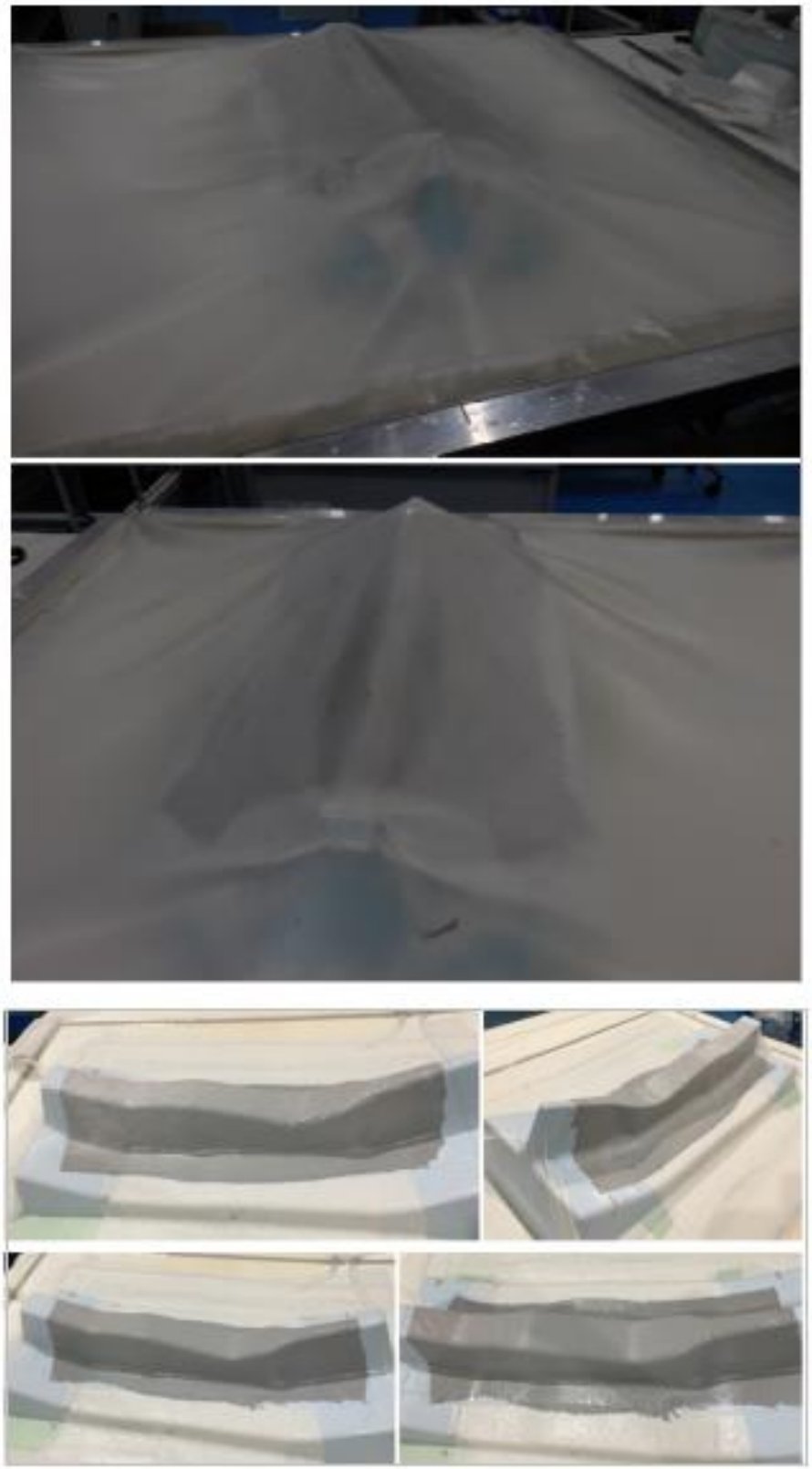


Figure 35: Forming of preforms

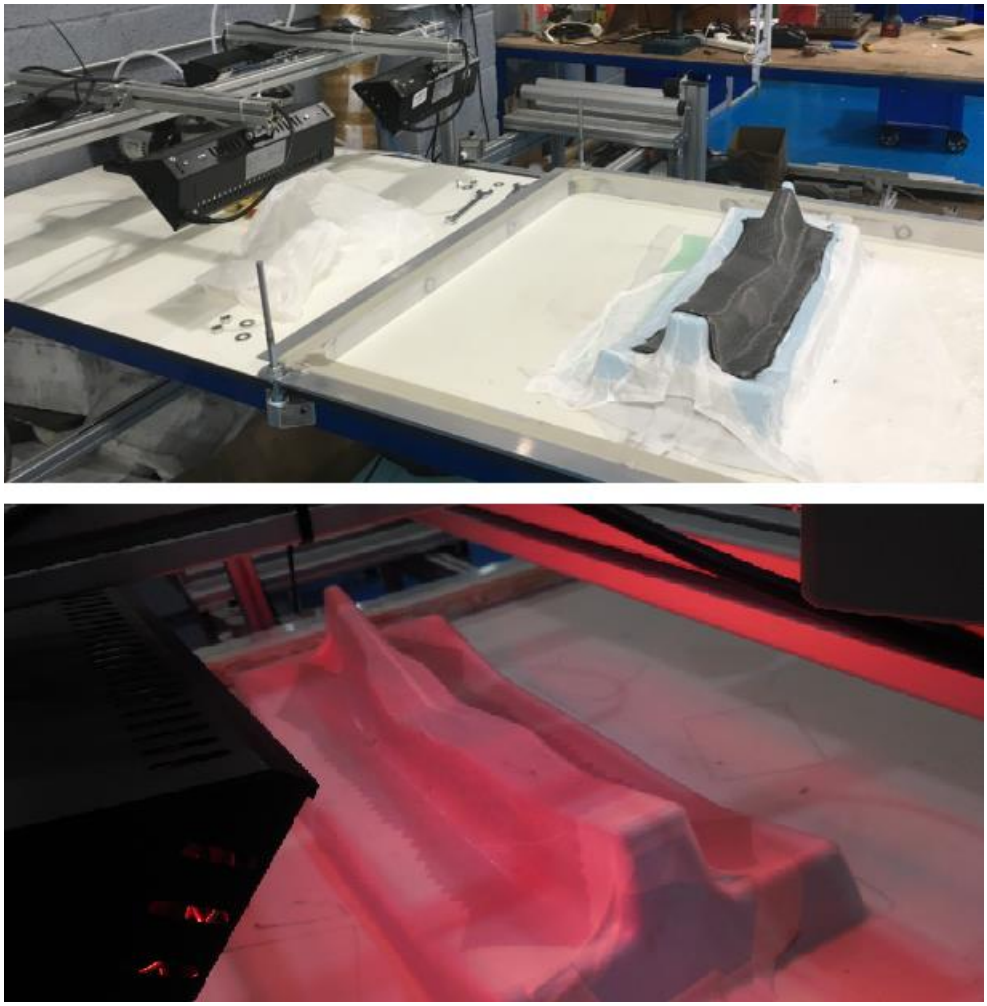


Figure 36: Heating set-up with Infra red lamps (rig above tool/preform)

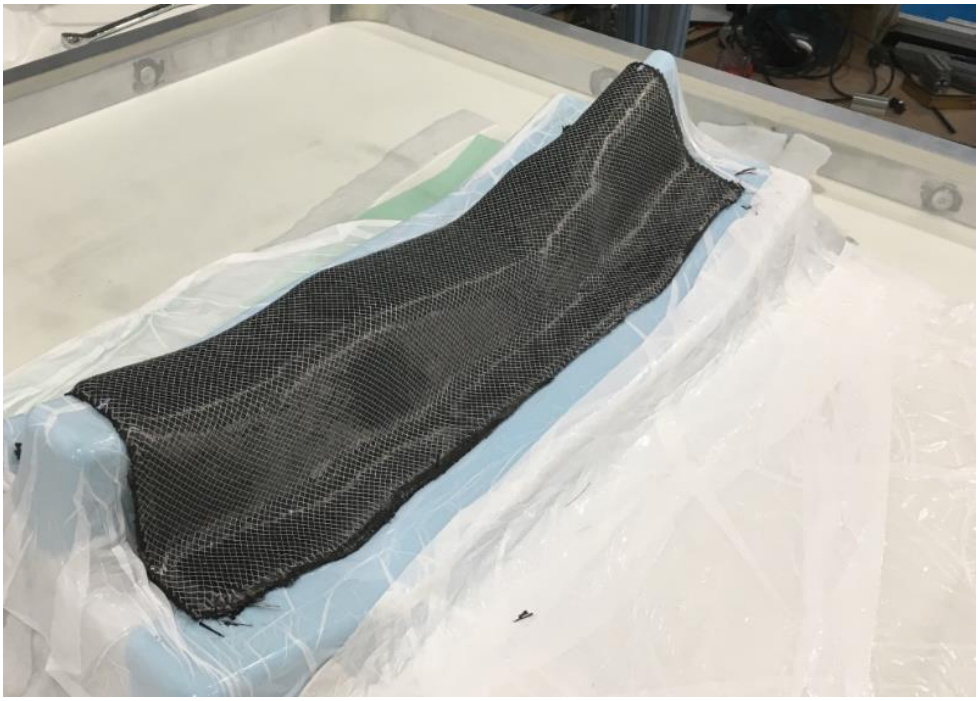


Figure 37: Removal of the preform from the tool

4. Effects of Stitch Tension on the Processing Parameters of Non-Crimp Fabrics

4.1. Unidirectional Non-Crimp Fabrics

Three different stitch tension values were selected in order to manufacture three types of carbon fibre fabrics. Figure 38 shows an image of the NCF fabric and figure 39 the notations of the parameters in the fabric. In this work, the permeability of carbon fibre non-crimp (NCF) fabrics is measured, aiming at studying the effect of varying the stitch thread tension on the fabric architecture and examining the effect on the fabric permeability.

The NCFs studied here comprise of unidirectional carbon fibre bundles (50 K), which are aligned in the warp direction, Zoltek Panex 35 [63]. On both faces of the fabric, glass fibre support threads (68 tex) are added in the weft direction at a spacing of 5.6 mm on both sides of the fabric. The support threads are attached to the carbon fibre bundles using a polyester stitch thread which alternates with the carbon fibre bundles (in the warp direction). The stitch type is pillar. Three different stitch tension values were selected for the manufacture of carbon fibre fabrics. Variations in the internal structure of the fabric such as the stitch material, stitch length distance between the stitches and stitch pattern can affect the permeability of the fibre reinforcement.

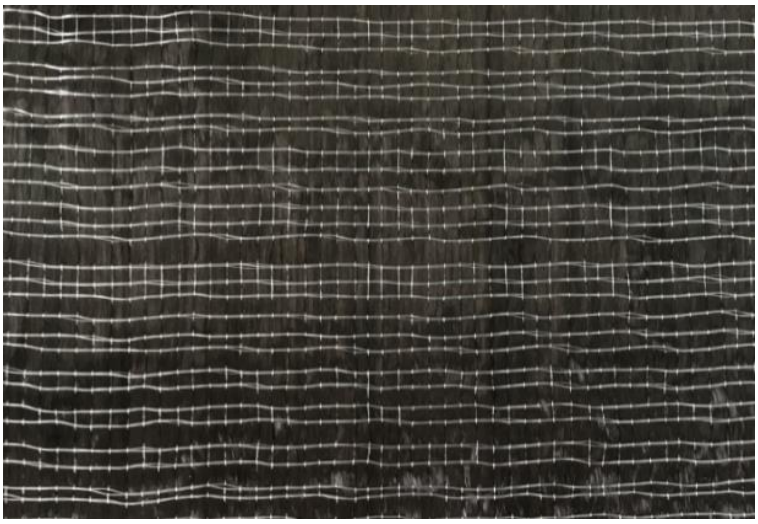


Figure 38 Overview of fabric

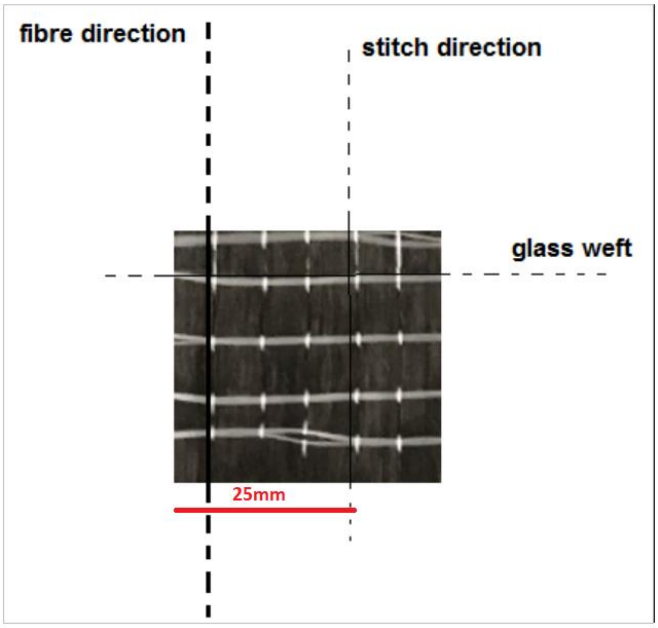


Figure 39 Stitch architecture in the fabric

The fabric architecture is illustrated in figure 40. During manufacture of the fabrics, the tension in the stitch threads can be set. Here, three fabrics with different values of the stitch thread tension were manufactured to experimentally study the effect of the stitch tension on the fabric properties. The material parameters are listed in tables 2 and 3.

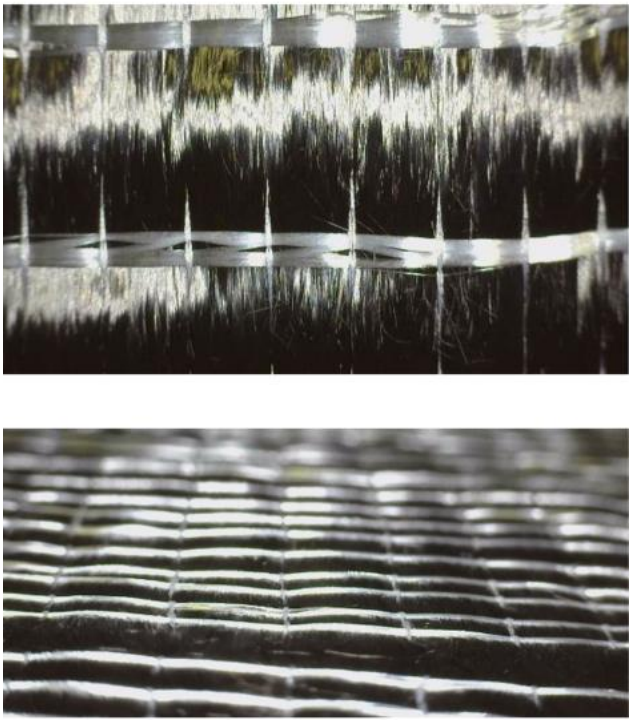


Figure 40 Overview of the fabric: top surface of the fabric shown at a 30° angle to emphasize the stitch and weft thread geometry

Set	Fibre type	Stitch material	Stitch type	Stitch gauge (number of stitches per 25.4mm)	Stitch length (mm)	Stitch tension (cN)
1	Zoltek Panex 35	Polyester	Pillar	5	3	14.6
2	Zoltek Panex 35	Polyester	Pillar	5	3	12.4
3	Zoltek Panex 35	Polyester	Pillar	5	3	10.2

Table 2 Stitch parameters

Three different stitch tension values were selected to manufacture three types of carbon fibre fabrics. Due to the production set-up conditions, the total width of the roll was 2000mm, divided into 4 500mm rolls. L1 and L2 are the left located fabric during production, R1 and R2 are located at the right of the machine during roll on cardboard tubes.

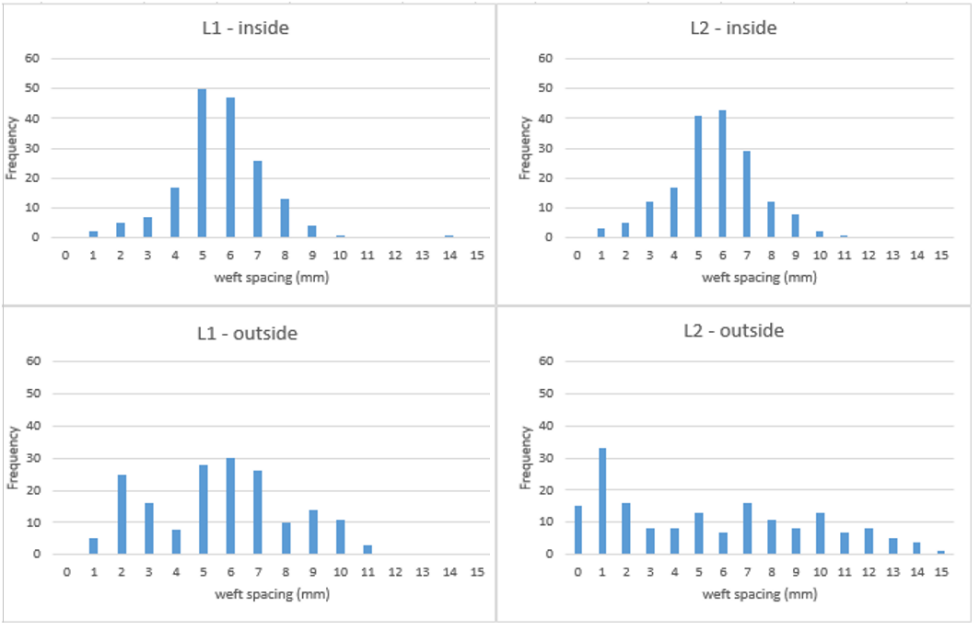
Fibre type	Panex 35
Weft material	glass
Weft tex	68
Weft - gauge	4.5
Stitch length warp (mm)	3

Table 3 Materials parameters

From the images taken using a digital microscope (Dinolite AM413T – placed on the surface of the fibre reinforcement) there are no visible difference between the fabrics with the highest and the fabrics with the lowest stitch thread tension. Moreover, no significant differences were observed with cut pieces of fabric (a 500mmx500mm piece of fabric was cut each time for each fabric version) and the fabric that was on the roll (the microscope images were taken 2 metres inwards the fabric roll in order to avoid any potential effects of the cutting procedure). The main quantifiable difference between the fabrics with different stitch tension is the quantity of the stitch that is in the fabric (a higher amount of stitch thread material goes into the fabric with the low stitch thread tension).

Examining the quality of the fabrics – experimental set-up:
The specification for the spacing of the weft thread (material; glass) is gauge 4.5 (4.5 stitches per 25.4mm). Both the inside (top of the fabric during production) and outside (bottom of the fabric during production) were examined. The spacing of the weft spacing was then measured and histograms for the fabric can be seen below in figure 41. The measurements were taken using a ruler.

The measurements were taken at a new area of the fabrics (~3metres inwards in the fabric roll to avoid any distortions that could take place during production/handling). The L1 production roll appears to be of higher quality, as the spacing is more consistent when compared with the other three manufactured rolls. This material was used for subsequent processing, characterization and analysis.



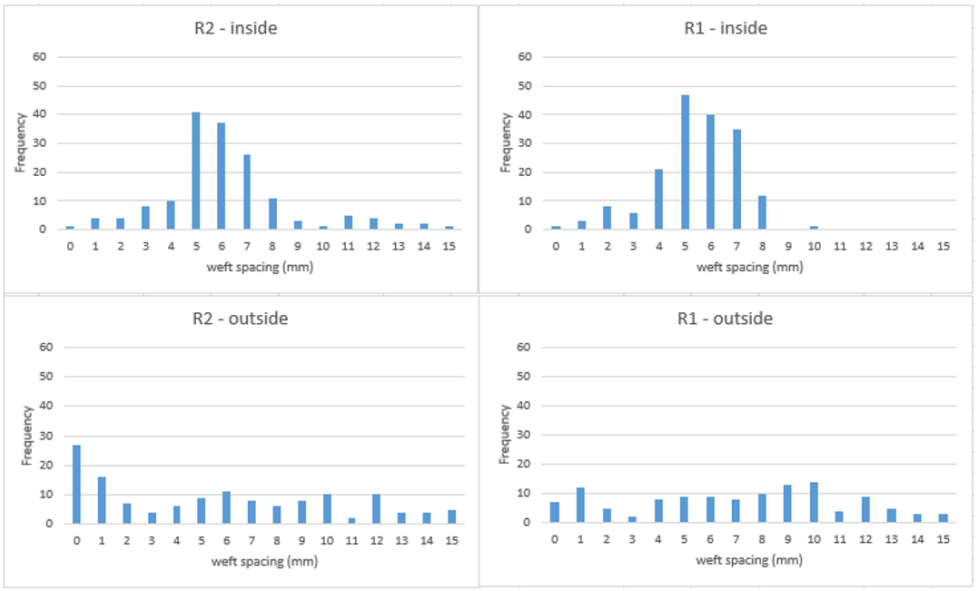


Figure 41 Weft support thread spacing occurrence of L1, L2, R1 and R2

The effect of stitch tension on the quality of the fabrics was characterized quantitatively. The in-plane waviness of the carbon fibre bundles was selected as a descriptor of the quality. The number of in-plane “waves” of the bundles was counted for fabric specimens with a length of one metre. To avoid any distortions which may potentially be induced during fabric production and handling, no specimens were taken from the first 3 metres from the end of the fabric rolls. The results are shown in figure 42 and indicate that the highest stitch thread tension tends to result in the lowest number of in-plane waves of

fibre bundles. It was also observed that the number of in-plane waves was higher on the top surfaces of the fabrics than on the bottom surfaces. It is thought that this may be a result of how the fabrics were pulled and rolled-up during production.

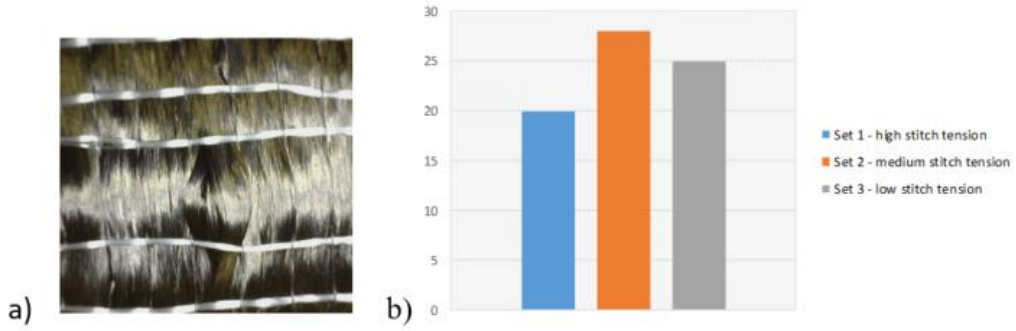
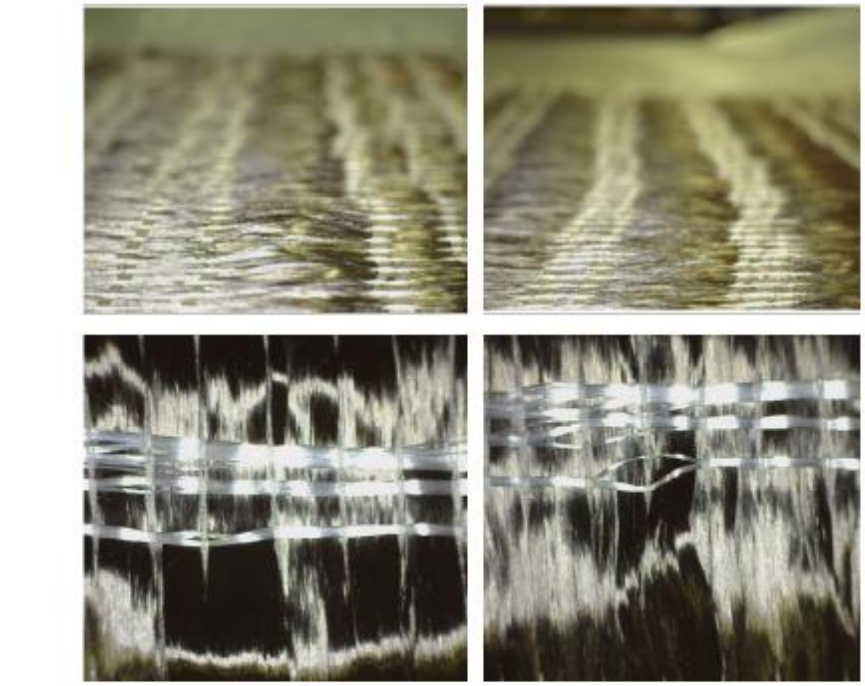


Figure 42 Defect analysis of the fabrics: a) image of an in-plane wave b) number of in-plane waves of fibre bundles at a specimen length of one metre.

A digital microscope (Dinolite AM413T) was placed at the edge of the fabric at an approximately 20^{o} angle in order to examine the glass weft architecture as well as the carbon fibre tow alignment. The out of plane fibre buckling although it does not appear frequently in the fabric it can result in in-plane fibre buckling. The in-plane fibre buckling appears more frequently in the fabric and can affect the fabric characterization results and material properties. As with the out of plane fibre buckling it appears at a higher rate on the inside (top side) of the fabric and this is shown in figure 43.



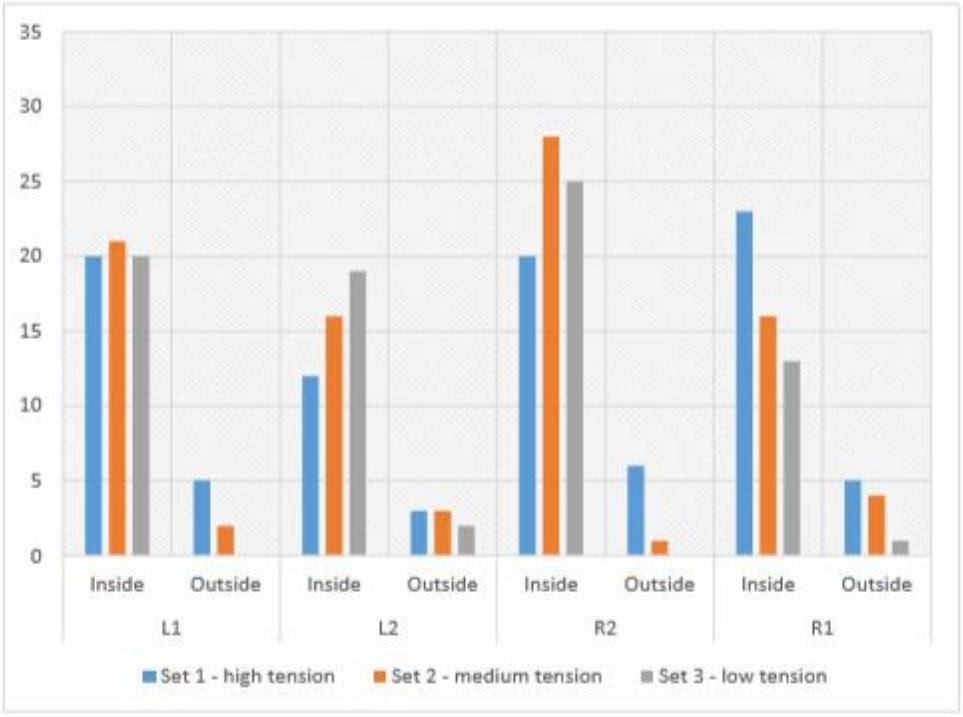


Figure 43: Carbon fibre tow distortions and measurements

The number of in-plane tow waves was measured from a one metre fabric sample for the different rolls (L1, L2, R1, R2). The measurements are shown for the different fabric rolls at different tension settings (low, medium and high). A higher number of in-plane tow waves are observed on the inside (top side of fabric during manufacture), especially on the R2 fabric roll. This might be attributed on how the fabric is pulled and rolled on the cardboard roll during production. Moreover, the out of plane waviness can result in in-plane waviness during handling/manufacturing of the fabrics.

4.1.1. The Effect of Stitch Tension on the Permeability of Unidirectional Non- Crimp Fabrics

The permeability of the fabrics was analysed at three fibre volume fractions, which were obtained by combining an appropriate number of fabric layers in the specimens with the height of the cavity in the permeability measurement tool (Table 4). Results are plotted in figures 44 and 45.

In the range of fibre volume fractions studied here, the principal in-plane permeability values, K_1 and K_2, appear to decrease almost linearly with increasing fibre volume fraction, V_f. Values of K_1 are similar for Set 1 (high stitch tension) and Set 3 (low stitch tension), while values for Set 2 (medium stitch tension) tend to be higher. On the other hand, K_2 is similar for Set 2 and Set 3, and significantly lower for Set 1. The ratio of anisotropy in permeability, K_1/K_2, shows significant scatter, but appears almost constant for all fabrics. As expected for unidirectional fabrics, K_1/K_2 indicates strong anisotropy. For all tests, the main flow direction is aligned with the fabric warp direction.

target V_f	number of layers	cavity height / mm
0.40	2	2.5
0.50	1	1.0
0.60	3	2.5

Table 4 Combinations of numbers of fabric layers and cavity height to obtain target fibre volume fractions

When interpreting the experimental data, it is to be considered that the stability of the fabrics is generally low. This may introduce uncertainty in the measured permeability values due to:

- deformation of the fabric during handling, which was severe for some of the tested specimens
- The high number of fibre filaments (50K) might be giving a more inhomogeneous porosity throughout the fabric. This might have an effect on the reproducibility of the fibre arrangement and thus the high variability between the experimental trials

The effect of nesting of fabric layers is also to be considered here. Nesting may occur at the highest and lowest fibre volume fractions (2 and 3 layers of fabric, respectively), but not at the medium fibre volume fraction (only one layer of fabric). This may result in formation of different flow channel networks in the specimens at different fibre volume fractions. In particular, the flow channels at medium V_f, where no nesting occurs since only one fabric layer is used, are greater in cross-section than they would be at the same V_f with nesting. This may explain why values of K_1/K_2 appear to be higher at a target fibre volume fraction of 0.50, and why K_1 and K_2 as a function of V_f show almost linear behaviour. This is attributed to the high variability of unidirectional fabrics. As the number of layers in a fabric increases so does that stability. This is also observed in fabrics that have a more stable stitching pattern (pillar). The inherent variability in a unidirectional (UD) fabric has an effect on the permeability measurement values of a fabric. Alterations during handling, cutting and subsequent processing, has a significant effect in the permeability measurements of the fabric. The higher the local porosity, the higher the influence on the permeability variations.

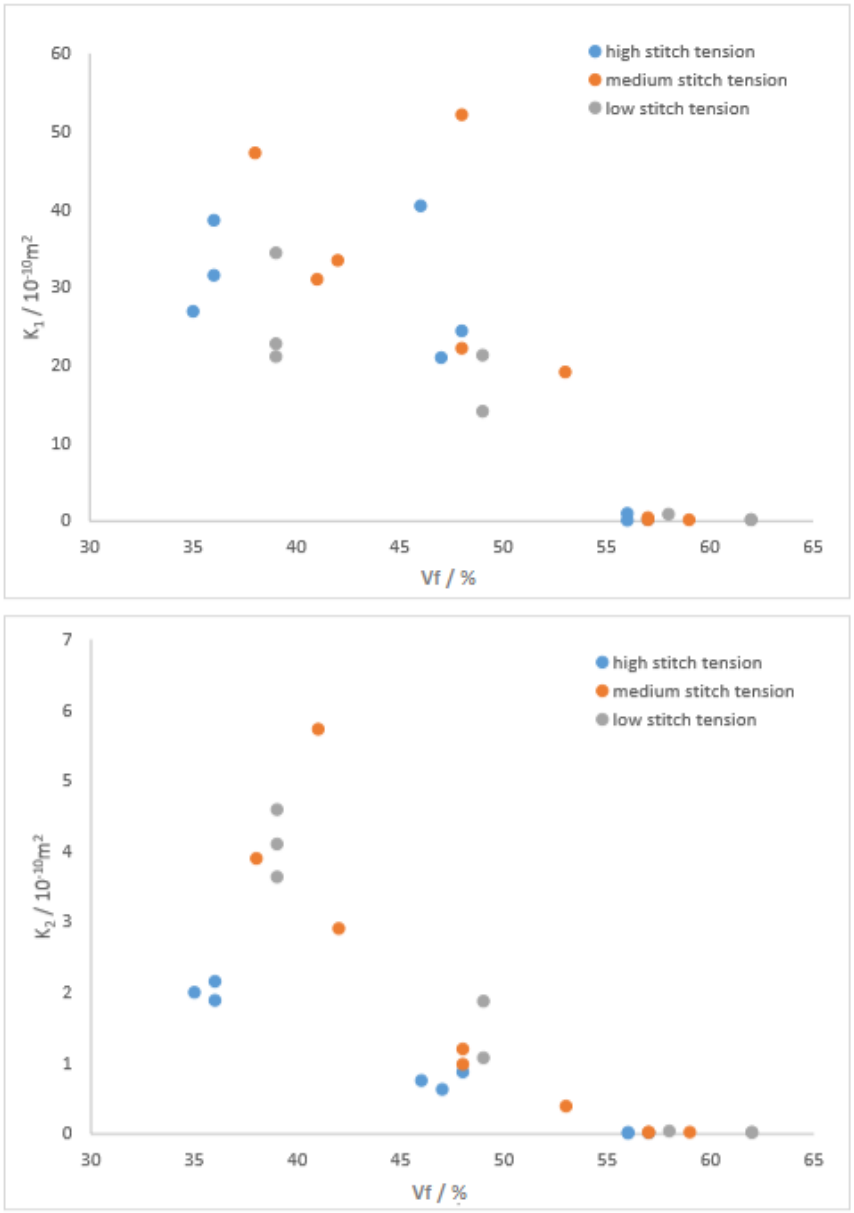


Figure 44 Experimentally determined data for principal permeability values, K_1 and K_2, as a function of the fibre volume fraction, V_f

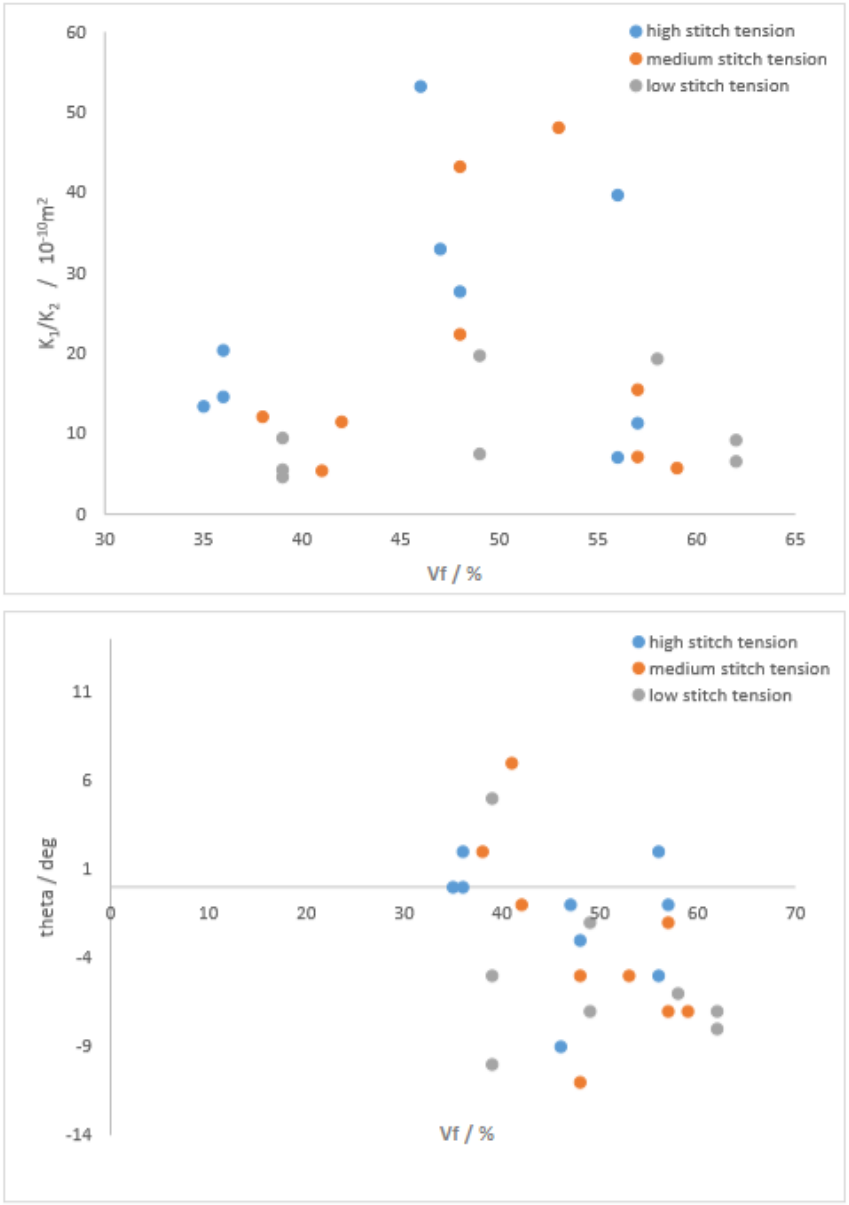


Figure 45 Experimentally determined data for ratio of anisotropy, K_1/K_2, and angle of flow (describing the orientation of the main flow direction) as a function of the fibre volume fraction, V_f

High tension in the stitch thread pulls the glass support threads from the surface of the fabric into the gaps between the carbon fibre bundles. This results in changes in the cross-sectional shape of the carbon fibre bundles and of the gaps between the individual bundles. Geometrical changes resulting from increased tension in the stitch thread constrain the movement of fibre bundles and increase the stability of the fabrics. This explains that the in-plane waviness of fibre bundles is lowest for the highest stitch tension.

4.1.2. The Effect of Stitch Tension on the Meso-structure Geometry of Unidirectional Non-crimp fabric Preforms

Cross-sections of four layer stacks for each fabric (dry fabric – at the preform manufacturing stage) of the warp direction (direction of the stitch thread and the carbon fibre tow) are shown in figure 46. X-ray computed tomography (XCT) is a radiographic based imaging method that produces 2D cross-sectional and 3D volume images of the object under inspection. The internal geometry of a part can be examined for quality (check for defects, tolerances and density). An X-ray source generates an X-ray beam, which propagates through the object under inspection. The resulting intensity of the X-ray beam is measured using an X-ray detector. This process is repeated at many angles to obtain a stack of 2D X-ray projections. A projection algorithm is applied to the data to compute the attenuation coefficients of the material where they are assigned a grey value which relates directly to the material density. The aim was to compare as best as possible the high and the low stitch thread tension in terms of gap size. Changes in the shape of gaps between fibre bundles also affect flow paths during resin injection. As a result, the permeability parallel and transverse to the carbon fibre bundles may change with increasing stitch thread tension. This is evident particularly for K_2, where the experimentally observed significant reduction in values for Set 1 is consistent with a reduction in the transverse permeability due to lateral compression and increasing thickness of the carbon fibre bundles at the highest stitch thread tension. However, from the images taken using XCT it is difficult to conclude the effect of the stitch thread tension.

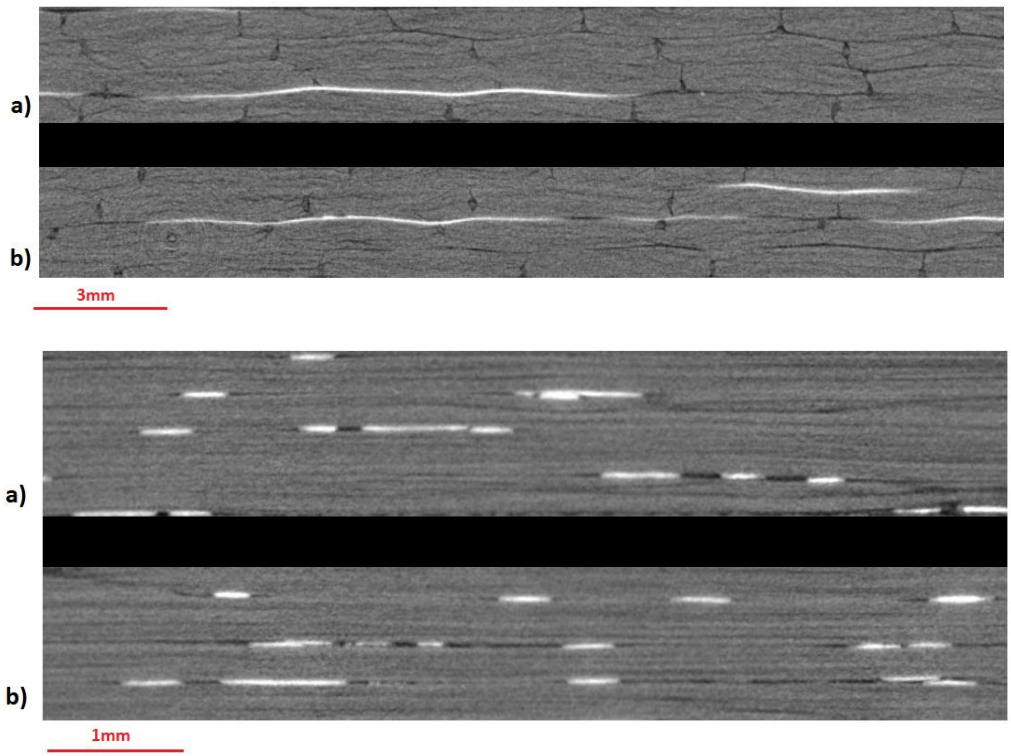
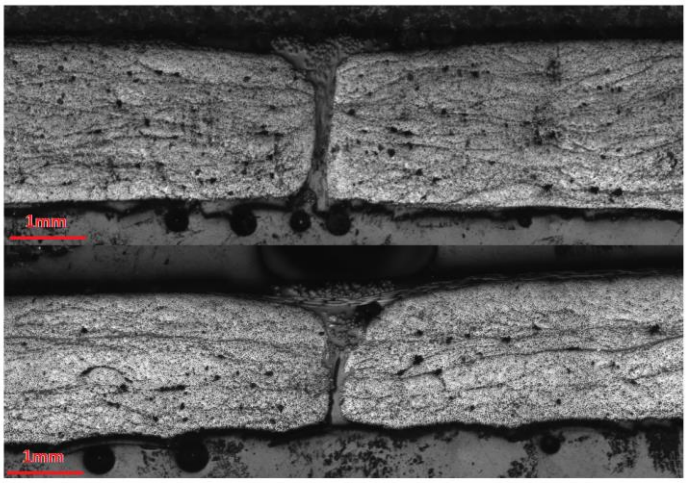


Figure 46 Vacuum bag set-up of a 4 layer dry stack: Top image permeability K_1, a) low stitch tension, b)high stitch tension. Bottom image permeability K_2, a) low stitch tension, b)high stitch tension

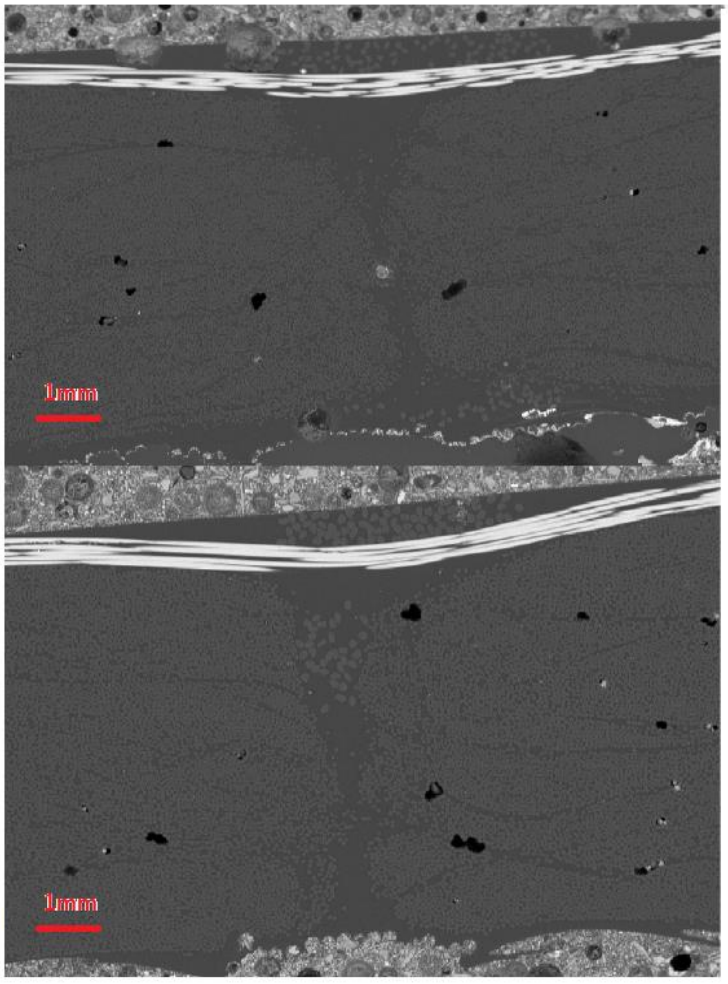
For unidirectional NCFs of the specific architecture studied here, changes in the stitch thread tension can affect the cross-sections of fibre bundles and inter-bundle gaps in the fabric. Constraining the bundle mobility by increasing the stitch tension tends to result in decreasing levels of fibre bundle waviness. The expected result is that the higher the stitch thread tension, the higher the crimp in the weft direction. The higher warp stitch tension will translate into the glass threads in the weft to be "pulled" down from the surface of the fabric and create higher crimp in the fabric. Different samples were manufactured, using vacuum bag infusion (using an epoxy resin), and the cross sections of the different materials were examined using optical microscopy as well as scanning electron microscopy (SEM). The images can be seen in figure 47. As well with the additional methods, it is difficult to draw conclusions from the images as the inherent variability of the material results in different local deformations throughout different areas of the fabrics.

a)



b)

a)



b)

Figure 47 Top image (warp direction): images taken using an optical microscope (a)high stitch tension, b)low stitch tension), Bottom image (warp direction): images taken using SEM (a)high stitch tension, b)low stitch tension)

Experimental observations suggest that the in-plane permeability of fabrics, which is determined by the size and geometry of flow channels forming in the material, is affected by the stitch tension. Particularly the permeability transverse to the fibre bundles appears to decrease with increasing stitch tension. However, trends are hard to identify, since low stability of the fabric means that experimental data show a high level of scatter. The higher the warp stitch thread tension it will translate into the glass threads in the weft direction to be "pulled" down from the surface of the fabric and rearrange the shape of the tows. The inter-yarn gaps shape changes, affecting the resin flow paths. As a result, the permeability in the warp and weft direction changes with different stitch thread tensions. In addition, an increase in the stitch thread tension can increase the stability of the fabric (handling and subsequent processing), restricting the movement of adjacent tows that can affect the alignment of the carbon fibre tows and consequently the process-ability of the material.

4.2. Biaxial Non-Crimp Fabrics

Three fabrics studied here are biaxial -45^{o}/+45^{o} carbon fibre fabrics, comprising of Toray T620 50C fibre type [64]. The stitch thread (pillar stitch pattern, 0^{o} direction – machine direction) is made of polyester. The stitch gauge is 6 and the stitch length spec for the original/benchmark fabric is 2.12mm (which can be affected during the tension value change during machine set-up). The stitch run-in refers to the quantity of the stitch thread that goes into the fabric. The higher the stitch run-in the lower the stitch thread tension. In table 5, the different fabric versions are listed and a close up of the fabric is shown in figure 48 and figures 49 and 50 a comparison between the fabric with the low and the high stitch thread tension.

Version	Fibre type	Stitch material	Stitch type	Stitch gauge	Stitch length (mm)	Stitch tension (cN)	Stitch run in
high stitch tension	T620SC 50C	Polyester	Pillar	6	2.12	10.8	3380
medium stitch tension	T620SC 50C	Polyester	Pillar	6	2.12	9.3	3515
low stitch tension	T620SC 50C	Polyester	Pillar	6	2.12	8	3700

Table 5 Materials parameters

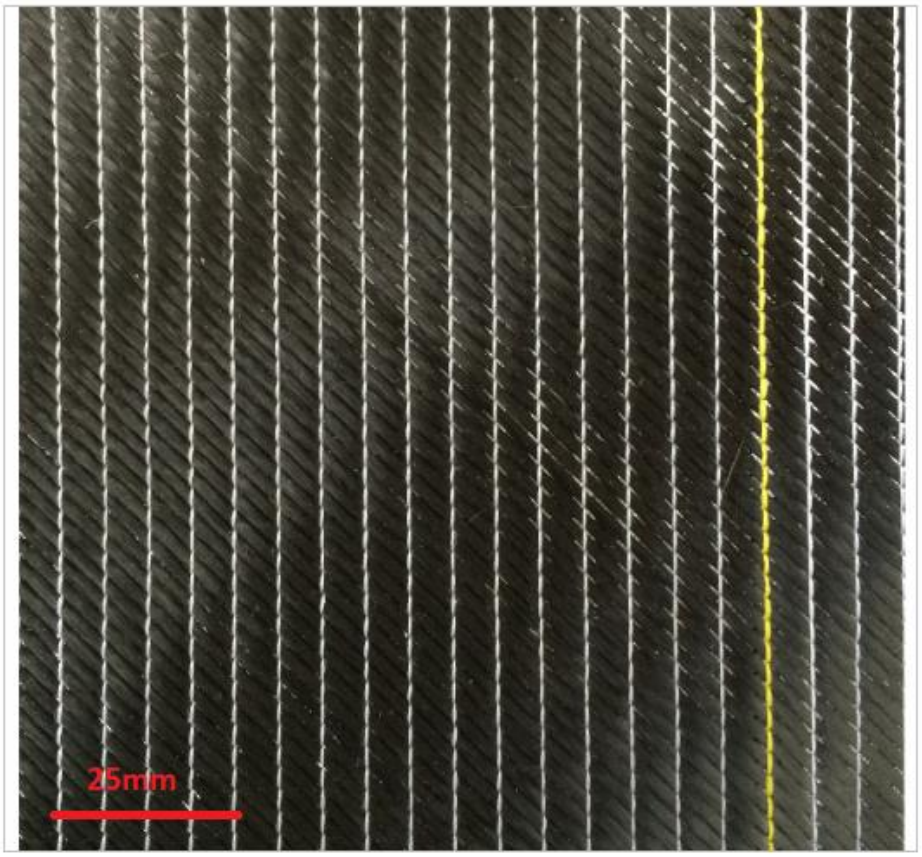


Figure 48 Closeup of the fabric: stitch thread in the warp direction

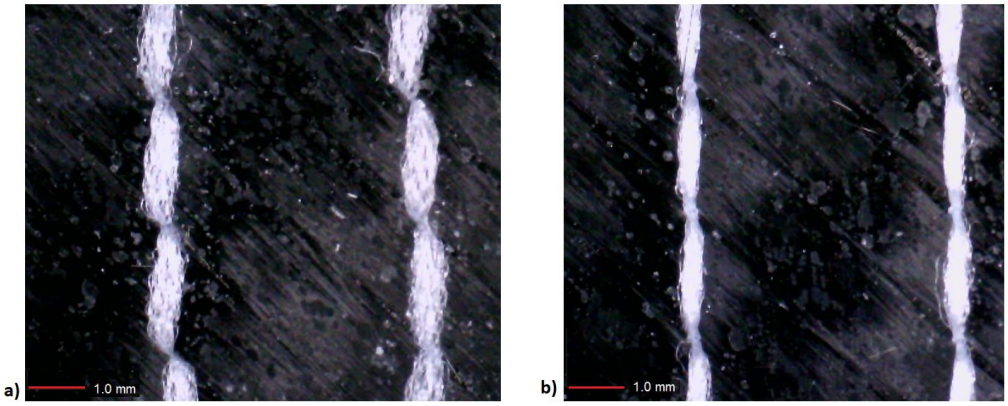


Figure 49 Top side of fabrics: a)high stitch tension, b)low stitch tension

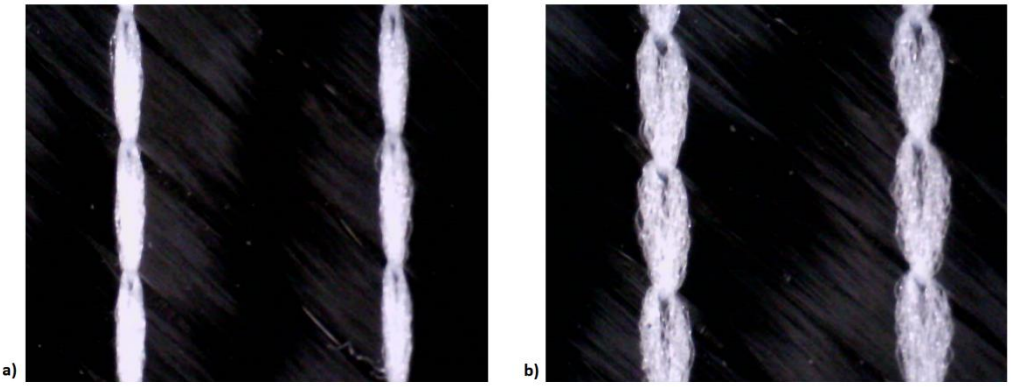


Figure 50 Back (loop) side of fabrics: a)high stitch tension, b)low stitch tension

4.2.1 The Effect of Stitch Tension on the Permeability of Biaxial Non-Crimp Fabrics

In this study, the permeability of carbon fibre non-crimp (NCF) biaxial -45º/+45º fabrics is examined, aiming to study the effect of varying the stitch thread tension on the permeability of the materials. The results are plotted in figures 51 and 52. Variations of the stitch thread tension will translate into rearrangements in the fibre structure and thus affect the permeability of the reinforcement. The higher the stitch tension, the tighter and closer packed the arrangement of the fibre filaments that can lead into alterations of the flow during liquid resin injection for composites manufacture.

Three fabrics with different stitch tensions are analysed here. The cavity height of the permeability measurement rig was set at 2mm and the permeability was calculated at three distinct fibre volume fractions. Three, four and five layers were used for the 37%, 50% and 62% fibre volume fraction respectively. In the range of fibre volume fractions used in this research, the principal in-plane permeabilities appear to increase for the fabric with the high stitch thread tension. This might be attributed to the fact that the stitch increasing the size of the gaps that are created and thus increase the dimensions of the flow channels. The values of the K_1 and K_2 permeabilities for the medium and low stitch thread tension appear to be similar. The ratio of anisotropy K_1/K_2 appears to be constant for all the fabrics tested here, with relatively small scatter. The main flow direction for the fabric with the high stitch thread tension is close to 30 degrees whereas for the fabrics with the medium and low stitch thread tension is between 10 and 20 degrees.

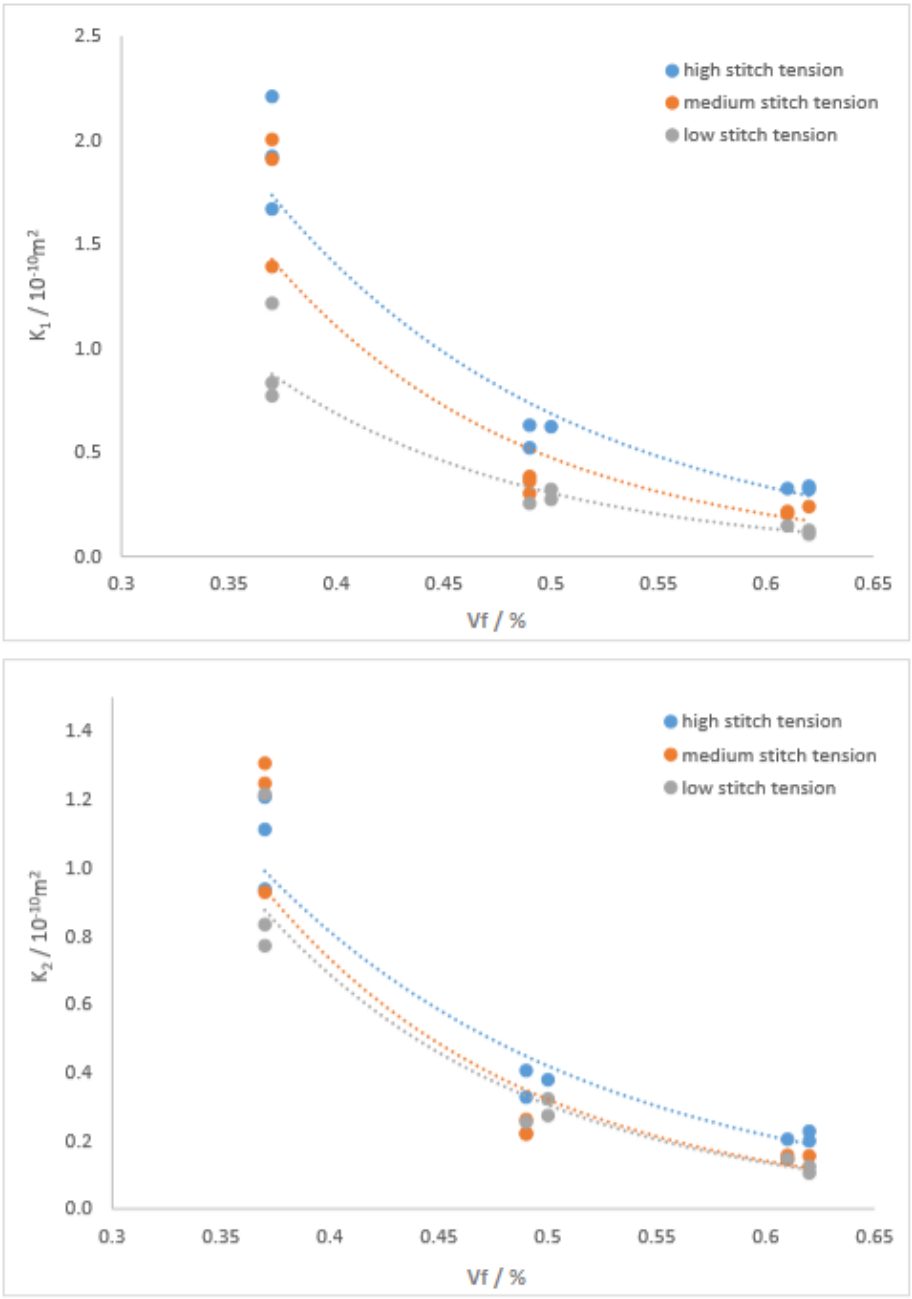
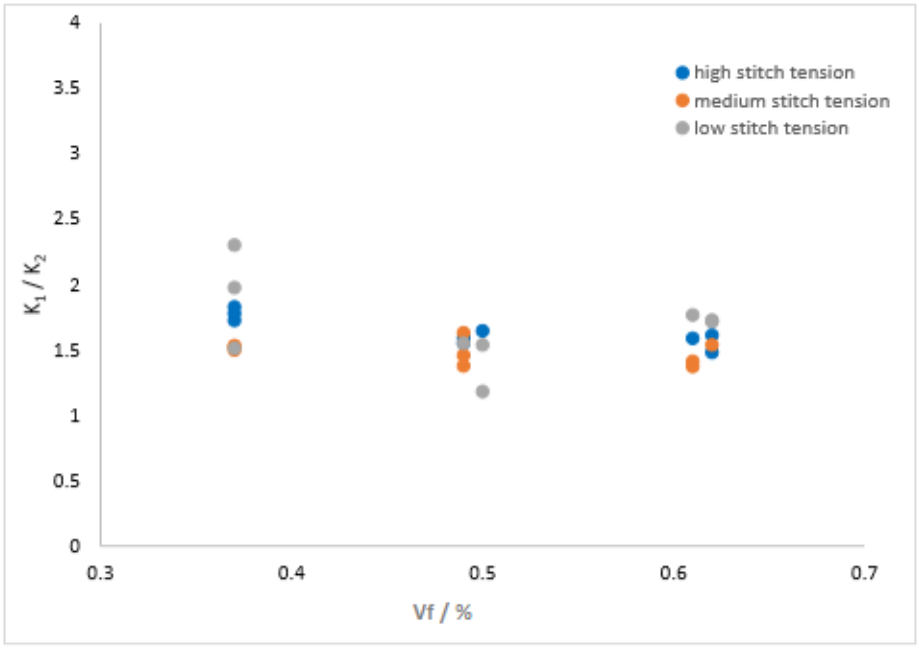


Figure 51 Experimentally determined data for principal permeability values, K_1 and K_2, as a function of the fibre volume fraction, V_f



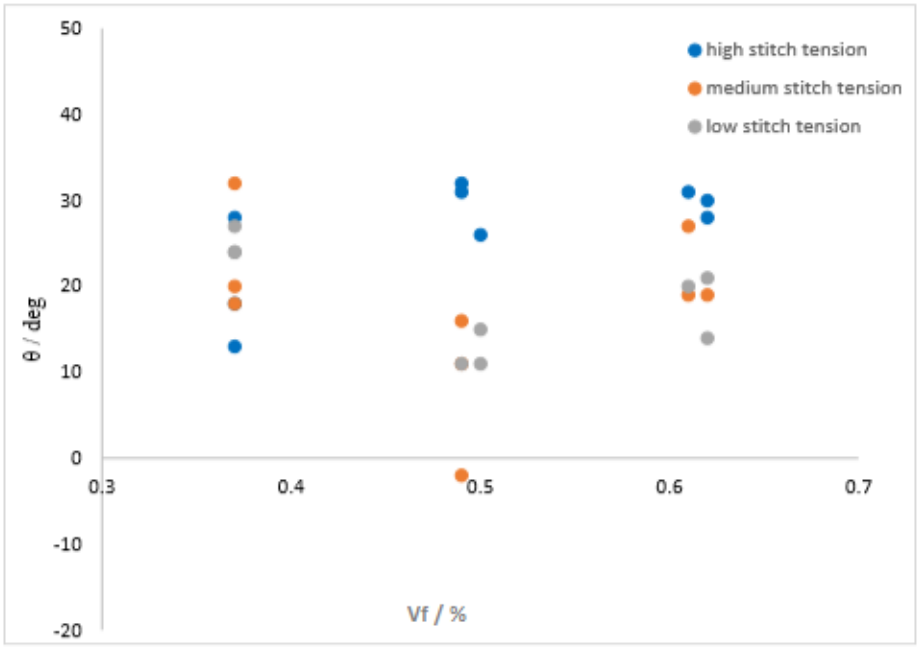


Figure 52 Experimentally determined data for ratio of anisotropy, K_1/K_2, and angle of flow (describing the orientation of the main flow direction) as a function of the fibre volume fraction, V_f

4.2.1 The Effect of Stitch Tension on the Meso-structure Geometry of Biaxial Non-Crimp Fabric Preforms

Experimental observations suggest that the high stitch thread tension will increase the permeability of the fabric in both principal directions. This is also evident in XCT images taken from a four layer stack of the low and the high stitch thread tension fabrics (figures 53 and 54). This can be attributed to that the stitch thread is creating gaps, the channels of which can allow for the resin to flow faster. For the lower fibre volume fraction (below 40%) the silicone oil might not be fully impregnating the fabric, but instead flow through the spaces and voids between the fabric stack. In this instances, Darcy's law for flow is not valid and the permeability cannot be defined accurately. It is difficult to conclude on the permeability results of the medium and low stitch thread tension fabrics as the results show similarities between the two. However, a good indication towards the understanding of how the yarn tension affects the physical properties of non-crimp fabrics, is that the high stitch thread tension of the specific fabric versions that were manufactured for this research study has a significant effect on its in-plane permeability.

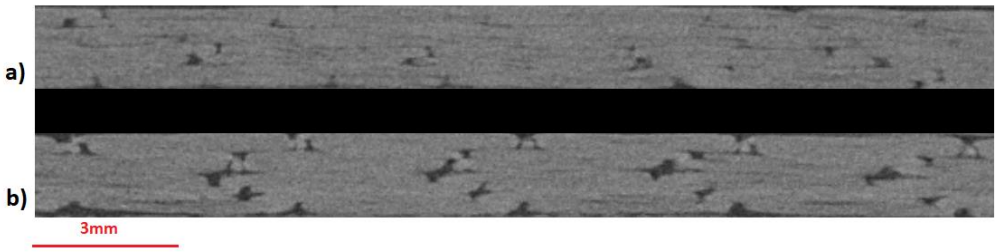


Figure 53 K_1 permeability a)low stitch thread tension, b)high stitch thread tension

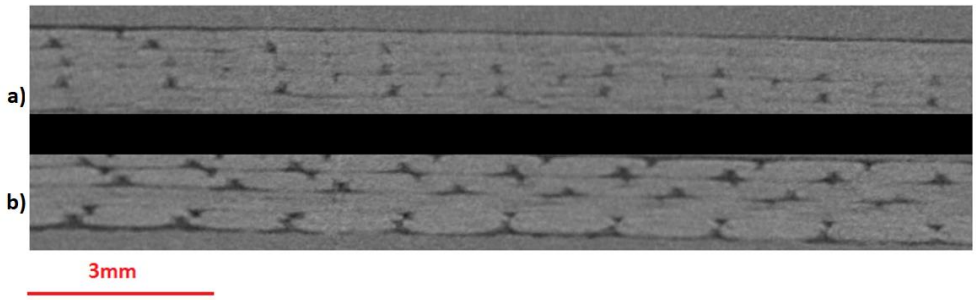


Figure 54 K_2permeability a)low stitch thread tension, b)high stitch thread tension

4.2.3 The Effect of Stitch Tension on the In-plane Shear of Biaxial Non-Crimp Fabrics

The material in this study comprises of two layers of carbon fibre tows in a -45°/+45° arrangement, with a polyester stitch thread as the support structure holding the fibres together in a pillar pattern. Three different stitch thread tensions are studied in this work (table 6). The stitch style is pillar with a stitch length of 2.12mm. Five samples for each stitch thread tension were tested using the picture frame method. The displacement speed on the mechanical testing equipment was 100mm per minute. A comparison of shear force vs shear angle for the three fabrics is illustrated in figure 55, all fabrics tested for positive shear (direction of stitch thread).

Version	Fibre type	Stitch material	Stitch type	Stitch gauge	Stitch length (mm)	Stitch tension (cN)	Stitch run in
high stitch tension	T620SC 50C	Polyester	Pillar	6	2.12	10.8	3380
medium stitch tension	T620SC 50C	Polyester	Pillar	6	2.12	9.3	3515
low stitch tension	T620SC 50C	Polyester	Pillar	6	2.12	8	3700

Table 6 Architecture parameters for the different fabric versions

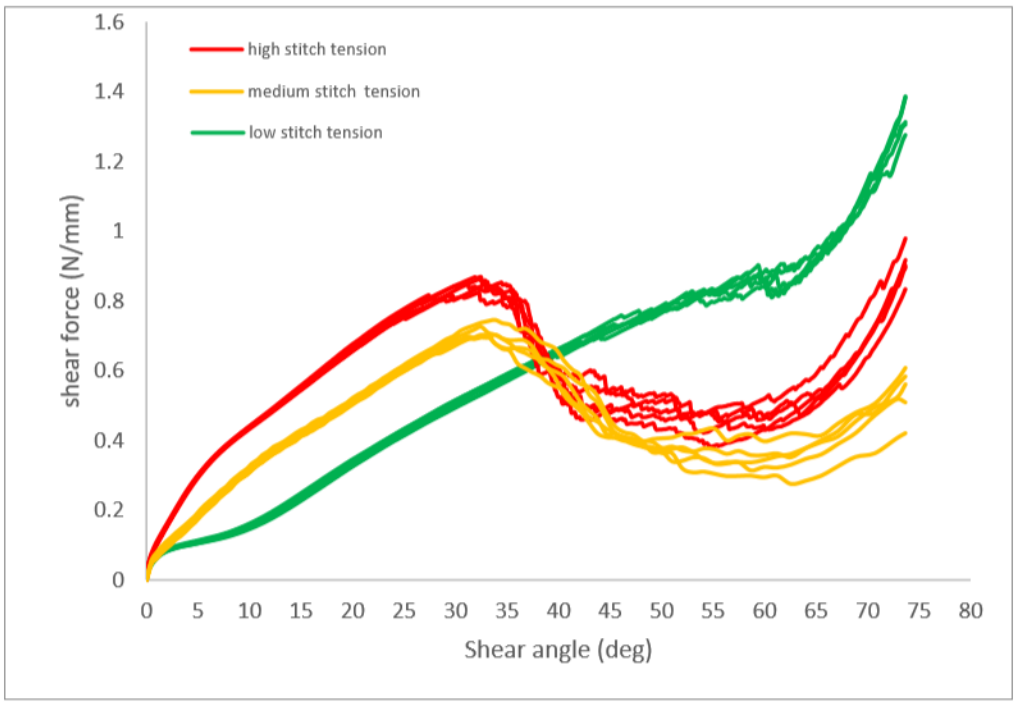


Figure 55 shear force vs shear angle of the different fabrics

Experimental observations show that shear behaviour of the fabrics is affected by the stitch thread tension and there is a linear effect to the degree of shear they experience. High stitch tension results in reduced formability of the fabric on a complex geometry. As the stitch thread rearranges the fibre filaments, these are packed in a tight formation where the bundles movement tends to be constricted. The fabric produced with the low stitch thread tension exhibits reduced shear deformation where this type of material can be potentially be used in applications where a high drapeable fabric is required. For the stitch materials (varying the stitch thread tension), two main regions are observed for the positive shear: one before and one after stitch breakage. Since the stitch thread tension was the lowest possible value for the production before the fabric becomes completely unstable, the lower shear force can be explained for the low stitch thread tension fabric.

4.2.4 The Effect of Stitch Tension on the Forming of Biaxial Non-Crimp Fabric Preforms

For the biaxial fabrics, the angle between the two fibre orientations during forming was experimentally determined by means of a new digital image analysis. Apodious digital imaging (figure 56) was implemented for this study [65]. This system is typically used for quality purposes during preform manufacture. This commercial unit is used primarily for quality measurements of composite materials where companies aim to examine the quality of preforms. A "benchmark" preform is manufactured and then all subsequent preforms are compared to a "quality pass" part. The preform is scanned and analysed by computer software, computing the coordinates systems and nodes. Each triangle mesh that contains the fibres angles is compared with the neighbouring one for deviations.

The preforms were manufactured with a single diaphragm forming process for this study. Two preforms for each extreme case were analysed and compared. The information captured with the equipment can be presented in a number of ways, each depending on the result for the desired analysis. The shear angle is plotted against the fibre angle occurrence in order to visualise the difference between the materials.

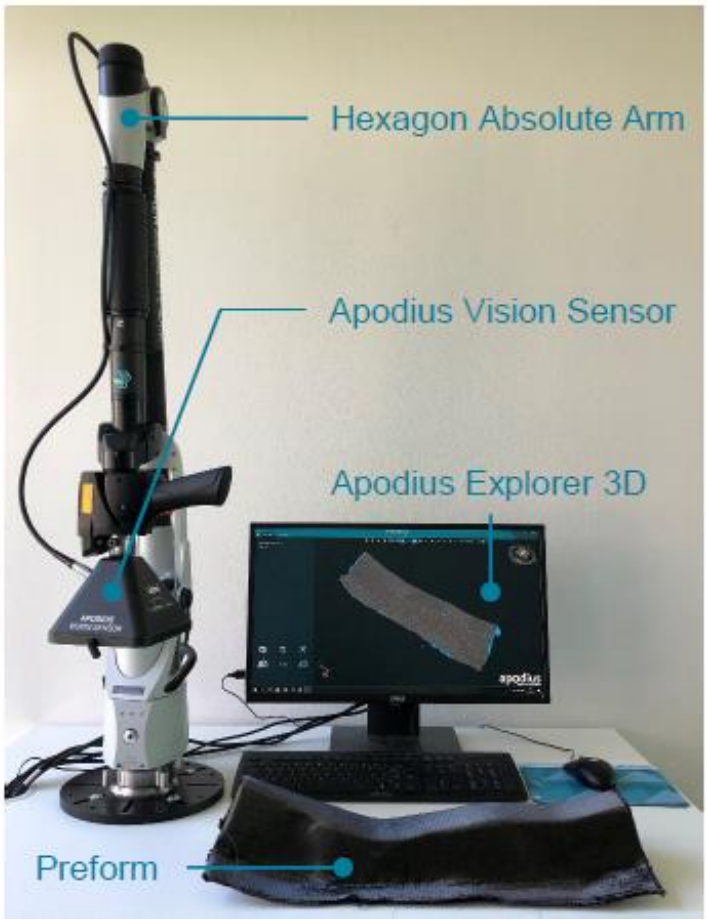


Figure 56 Apodius system

The preform part is first scanned and digitized. The preform is then analysed for fibre misalignment during forming. The mesh triangle edge can be set to different values. A 3mm triangle mesh was chosen for the trials. An algorithm assigns values for the average fibre orientation to every generated mesh triangle. The fibre analysis and the mesh can be seen in figures 57 and 58. Figure 59 through 62 show the analysis of the preform using the fabric with high stitch thread tension while figure 63 through 66 the fabric with the low stitch thread tension.

Experimental set-up;

400mmx250mm samples were manufactured. A 2 layer stack was used for the manufacturing of the preforms. Epikote 05390 powder binder (10gsm) was applied on the surface of the stitched fabrics.

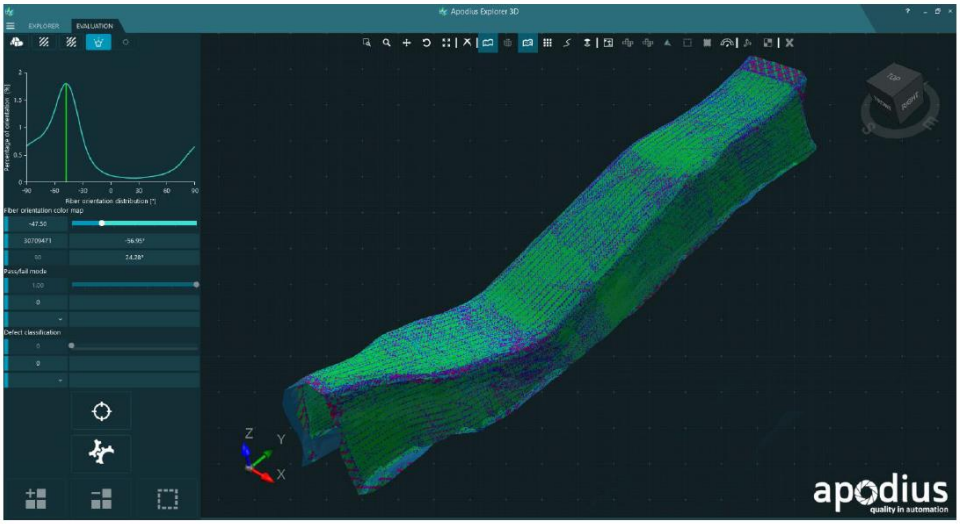


Figure 57 Preform analysis

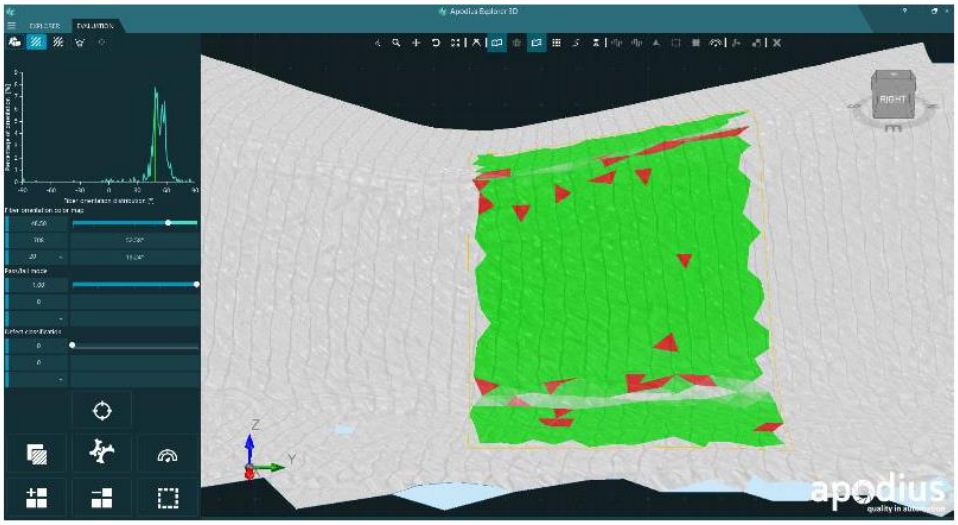


Figure 58 Mesh generation

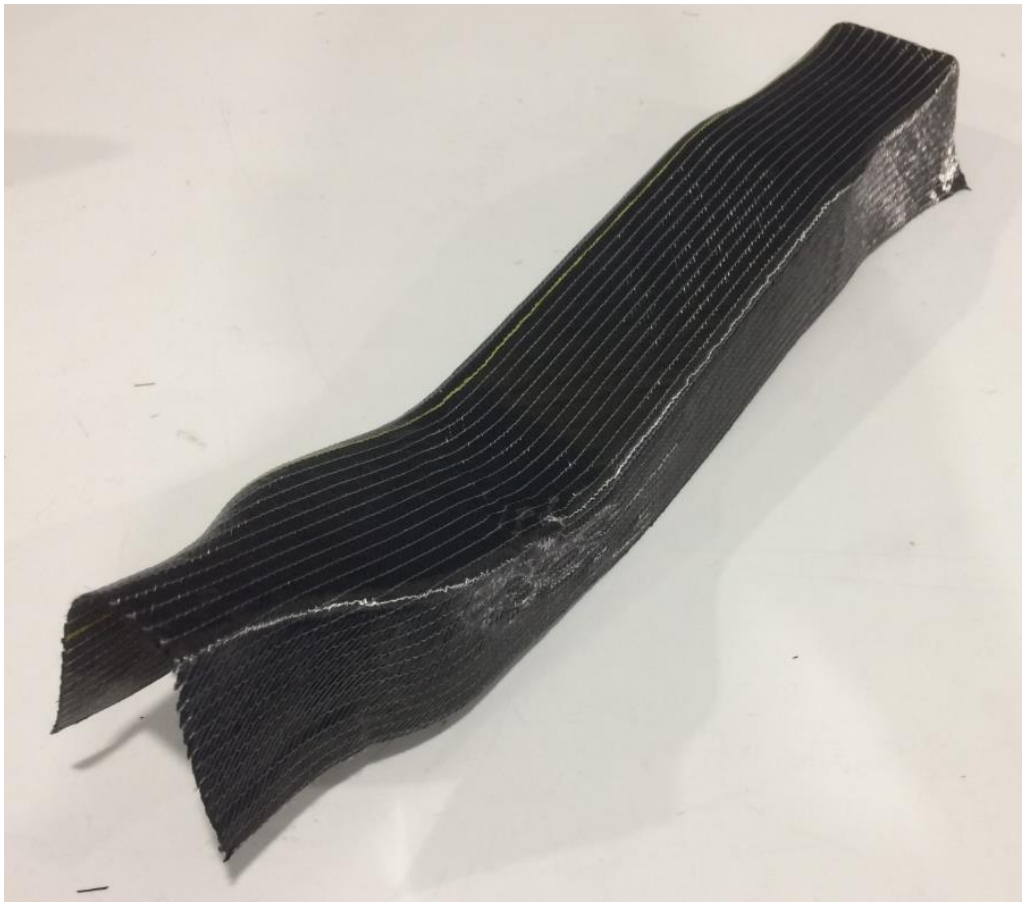


Figure 59 Manufactured preform with the high stitch thread tension

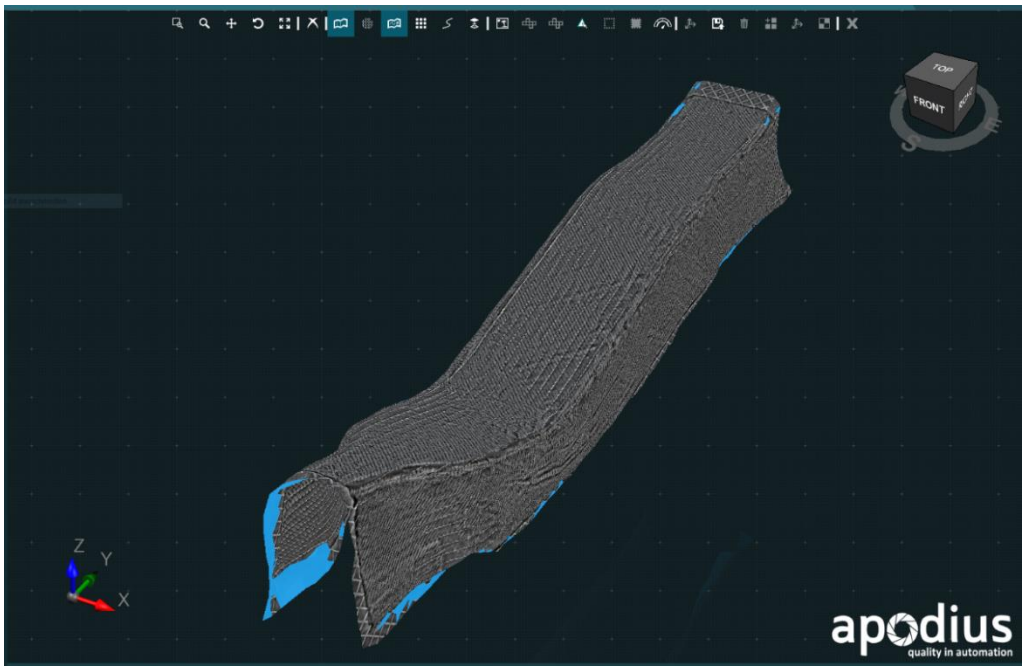


Figure 60 Scanning of preform with the high stitch thread tension using the Apodious system

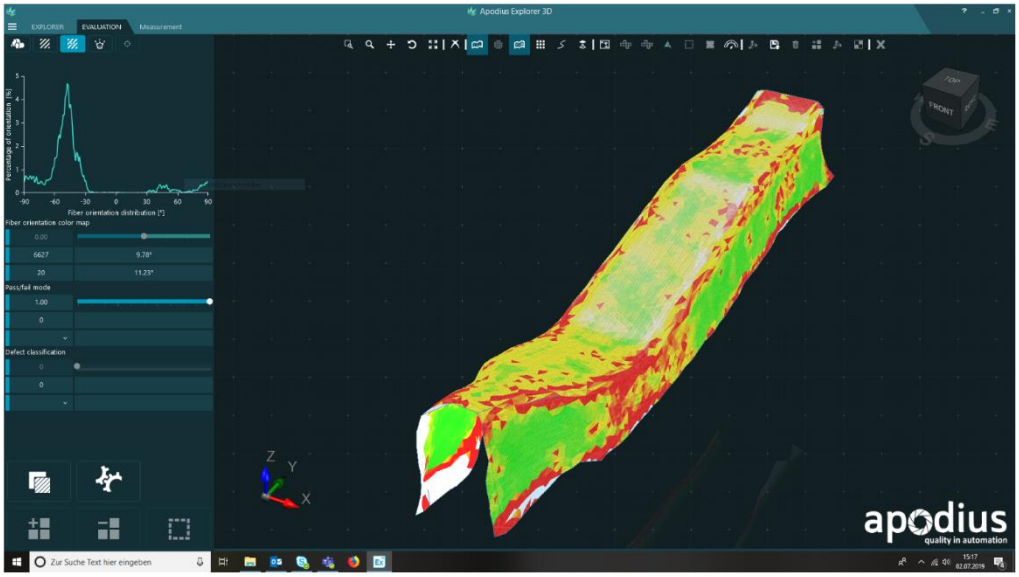


Figure 61 Analysis of the preform with the high stitch thread tension using the Apodious software

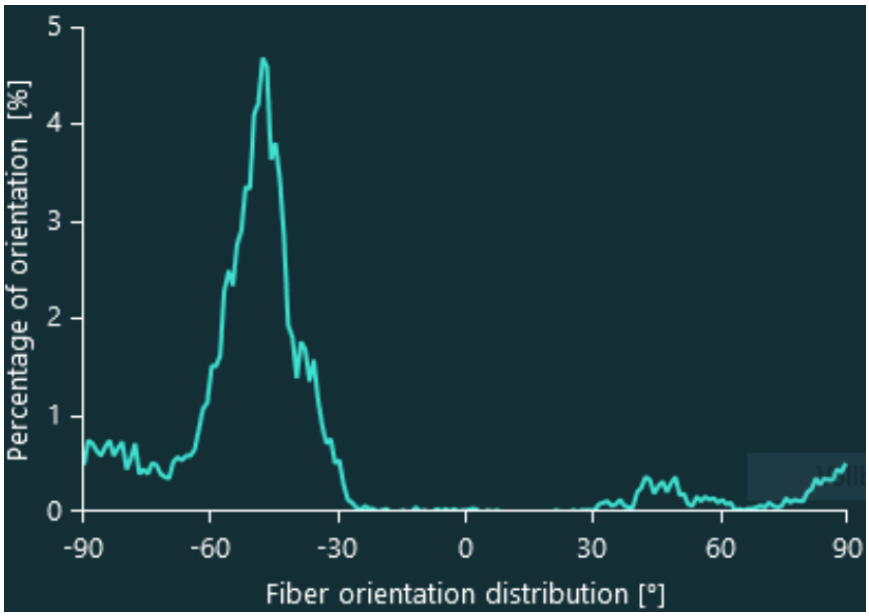


Figure 62 Fibre orientation destribution of the preform with the high stitch thread tension

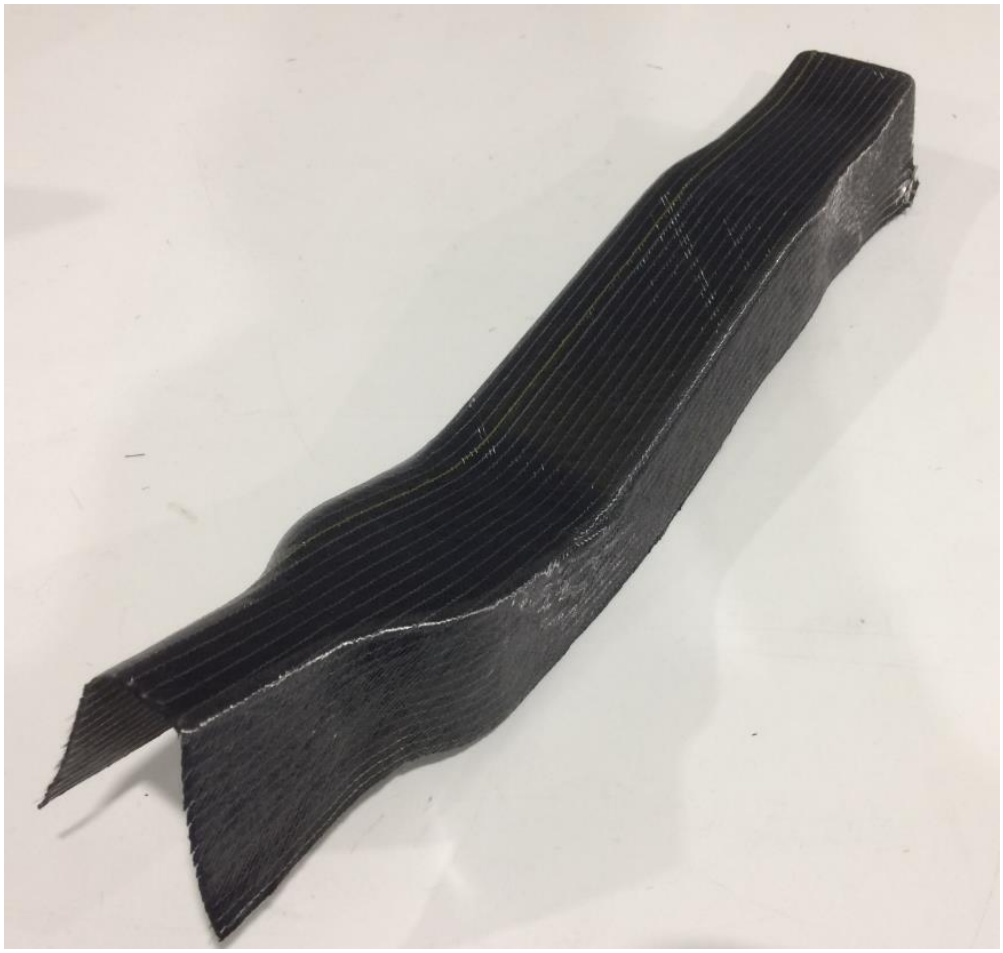


Figure 63 Manufactured preform with the low stitch thread tension

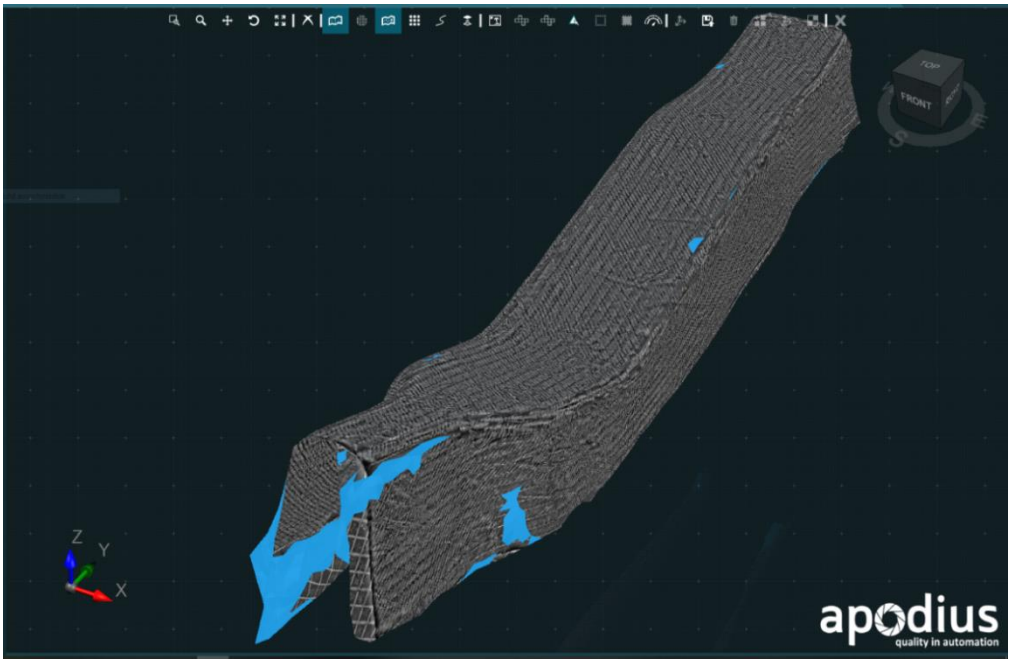


Figure 64 Scanning of the preform with the low stitch thread tension using the Apodious system

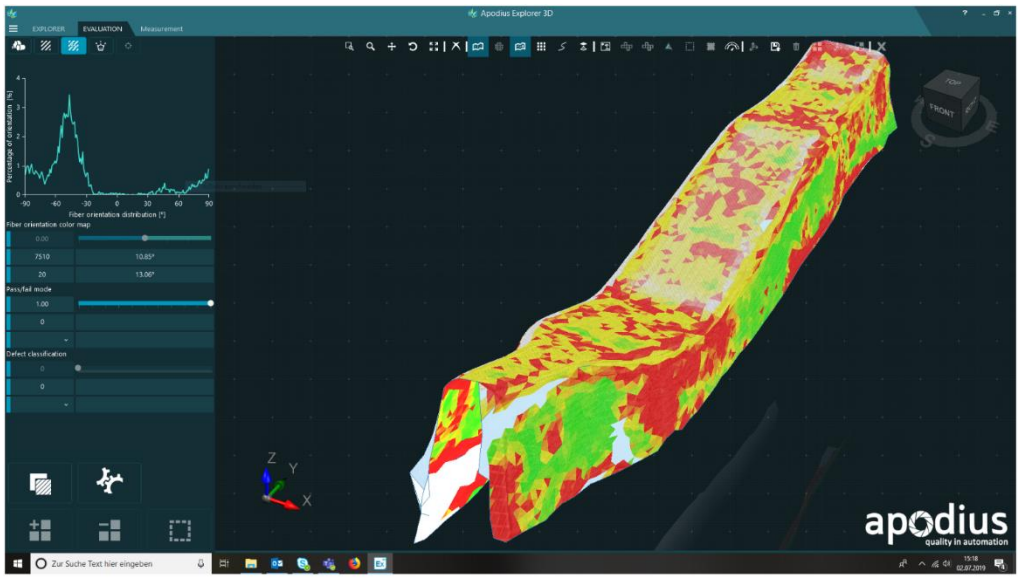


Figure 65 Analysis of the preform with the low stitch thread tension using the Apodious system

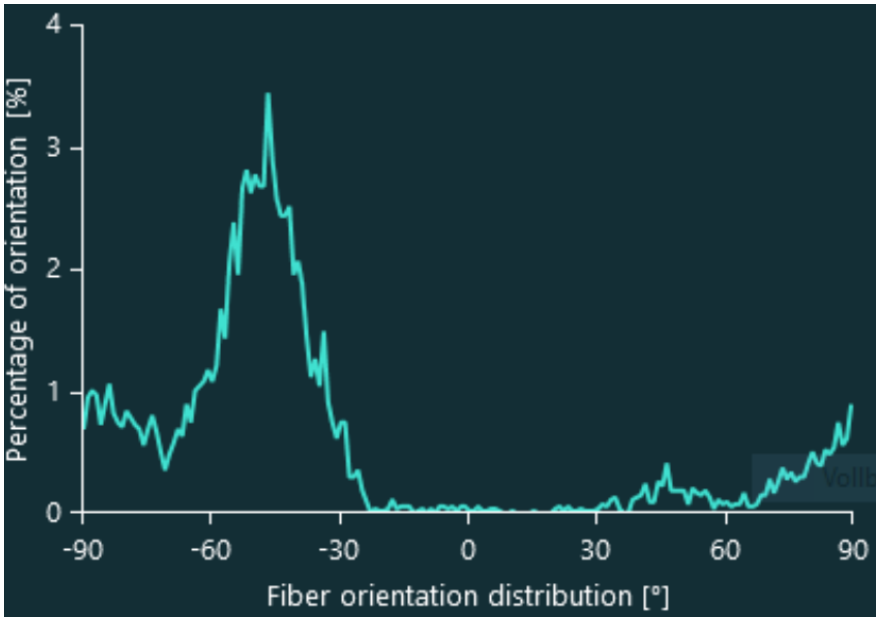


Figure 66 Fibre orientation distribution of the preform with the low stitch thread tension

Statistical evaluation of the results show that the angle can be described by means of normal distribution. Figures 62 and 66 illustrate the fibre angle and the corresponding normal distribution for the high and the low stitch thread tension respectively. The Apodious system was used to measure the fibre orientations. The system generates a point cloud in order to create a triangular mesh with specific edge length of 3mm. The algorithm of the system assigns values for average fibre orientations from -90^{o} to +90^{o} to every generated mesh triangle. The corresponding fibre orientations are displayed color coded, where the selected fibre orientations are displayed in green and the deviating fibre orientations in red.

The majority of the fibres angles are between 30^{o} and 60^{o} degrees, with the highest percentage at 45^{o}. Because of the geometry of the part, a high percentage of flat areas will not interfere with the deformation of the fabric during the forming process and thus the fibre will remain at 45^{o}. A lower, by 10%, distribution in these fibres angles is observed for the biaxial fabric with the low stitch thread tension. This does not correspond well with what is expected with a material that is more formable, as even from the results from section 4.2.3 the shear behaviour of the material is comparable to that of a woven fabric. In the results from section 4.2.3 it can be seen that the fabric with the high stitch thread tension, the shear force is higher than the other fabrics.

Although optical observations show a clear difference between the two preforms, where for the fabric with the high stitch thread tension, severe defects are caused and are detected on the side of the preform where the double curvature of the tool is (figure 67), it is difficult to draw comparison between the fibre angle distributions. The stitches cause disturbances during forming, where fibre movement can lead to defects such as “bunch up” and bridging. The variations of fibre angle for the both fabrics is similar, which might be attributed to the low mesh resolution. The shear resistance measured during positive shearing, increases for the NCF with increasing stitch thread tension as it seen from the picture frame testing results.

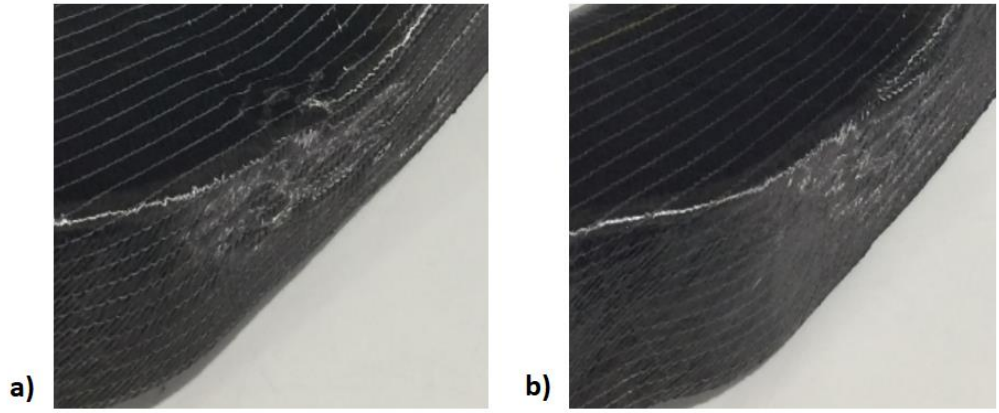


Figure 67 Comparison between the fabric preform parts with the high (a) and the low stitch thread tension (b)

5. Development of Novel Scrim-based Non-Crimp Fabrics

5.1. Scrim architecture

5.1.1. Testing of commercially available Scrims

Commercially available scrims were sourced as well as bespoke custom ordered constructions. Different yarn (in the scrim) parameters can exist and can be altered (figure 68). Each yarn comprises of a bundle of filaments ranging from 20 to 200 individual filaments (this can vary with different scrim manufacturers). The scrim yarn is measured and defined in dtex. The spacing between the yarns in the scrim range between 2mm and 25mm. Increasing the number of yarns within the scrim increases the number of contact points and generates higher fabric stability, but with an associated increase in the supporting structure's (scrim) weight.

The most common used yarn sizes from manufacturers are 74, 550 and 1100 dtex. It is possible to have different dtex values for the different orientated yarns, however the warp (0^o direction) cannot be very light compared with the weft direction due to equipment limitations of the supplier's equipment (difficulty for the 0^o orientated yarns in the scrim to maintain the same tension as the weft yarns and consequently produce bond between the 2 yarn directions. Theoretically any angle is possible (0^o - 90^o). The main types of scrim that are readily available are either $0^o/90^o$ (biaxial) or $-30^o/0^o/+30^o$ (triaxial). However, with the fibre deposition technology being developed, these orientations can be further processed/changed to suit the desired properties of the manufactured fabric.

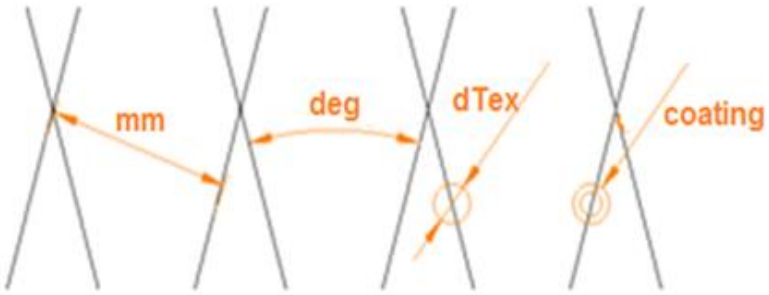


Figure 68 Scrim parameters

Typical materials for the scrim are polyester, E-glass, PE (polyethylene) and PET (poly(ethylene terephthalate)). Low melt point yarns can be unstable and difficult to manufacture into scrims. Moreover, different types of coating chemistry exist: however, it was not possible to obtain details/information from suppliers that could be used to manufacture scrim materials. This was an issue as a high number of trials using different types of scrim materials were necessary in order to determine first and foremost a suitable material for fibre deposition using a new manufacturing method that is discussed in a subsequent chapter.

The type of coating of the scrim is typically PVA (polyvinyl alcohol) or PVAC (polyvinyl acetate) with different chemistries used by different companies. The percentage of coating typically ranges from 20 to 60% of the total yarn weight. The core of scrim is typically polyester. A low melting temperature coating of the yarn is potentially attractive for the deposition stage of manufacture, and should pose little technical challenge to the manufacturer. Moreover, scrim weight can be optimized where the scrim manufacturer could potentially decrease the adhesive quantity on the nodes (where two scrim yarns intersect) and thus reduce the overall weight.

The scrim manufacturer attributes a 10 – 20% weight tolerance for the scrim, meeting the lower end of the spectrum for an optimum lighter material would be beneficial for a lightweight fabric with less parasitic weight for the support structure and thus overall weight of the manufactured fabric. The fabric

stability depends on the level of adhesion between the tows and the scrim. The optimum yarn coating for adhesion was found to be PVAC (polyvinyl acetate), with the most suitable (higher tow-scrim adhesion) PVAC chemistry being the one used by only one company. The PVAC can be modified further to produce a lower melt chemistry that can help generate deposition stability with lower temperatures, but could potentially reduce the adhesion between the scrim and the tows.

Two scrims sourced from the company Bafatex [66] are shown in figure 69 (same coating type, different number of yarns in the warp direction, different dtex and different overall scrim weight) for comparison. The architecture of the scrim contributes to the characteristics of the fabric and consequently to the composite itself. The number of filaments in the yarn, the spacing and orientations of the yarns, the cross-sectional dimensions and shape of the yarn, the type of coating, coating percentage and coating melt temperature of the yarn will determine the properties of the new fabric.

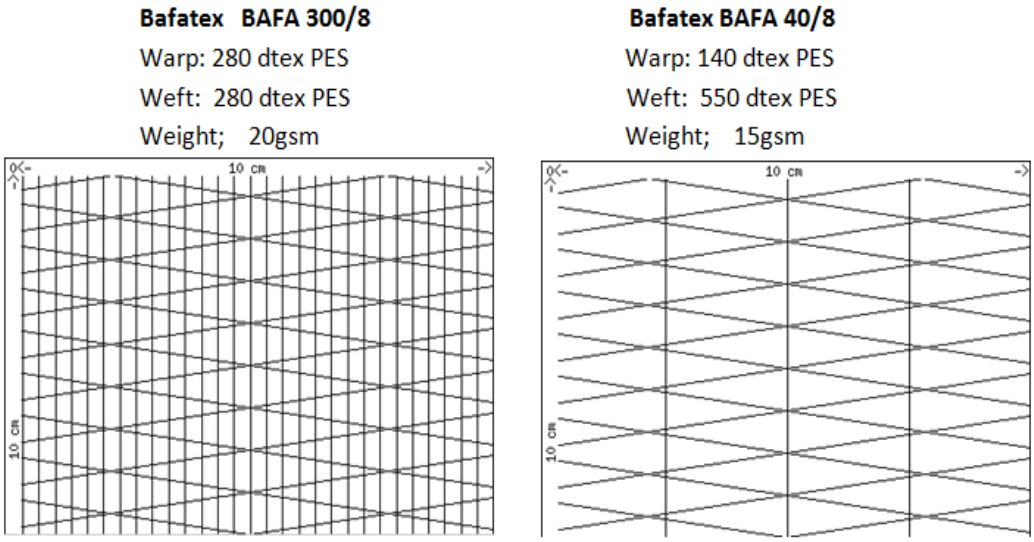


Figure 69 : Scrim construction schematics: On the left a conventional readily available scrim (Bafa 300/8) and a bespoke manufactured for Hexcel scrim (Bafa 40/8) a construction with a reduced number of 0^{o} oriented yarns

5.1.2. Manufacture and Testing of bespoke Scrims: early development

The 0^o orientation polyester yarns were supported on the 90^o orientation yarns to ensure a good degree of contact. Three yarn types were used (EMSGrilon C-60, Eytechnologies HM2270 and a new product Wykes 4808). An infra-red lamp placed at a 10mm distance from and parallel to the yarns was mounted on the equipment frame. The speed setting for sufficient adhesion was 200rpm (30m/h) for the Wykes and 100rpm (15m/h) for the other 2 yarn types. A small roller was mounted on the equipment frame (after the IR lamp), pushing slightly down the 0^o yarns to ensure contact of the 0^o and 90^o yarns. The experimental set-up is shown in figure 70. It was observed that a lower machine speed was required in order for the higher dtex yarns to acquire a better adhesion level (15 metres per hour production rate).

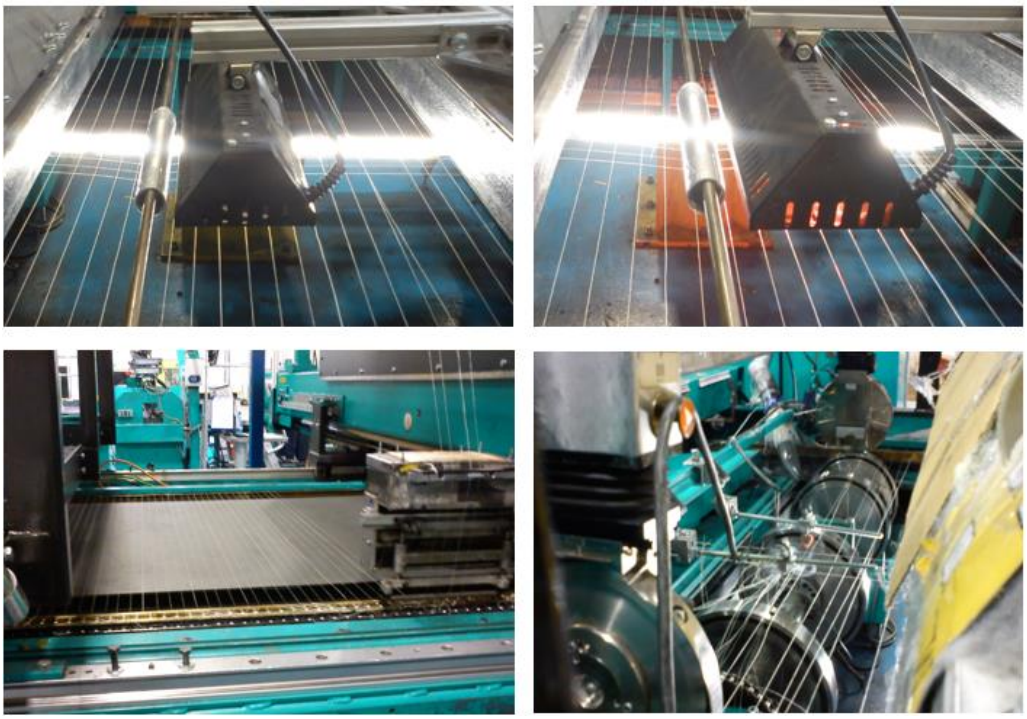


Figure 70 Manufacturing of the scrim material

Issues:

- Debris build up on the equipment due to the melting of the yarn coating: the equipment had to be cleaned every few metres of produced material and examined for any inconsistencies
- The entire set-up required bypassing most of the roller set-up on the production line
- Overall, it is difficult to manufacture the scrim materials on the ncf production lines as low yarn tension is required downstream of the equipment in order to avoid damaging the scrim nodes (intersection of the warp and weft yarns)

Other yarn options for scrim manufacture (these are only in concept form and they are not readily available from the manufacturer) that could potentially improve the end result:

- C-60 yarn from EMS Grilon with 500 dtex with the same core (150 dtex PET) but reduced percentage of coating melting yarn as the 840 dtex version.
- Reduction of the amount of melting polymer (currently the yarn consists of 80% melting polymer (coating) and 20% core yarn).
- Change that to a 50/50 ratio (coating/core). Thus the core yarn is thicker in comparison to a standard combi yarn. This would roughly amount to 660 dtex in total.
- Glass core yarn could potentially be used (same effect as above, but more dominant)
- Mono-filament core yarn: however this might lead to higher crimp as a single yarn could not spread on the surface of the fabric when compared with multi-filament yarns

5.2. Scrim-based Fabric manufacture: early development

During production of the scrim material, the weft yarns are supported through a spring/fixture that adjusts the angle of the placement. The weft yarn is supported on the warp yarn, this is a manufacturing limitation. Only biaxial ($0^o/90^o$) or triaxial scrim types are readily available from manufacturers, available with different parameters such as dtex, yarn spacing and yarn coating. Any orientation and dtex is possible to manufacture, however standard specification type scrims are mainly available due to costs since changing to different settings from the main available products will increase the product price significantly.

Different types of coating are available, however as with the above parameters listed standard coating types are available at a higher cost as it requires a time consuming and expensive procedure to change the type of the chemical (requires cleaning the chemicals containers and then changing the type of coating). Also there is a difference between the melting and bonding temperature of the yarns. Moreover, it is difficult for the manufacturer to create a low melt scrim coating as this will reduce the stability and handleability of the material during processing and manufacturing. However, a lower weight scrim can be achieved with a standard product by reducing the adhesive quantity that is used when attaching the nodes together (of the warp and the weft yarns of the scrim).

A limitation of the warp yarn properties is that it usually has to be heavier than the weft yarn due to equipment limitations. Different yarns can be manufactured with different percentages of elongation. This might potential inhibit the drape characteristics of the manufactured fabrics and possibly the in-plane permeability values. The two main scrim categories are laid (warp and weft yarns heat set together) or woven (warp and weft yarns interlaced). Manufacturing a bespoke material for the experimental study will have an impact on the price of the product as minimum orders are required, lead time and degree of difficulty in manufacturing it especially when deviating from the standard products that are sold through the manufacturer is also important.

In table 7 and 8, all the scrim materials that were tested are listed [67 – 71]. The yarns for the scrim manufacture, and infra red lamp used, are listed in the references [72 – 76] and in table 9. All the information (from specification sheets, research, discussion with the manufacturers and physical examination) for the different types of scrim materials that were used to manufacture the carbon fibre fabrics were compiled and are listed as well as the yarns that were used to manufacture scrim materials for the experimental trials. The parameters of the scrim include the scrim type, the cell geometry, the dtex (cross-section), number of yarns in the warp and the weft, the type of the core material in the yarn, the melting temperature, the overall weight of the material, the coating type, the elongation at break and the tensile strength. One of the main objectives for the selection of a suitable scrim material was the sufficient adhesion between the carbon fibre and the scrim. As the coating chemistry from the manufacturer was not disclosed, a high number of scrim materials were trialled. The suitable materials are discussed in a subsequent section of the study. James Dewhurst uses a PVAC coating that was suitable for the manufacture of the fabrics.

The quality of the adhesion of the tow to scrim is qualified by a delamination force test, and by inspection. Similar tests can be found in the literature [77,78]. A 500mmx500mm piece of laminated scrim and tow is cut. The scrim is then clamped down, from both sides of the tow, by means of G-clamps and by using a wooden plate damaging the test materials is avoided. A 10mm gap between the edge of the tow and the batten on each side of the tow is freed. The tow is slowly pulled at one end, so that a clip used for the tow's edge to be clamped. The clip is attached to a spring balance, and the balance is pulled so that the tow is delaminated from the scrim. The angle between the scrim and the tow is kept at 90° during the pull test. The tow and scrim were inspected each time, examining for evidence of damage to the scrim, where the scrim has melted or if it showing signs of other heat damage that might be caused from the roller that deposit the tow.

Company	Product	cell geometry	Dtex (coated)	warp / weft	Core material
SCRIMS					
BAFATEX	200/20	diamond	74	warp; 200 threads/1m weft; 20mm distance between yarns	polyester-filament-yarn
BAFATEX	80/30	diamond	warp;74, weft; 80	warp; 80 threads/1m weft; 30mm distance between yarns	polyester-filament-yarn
BAFATEX	100/20	diamond	500	warp; 100 threads/1m weft; 20mm distance between yarns	viscose yarn
BAFATEX	200/10	diamond	280	warp; 200 threads/1m weft; 10mm distance between yarns	polyester-filament-yarn
BAFATEX	200/20	diamond	550	warp; 200 threads/1m weft; 20mm distance between yarns	polyester-filament-yarn
BAFATEX	200/18	diamond	1100	warp; 200 threads/1m weft; 18mm distance between yarns	polyester-filament-yarn
BAFATEX	100/8	diamond	280	warp; 100 threads/1m weft; 8mm distance between yarns	polyester-filament-yarn
BAFATEX	300/8	diamond	280	warp; 300 threads/1m weft; 8mm distance between yarns	polyester-filament-yarn
BAFATEX	40/8	diamond	warp;140, weft; 550	warp; 40 threads/1m weft; 8mm distance between yarns	polyester-filament-yarn
ADFORS	(LWPET) FLS KPM210	square	78	12 X 8mm 0/90o orientations	polyester-filament-yarn
James Dewhurst	glass scrim	square	340	8 X 8mm 0/90o orientations	plain glass
James Dewhurst	code; 106A78D	square	warp;167, weft; 150	25 X 8mm 0/90o orientations	polyester-filament-yarn
James Dewhurst	code; 1001A343T	square	280	5.5 X 4.5 mm 0/90o orientations	polyester-filament-yarn
James Dewhurst	TR005G	diamond	680	-	glass
James Dewhurst	040A134D	diamond	167/280	-	polyester-filament-yarn
James Dewhurst	011G25D	diamond	340	-	glass
James Dewhurst	1031A78D	diamond	167/150	40X 30mm 0/90o orientations	polyester-filament-yarn
James Dewhurst	852A78D	diamond	150/150		polyester-filament-yarn
Formax	XCIM234 (FCIM100)	square	-	-	Warp; 3K carbon fibre
PORCHER	M4113SR22N	square	warp;167, weft; 140	25 X 08cm 0/90o orientations	PET
PORCHER	P3x3	square	N/A	0.3 x 0.3 mm	polyester-filament-yarn
PORCHER	D3553S002	diamond	34tex	8 x (0.6 x 2) D mm	glass
PORCHER	D4099S002	diamond	167/140	20 x (10 x 20) D m	polyester-filament-yarn
PORCHER	D4285S036	diamond	280	40 x (5.5x20) D mm	polyester-filament-yarn
PORCHER	D3943C018C1350A	square	76/80	3X3 GD	polyester-filament-yarn
Kirson	2100103	square	warp;76, weft; 80	2.5 X 1.5 mm 0/90o orientations	RPES

Table 7 Scrims trialled

Company	Melting temperature (°C)	Weight (gsm)	Coating	Elongation %	Properties (tensile)
SCRIMS					
BAFATEX	120-130	3.3	PVAC binder	~16%	Warp tensile; 53N/5cm, Weft tensile; 13N/5cm
BAFATEX	120-130	4	PVAC base binder	N/A	N/A
BAFATEX	100	14.4	PVAC base binder	N/A	N/A
BAFATEX	120-130	8.7	PVAC base binder	N/A	54x N/5cm
BAFATEX	120-130	15.7	PVAC base binder	N/A	N/A
BAFATEX	120-130	30	PVAC base binder	19.20%	820 N/5cm
BAFATEX	120-130	13	PVAC base binder	N/A	N/A
BAFATEX	120-130	15	PVAC base binder	N/A	N/A
BAFATEX	120-130	20	PVAC base binder	N/A	N/A
ADFORS	95	2.64	Thermoplastic	N/A	20 x 13 N/5cm
James Dewhurst	N/A	6.3	PVOH	N/A	N/A
James Dewhurst	N/A	8.7-10.7	PVAC	warp; 22%, weft 20%	Warp tensile; 90N/5cm, Weft tensile; 36N/5cm
James Dewhurst	N/A	72	PVAC	warp; 20%, weft 20%	Warp tensile; 456N/5cm, Weft tensile; 373N/5cm
James Dewhurst	N/A	10	PVOH	N/A	N/A
James Dewhurst	N/A	6	PVAC	N/A	N/A
James Dewhurst	N/A	15	PVAC	N/A	N/A
James Dewhurst	N/A	14.6 - 24.6	PVAC	warp; 25%, weft 25%	N/A
James Dewhurst	N/A		PVAC	N/A	N/A
Formax	N/A	65	N/A	N/A	N/A
PORCHER	120-130	10.5	EVA	warp; 20% - 40%, weft 15% - 30%	Warp tensile; 80N/5cm, Weft tensile; 30N/5cm
PORCHER	N/A	6	EVA	N/A	N/A
PORCHER	N/A	8	PVOH	N/A	N/A
PORCHER	N/A	7.8	PVOH	N/A	N/A
PORCHER	N/A	20	PVAC	N/A	N/A
PORCHER	N/A	6	EVA	N/A	N/A
Kirson	120	9	PVAC base binder	warp; 16% - 24%, weft 16% - 24%	Warp tensile; 85N/5cm, Weft tensile; 40/5cm

Table 8 Scrims trialled – continuation

Company	Product	cell geometry	Dtex (coated)	Core material	Melting temperature (°C)	Elongation %
YARNS						
EMS - Grilon	KE-60	yarn	110	coPES	60	80%
EMS - Grilon	KE-60	yarn	220	coPES	60	80%
EMS - Grilon	KE-60	yarn	330	coPES	60	80%
EMS - Grilon	K-178	yarn	55	PA12	178	80%
EMS - Grilon	K-178	yarn	200	PA12	178	80%
EMS - Grilon	K-85	yarn	840	coPA	85	N/A
EMS - Grilon	K-85	yarn	1650	coPA	85	N/A
EMS - Grilon	C60	yarn	400	Polyester	60	N/A
EMS - Grilon	C-85	yarn	400	Polyester	85	N/A
EYTECHNOLOGIES	HM-2270	yarn	1870 (denier)	glass fibre	85 (70 - softening temperature)	N/A
EYTECHNOLOGIES	HM-4818	yarn	771 (denier)	glass fibre	115 (105 - softening temperature)	N/A
EYTECHNOLOGIES	HM-2980	yarn	207 (denier)	polyester	115 (105 - softening temperature)	N/A

Table 9 Yarns trialled

Issues and difficulties encountered are listed in a subsequent chapter. A number of scrims was only in sample form (only a few metres). Other scrim products were not suitable for the trials (quality of material), expensive to order (minimum order required) or difficult to process (insufficient adhesion between the carbon fibre tows and the scrim). The scrim products that were used are listed in a subsequent chapter. Although a 100 linear metre roll (for a 1m width) is sufficient for samples to be manufactured, minimum order quantities are in the thousands of square metres. Other factors that can affect the production of a new scrim product are the width of the roll that is specified, the linear meters produced, and the consistency/quality requested of the product (this will affect the weight of the scrim) and alignment of the scrim yarns.

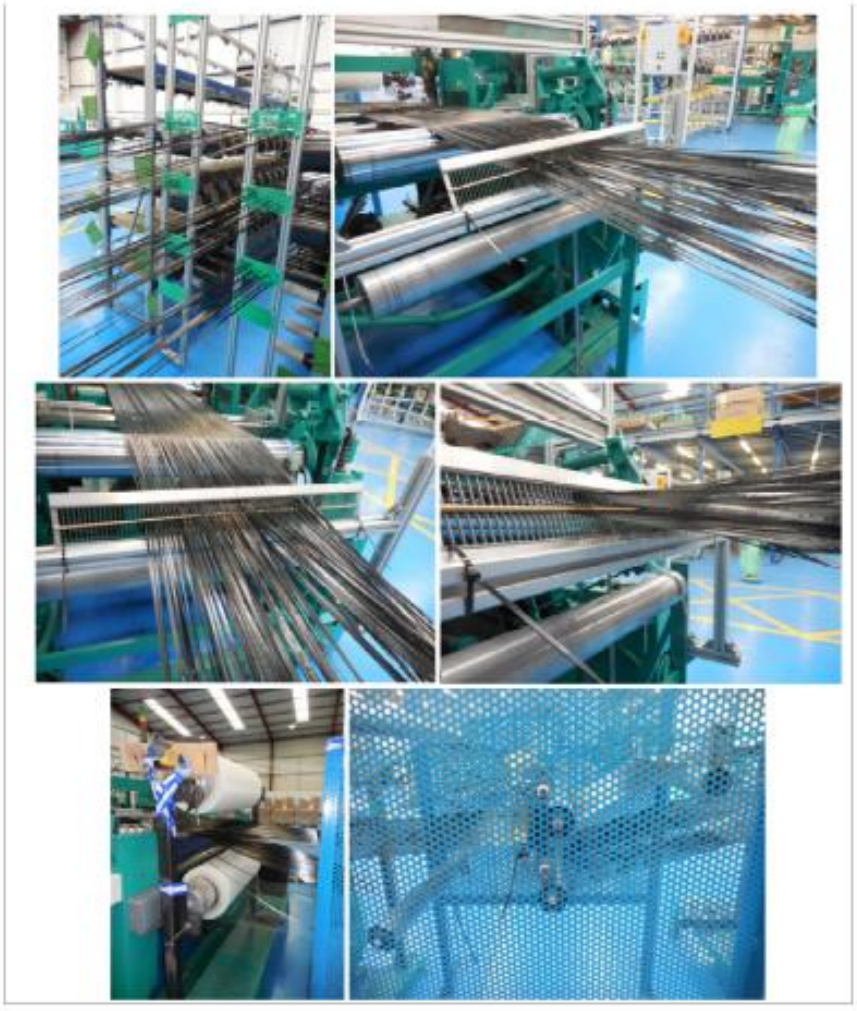
It is relatively easy to change the yarns spacing (although costly as it requires increasing the equipment set-up time, but can be achieved relatively easy as it is an in-house procedure) than changing the dtex, as well percentage of coating, of the yarns as this requires a different material supply from a different manufacturer. However, for a biaxial (usually a $0^o/90^o$ orientation architecture) scrim, it is very expensive to change the spacing of the yarns in the warp direction. The manufacturer is required to have a high number of yarn bobbins in the warp to change the yarn spacing, depending on the spacing of the required spacing of the yarns. Only one bobbin of material is required to change the weft by only changing the machine speed to change the weft spacing. This can reduce overall production costs. The automated fibre deposition technology that is used and discussed in a subsequent chapter, can allow for different scrim orientations thus reducing overall costs as well as production/cycle time.

Changing the dtex values is considerably more expensive than changing the yarn density. Moreover, a higher dtex can potentially introduce more crimp and as mentioned earlier it is more costly to change as it involves the scrim manufacturer ordering different types of yarns (the yarn manufacturer will require a minimum quantity order which the scrim manufacturer cannot justify). The carbon fibre bobbins had to be ordered, checked for availability

and consistency, transported to the process area and their quality had to be examined for any inconsistencies and defects.

5.3. Scrim-based Fabric development

The scrim supported fabrics were manufactured by using a laminating machine and support frames (figure 71) at the production line at Hexcel (application of heat and pressure) in order to have the scrim layers adhere to the carbon fibre tows. 120 to 130 bobbins of carbon fibre tows were required for each production of a single scrim supported fabric.



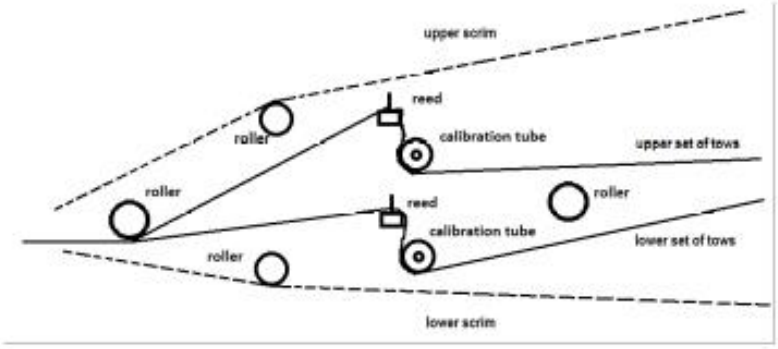


Figure 71: Laminating equipment for scrim-supported fabric manufacture and schematic (side view) of set-up

Setting up the carbon fibre bobbins takes approximately one work day. However, setting the rollers and support fixtures on the equipment so as to have the correct sequence that will enable the correct spreading of the tows and to acquire full fibre coverage was a more time consuming process, taking up several days of experimental time. Issues included the frame supports that the rollers could be mounted on could not be aligned to a very high degree (frame manufacturing issues). A 100 linear metres of each fabric (width: 500mm) were manufactured in order to allow for enough material for the testing to be completed (defective areas of fabric were cut/discarded). The set-up is shown in figure 72. As the only fabric manufactured and sold through Hexcel is a 300mm wide scrim-backed fabric, equipment was sourced in order to manufacture a wide sufficient material that could be used for the permeability measurement trials. Another time consuming part of the experimental trials was setting up, replacing (when broken) and monitoring the carbon fibre bobbins. This had to be repeated for each scrim version that was trialled. A reed was used at the start of the tow feed in order to acquire a more controlled tow width and therefore remove an unknown parameter that would potentially interfere with the permeability measurements at a later stage. Two rows (separating the upper and lower tows) were used. The upper set of the carbon fibre tows was offset covering evenly the gaps created from the lower set of tows.

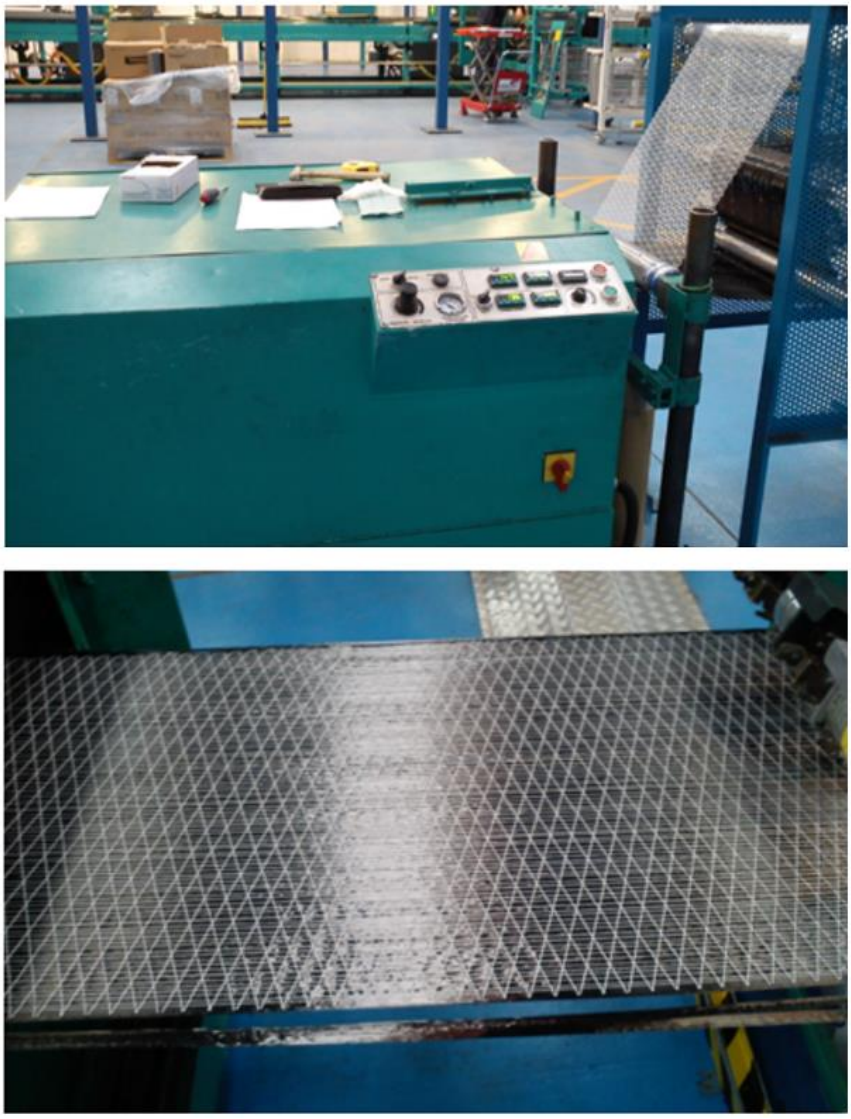


Figure 72 Laminator equipment and manufactured fabric

Issues:

- An additional reed was used (between the carbon fibre bobbins and the rollers) to help guide the tows (to avoid tow twisting)
- The scrim materials have different types and percentages of coating: the temperature and pressure in the laminator equipment had to be adjusted each time (multiple trials – time consuming) otherwise the adhesion between carbon fibre tow and scrim would not be successful. Several types of scrims had to be discarded since it was not possible to manufacture the fabric

Three types of scrim versions with the same number of yarns in the warp and different number in the weft were designed and manufactured for this project by James Dewhurst and are shown in figure 73 and 74. The scrim materials were also rotated at 90^{o} in order to produce additional fabrics with the different number of scrim yarns in the warp. Trials showed improved adhesion with this type of scrim (and type of scrim coating and core stability) and the material was suitable for manufacture of scrim supported fabric with no issues. The two studies are divided into two parts (sections 5.3.1 and 5.3.2).

1. 4x2: 2 yarns in the warp (at 0^{o} orientation) and 4 yarns in the weft (at 90^{o} orientation) per 10mm
2. 4x3: 3 yarns in the warp (at 0^{o} orientation) and 4 yarns in the weft (at 90^{o} orientation) per 10mm
3. 4x4: 4 yarns in the warp (at 0^{o} orientation) and 4 yarns in the weft (at 90^{o} orientation) per 10mm

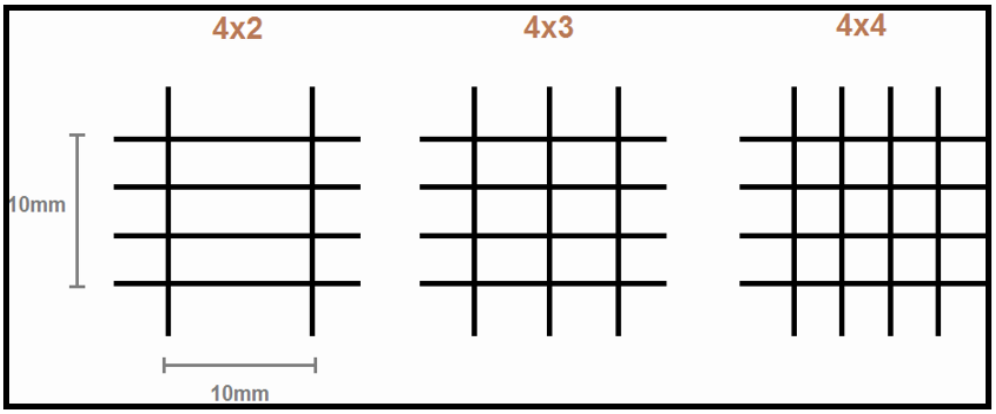


Figure 73 4x2 , 4x3, 4x4 scrim architectures overview

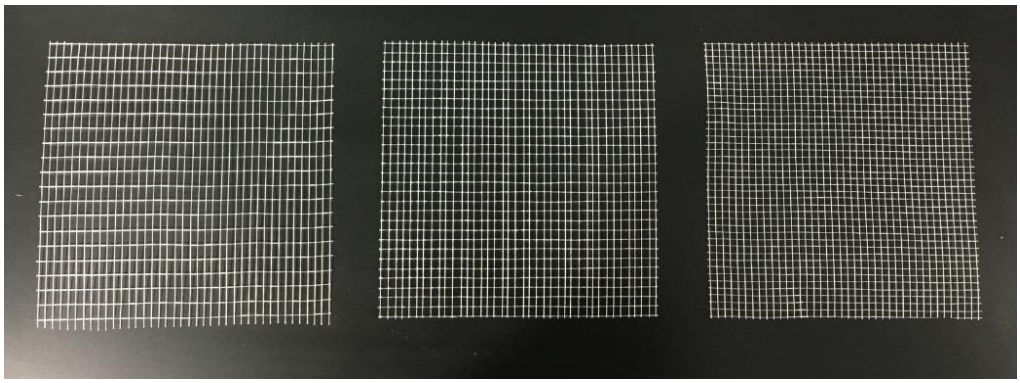


Figure 74 Scrim materials , 4x2, 4x3, 4x4

5.3.1. Scrim-based Unidirectional Fabrics: Part 1

This study focuses on the influence of geometrical parameters of scrim on the permeability of carbon fibre non-crimp fabrics. The carbon fibre fabrics studied comprise of unidirectional carbon fibre bundles (24 K), aligned in the warp direction. The scrim consists of thermoplastic threads arranged in a bi-directional open mesh construction, which are adhesively bonded onto the carbon fibre bundles. The scrim consists of yarns in the warp and the weft orientation at a 90^{o} angle. In figures 75 and 76, close up views of the 4x2 and 4x4 scrim materials are shown for comparison. The in-plane permeability of the fabrics, i.e. the two principal in-plane permeability values and the angle indicating the main flow direction, was characterized in unsaturated radial flow experiments at constant injection pressure. Experimental observations show that the in-plane permeability of the scrim-backed fabrics is affected by the scrim architecture. As the permeability of unidirectional carbon fibre bundles is inherently high parallel to the fibre direction and low in the transverse direction, when a scrim is added, flow is locally enhanced parallel to the fibre bundles, since the geometry of flow channels formed in the fabric is affected. In particular, new flow channels can form along transverse scrims threads which can increase the transverse fabric permeability.

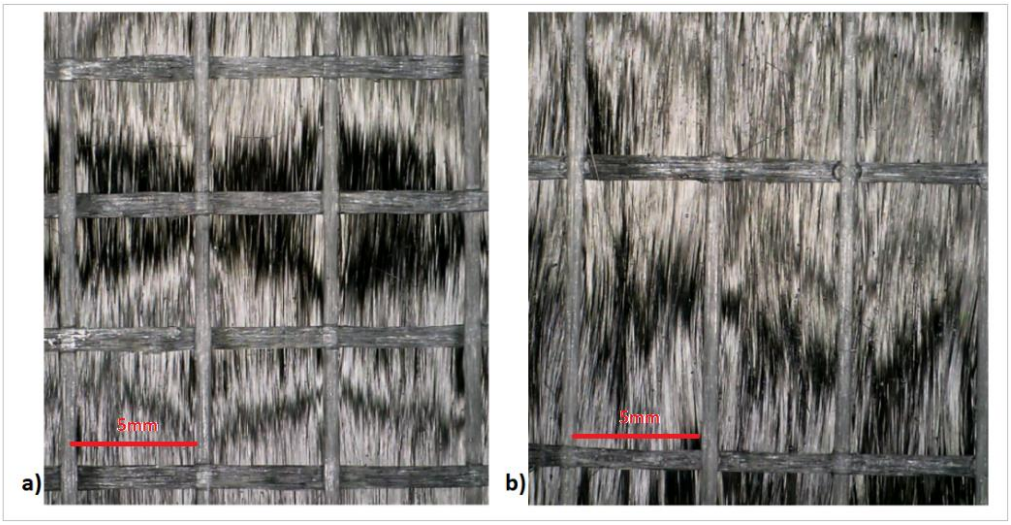


Figure 75 Top view: a)4x4 scrim, b)4x2 scrim

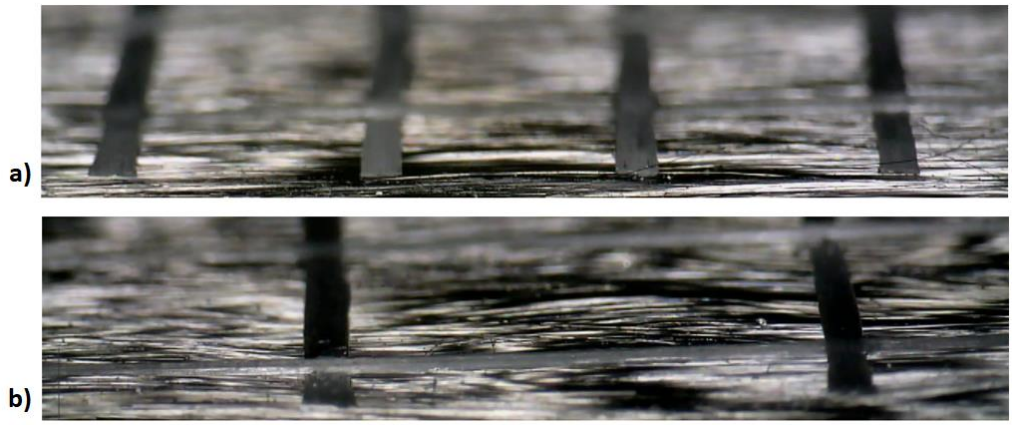


Figure 76 Side view (fabric titled at 85^{o} relative to the microscope set-up): a)4x4 scrim, b)4x2 scrim

The manufactured fabric can be seen in figure 77. The materials were examined for quality (consistency of the distance between adjacent scrim yarns) and the results are plotted in figure 78, where only for the 4x3 scrim the weft oriented yarns were approximately 10% off of the manufacturing specifications. For all other scrim types, the quality was satisfactory and following the specifications from manufacture.



Figure 77: Manufactured fabric - top (left) and bottom (right) view

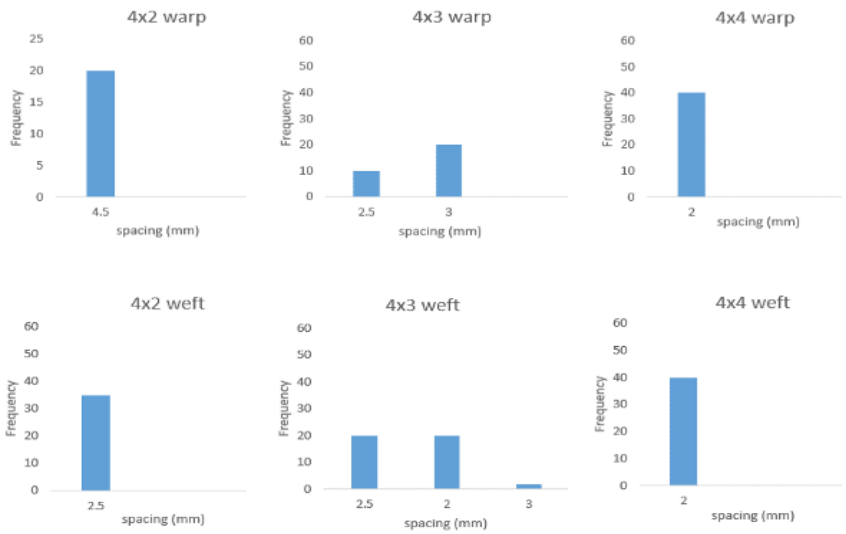


Figure 78: Measuring the distance between two adjacent scrim yarns for the three types of scrim material

5.3.1.1 Permeability of Scrim-based Unidirectional Fabrics: Part 1

The permeability of the fabrics was analysed at three fibre volume fractions, which were obtained by combining an appropriate number of fabric layers in the specimens with the height of the cavity in the permeability measurement tool (Table 11) and the results are listed in figures 79 and 80.

target V_f	number of layers	cavity height / mm
0.38	4	1.5
0.44	4	1
0.55	5	1

Table 10 Combinations of numbers of fabric layers and cavity height to obtain target fibre volume fractions

Non-crimp fabrics exhibit macro-scale uniformities that are determined by the movement of the fibre bundle [79]. This movement is affected by the porosity/voids between the carbon fibre bundles. In NCFs, where the stitch thread is the main influence on the fabric, is mainly mesoscopic uniformities.

The materials variability on non-crimp fabrics on permeability has been studied extensively and it the inherent material variability is evident in structural fabrics [79 – 82]. Inspection of the samples shows that the scrim threads create additional channel space on material 4x4 than material 4x2. The same effect was studied for non-crimp fabrics, where the flow is enhanced due to the gaps between the stitches [83]. Higher yarn density will influence the local permeability enhancing the preferential flow orientation which is determined by the carbon fibre packing in the fabric structure. Different scrim architectures and types have been found to have a significant effect in influencing the permeability of a non-crimp fabric. It was observed that the weft scrim yarns aid in increasing K_2 permeability, as the yarns "remain" on the surface of the tows, creating pathways (figure 81). Contrarily, when the scrim yarns are aligned parallel to the carbon fibre tows (in the 0^o direction), they appear to have little effect on the permeability values as the yarns in the scrim can nest between the carbon fibre filaments.

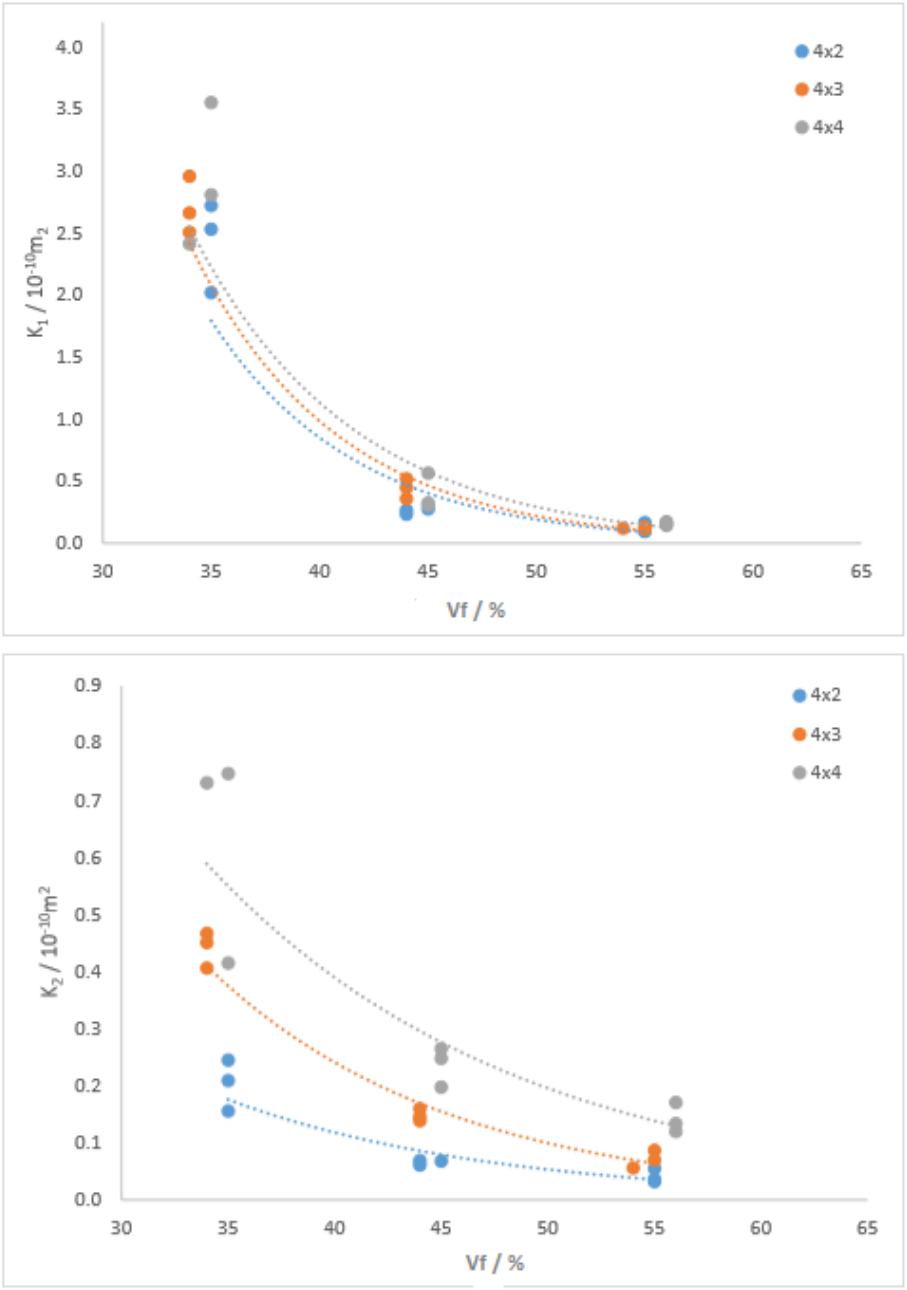


Figure 79: Experimentally determined data for principal permeability values, K1 and K2, as a function of the fibre volume fraction, Vf

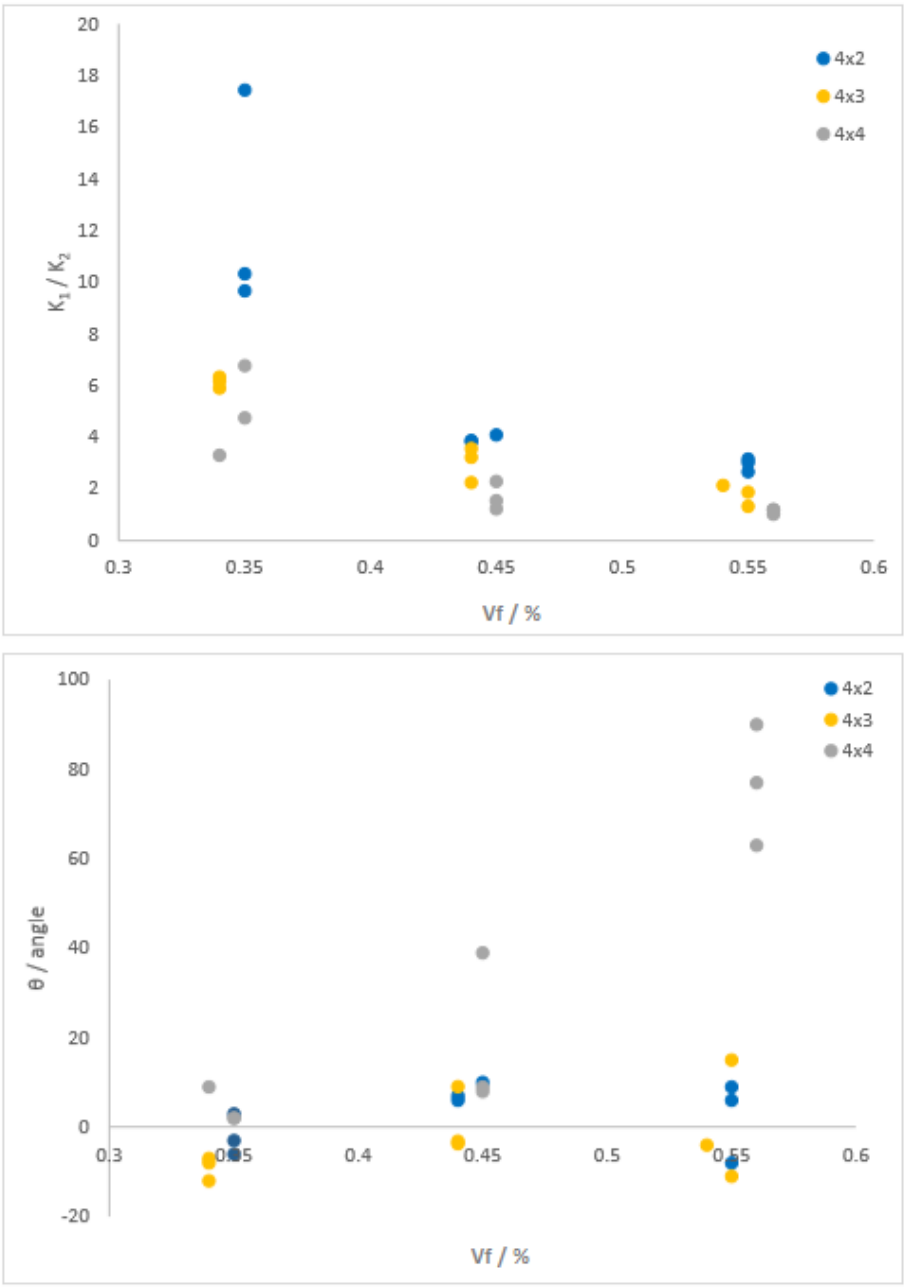


Figure 80 Experimentally determined data for ratio of anisotropy, K_1/K_2, and angle of flow (describing the orientation of the main flow direction) as a function of the fibre volume fraction, V_f

The main flow direction changes depending on the structure of the scrim version. For most fabrics and fibre volume fraction, trials show that the flow angle tends to deviate between 3 to 17 degrees. Only for the 4x4 scrim and at 55% fibre volume fraction the flow angle is between 63 to 90 degrees which might be explained by the higher compaction on the fabric, changing the flow due the higher scrim yarn count. In order to examine the behaviour of the scrim yarns in compaction, composite panels were manufactured using the 4x4 scrim supported fabric. Using vacuum bag infusion with epoxy resin, and using a one layer of fabric stack, composite test panels were manufactured. In order to have a view of the top surface of the panel at the same time as to examine the cross-section of the test panel, a different method was used. The material was examined using a digital microscope set at a distance of 10mm. Aluminium plates were used as supports to mount the samples. The composite was tilted at 85^{o} relative to test bench in order to be able to show the surface of the scrim yarns as well as the cross-section. In the warp direction (direction of the carbon fibre filaments) the scrim yarns appear to nest between the fibres whereas in the weft direction, the scrim yarns tend to flatten and remain on the surface of the carbon fibre tows. This might explain the increase in K_2 permeability, when the scrim yarn number is increased.

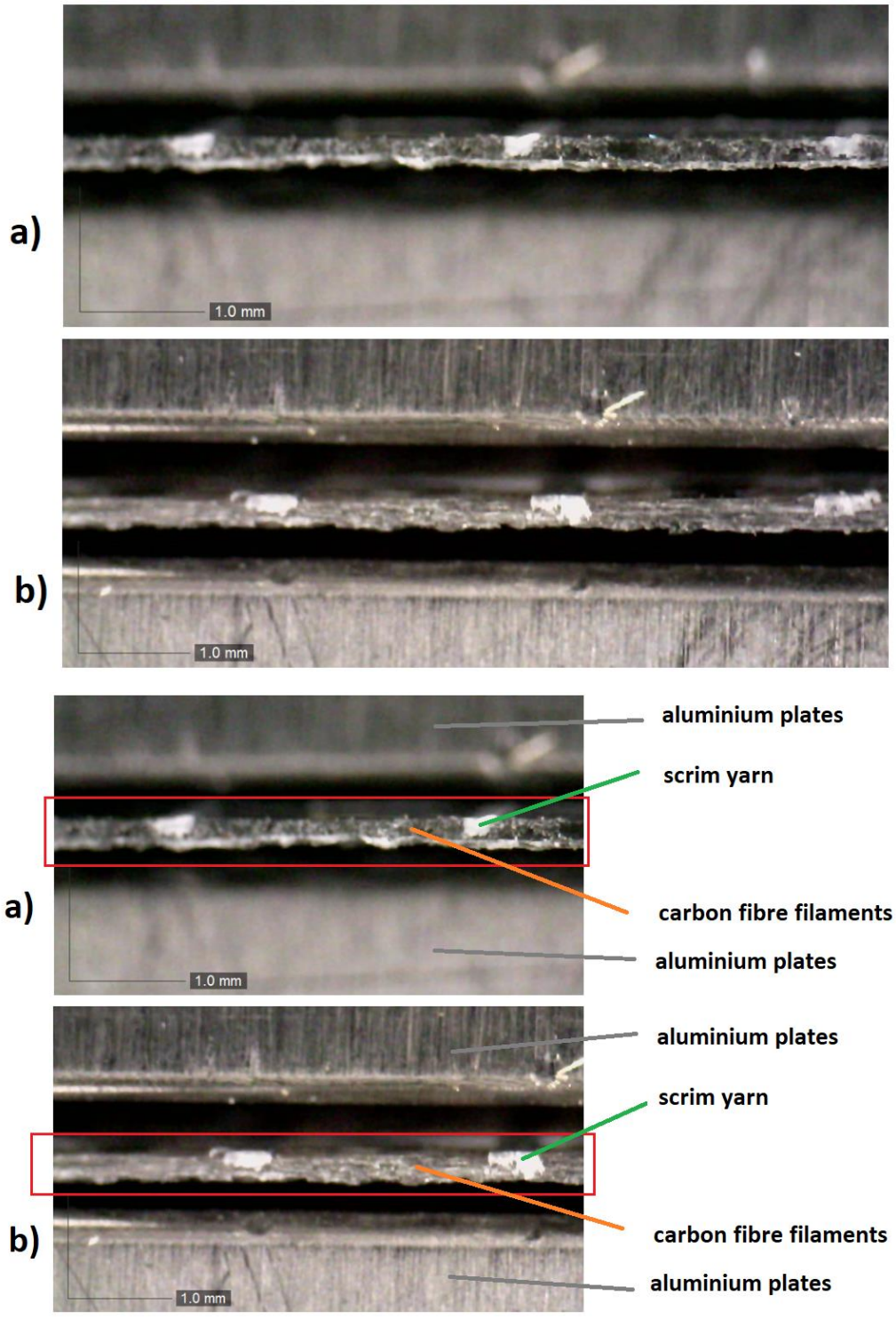


Figure 81 Top image: a) 4x4 scrim warp direction (direction of the fibre), b)4x4 scrim weft direction. Bottom image: same image with notations

Geometrical changes resulting from the different scrim architecture can alter a liquid's (in this study silicone oil) flow in different patterns. As a result, the permeability parallel to and transverse to the carbon fibre bundles can change with the different spacing of the scrim yarns. These gaps/channels will have a tightly packed arrangement of polyester filament yarns that might disrupt or aid the resin flow during composite manufacture. It has been studied that variations in the calculated permeability values are usually caused by local changes in fibre misalignment and changes in the thickness in different areas of a stitched fabric as well as nesting [84 – 88]. The scrim in the newly developed fabrics aids in supporting to a higher degree the fibre filaments which can lead to uniformity in the target fibre volume fraction.

In the principal permeability K_2, by increasing the spacing between two adjacent scrim yarns the permeability decreases. As a result, the ratio of fabric permeabilities parallel and transverse to the carbon fibres was found to decrease with increasing stitch thread density. Another effect of the transverse scrim yarns might be that they are" pushing down" onto the surface of the fabric and thus decrease the warp permeability due to reducing the cross-sectional area of the fibre bundle, where the flow channels are initially created. Moreover, this can result in changes in the cross-sectional shape of the carbon fibre tows, the warp scrim yarns and also the gaps between the carbon fibre tows. Moreover, the scrim yarns consist of individual filaments and for the three scrim versions the count number was 48. These filaments might be "spreading" to different degrees during compaction, thus altering the degree of influence on permeability.

5.3.1.2 Correlation between the scrim yarn spacing and permeability: Part 1

Measuring the distance between adjacent scrim yarns in the weft direction (perpendicular to the fibre direction) for each material:

4x4 – 2mm distance between 2 scrim yarns

4x3 – 2.25mm distance between 2 scrim yarns

4x2 – 2.5mm distance between 2 scrim yarns

Calculating the mean permeability (average of all points at a given fibre volume fraction – figure 82):

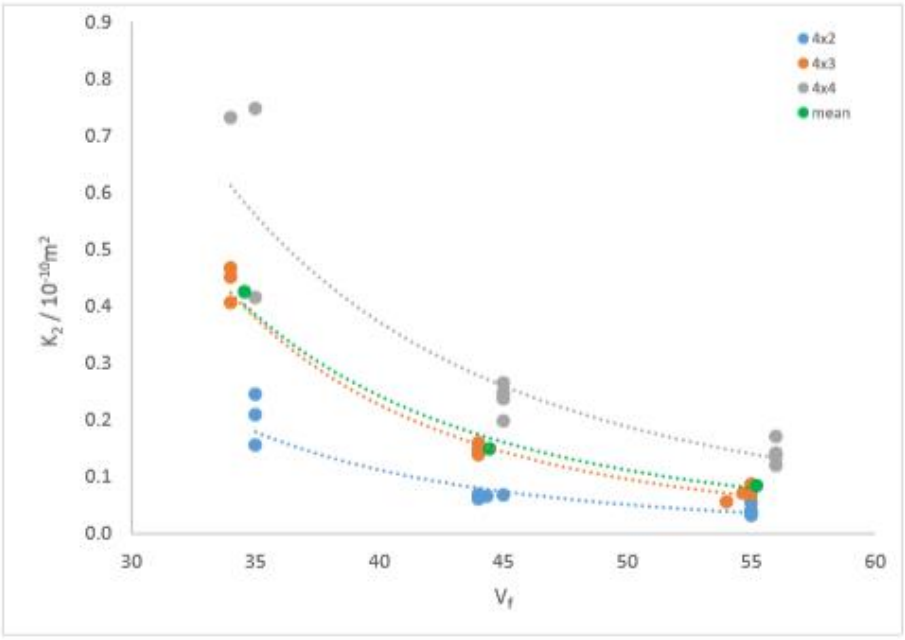


Figure 82: Calculated mean permeability

Mean permeability fitted curve:

$$K_2 = m * FVF^{-3.464} \quad (8)$$

Where m: constant

Proposing a relationship that would relate K_2 permeability with the distance between two adjacent scrim yarns (validation results are plotted in figure 83):

$$K_2 = 8^8 * 10^{-x} * FVF^{-3.464} \quad (9)$$

Where

x: distance between 2 adjacent scrim yarns

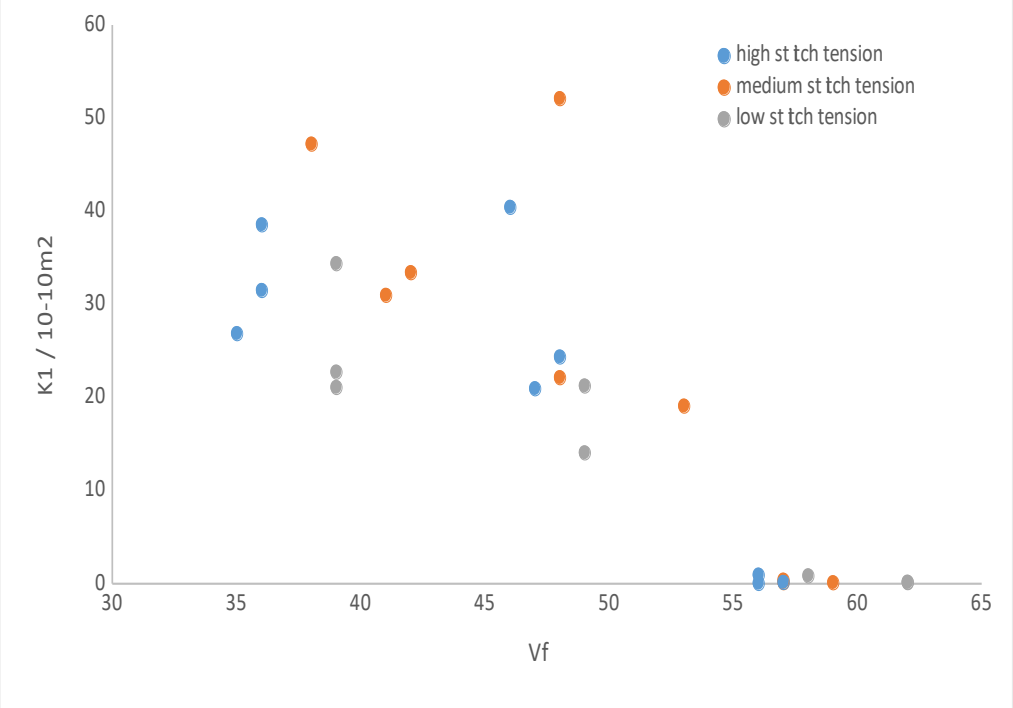


Figure 83 Predicted and calculated permeability

The K_2 permeability would decrease when the distance between two adjacent scrim yarns increases (figure 84). As the warp scrim yarns (0^o direction yarns – parallel to fibre direction) have a negligible influence on K_1 permeability, their number can be as low as possible (without sacrificing fabric stability) in order to reduce overall fabric weight.

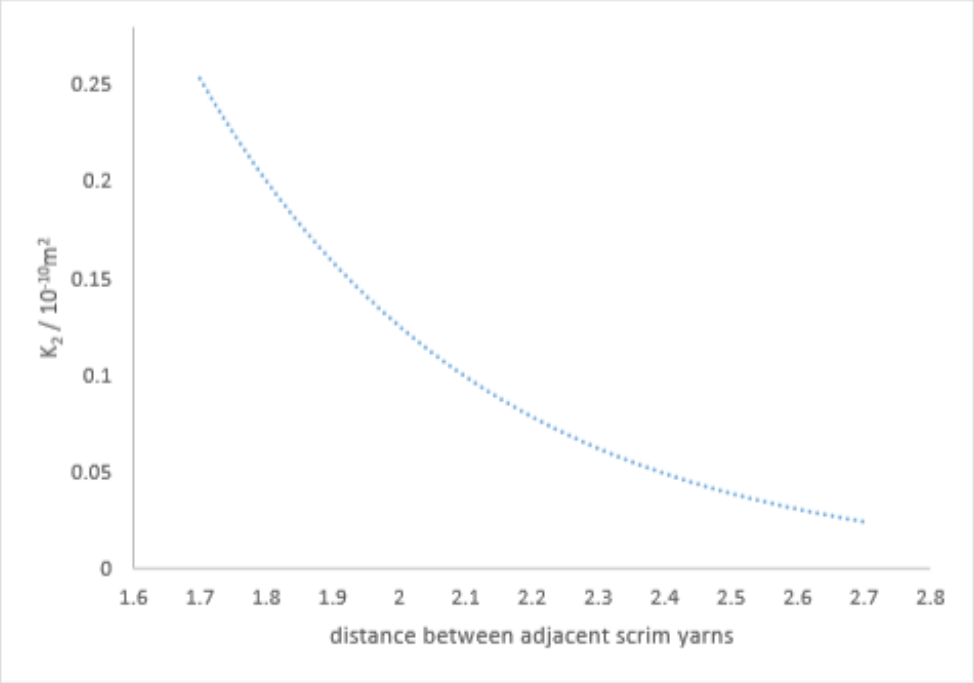


Figure 84: Correlation between the K2 permeability and the distance between the two weft scrim yarns at 55% fibre volume fraction

5.3.2 Scrim–based Unidirectional Fabrics: Part 2

The same scrim materials were used for this second study. However, the scrim was rotated at 90^{o} in order to examine when the spacing of the weft scrim yarns is the same and the warp changes what is the effect on the physical properties of the fabric. In this study again, the permeability of carbon fibre textile reinforcements for the purpose of comparing different architectures was investigated.

5.3.2.1 Permeability of Scrim-based Unidirectional Fabrics: Part 2

The permeability of the fabrics was analysed at three fibre volume fractions, which were obtained by combining an appropriate number of fabric layers in the specimens with the height of the cavity in the permeability measurement tool and results are listed in figures 85 and 86. It can been seen that when the number of scrim yarns are the same in the weft, the permeability is similar for all the scrim versions. The differences in the principal permeabilities is less pronounced in this set of materials. Although both permeabilities tend to increase with increasing scrim yarn density, as the scrim warp yarns tend to nest between the carbon fibre filaments the effect appears less significant. The ratio of anisotropy is similar to that of the first set of scrim materials set-up as well as the angle of flow. Overall, the scrim layers in the fabric might be preventing the fibres from nesting and increase K_2, as the major source of scatter in the permeability values is the nesting of the fibre filaments, and the different parameters of the fibre architecture. The ratio K_1/K_2 high value indicates a strong influence of the scrim material for all fabrics.

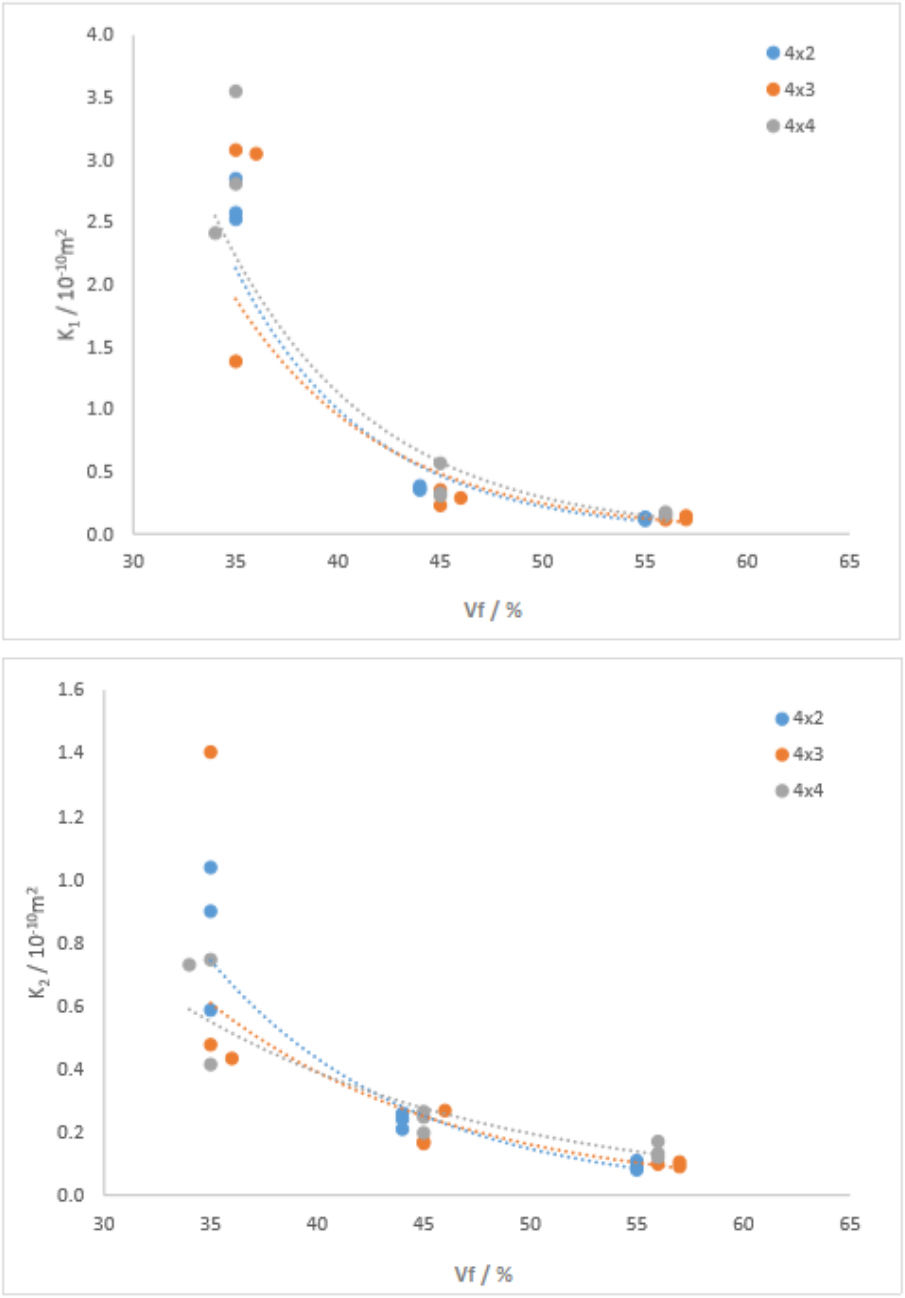


Figure 85 Experimentally determined data for principal permeability values, K_1 and K_2, as a function of the fibre volume fraction, V_f

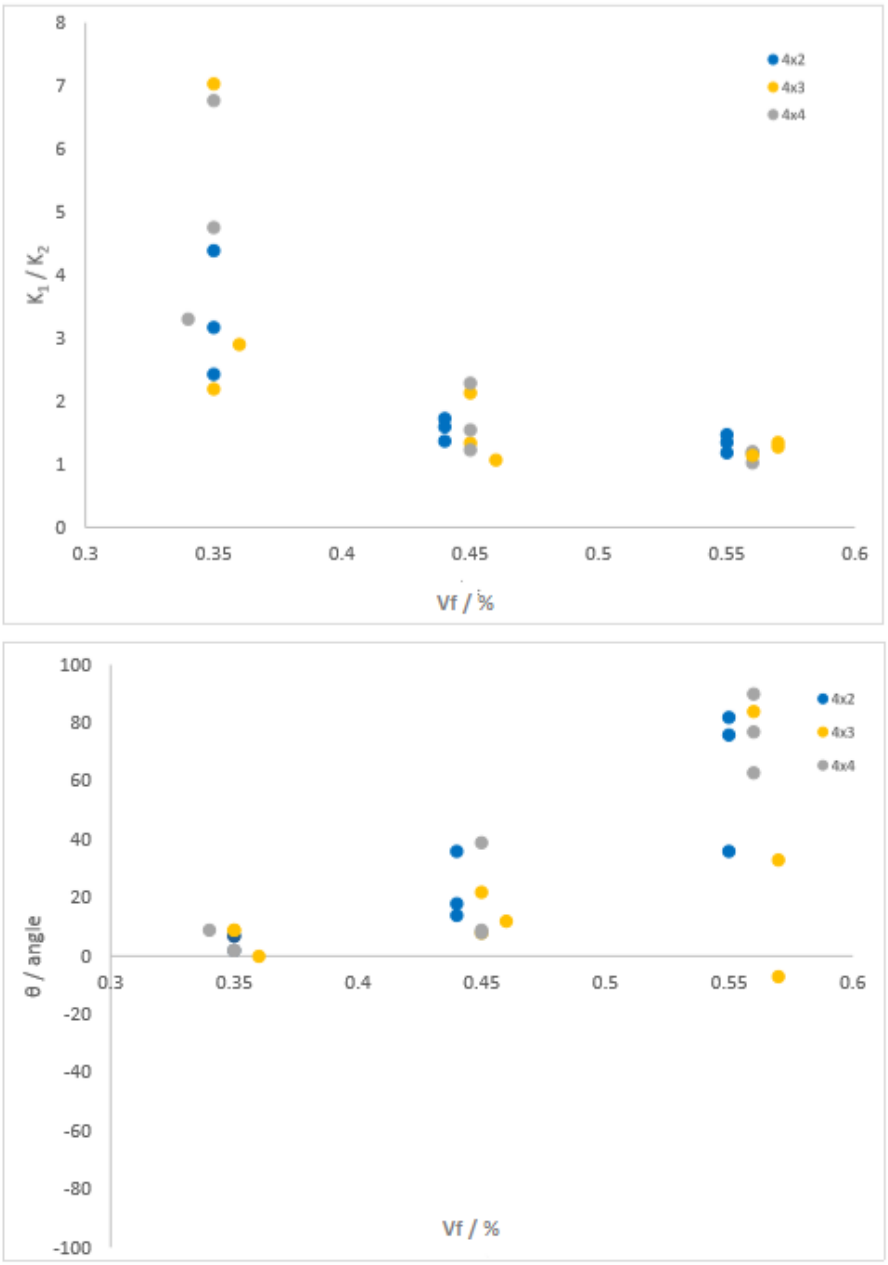


Figure 86 Experimentally determined data for ratio of anisotropy, K_1/K_2, and angle of flow (describing the orientation of the main flow direction) as a function of the fibre volume fraction, V_f

5.3.3 Scrim-based Biaxial Fabrics

Two layers of fabric, oriented at -45°/+45° were produced for the manufacture of biaxials NCFs in order to examine the effect of scrim on multiaxial non-crimp fabrics produced on the new Automated Fibre Placement process. The scrim yarn density is kept the same with the one with the first set of the unidirectional fabrics.

5.3.3.1 Permeability of Scrim-based Biaxial Fabrics

The permeability of the fabrics was analysed at three fibre volume fractions, which were obtained by combining an appropriate number of fabric layers in the specimens with the height of the cavity in the permeability measurement tool (Table 11) and the results are listed in figures 87 and 88.

target V_f	number of layers	cavity height / mm
0.36	3	2
0.48	4	2
0.62	5	2

Table 11 Combinations of fabric layers and cavity height to obtain target fibre volume fractions

For the K_1 permeability values, there is no distinct difference between the three scrim type materials. The warp scrim yarns might not contribute to a significant degree to the K_1 permeability. As the inherent low permeability of carbon fibre tapes in the transverse direction inhibits the flow front, the transverse scrims yarn can increase the permeability of the structural fabric. The yarns in the weft orientation can act as channels for the resin to flow and thus increase the permeability of the fabric. K_2 permeability tends to increase with increasing scrim yarn density and as with the first set of the unidirectional fabric, the scrim yarns maintain their shape on the surface of the carbon fibre bundles and thus provide flow channels. The ratio of anisotropy resembles that of conventional stitched fabrics, where K_1 and K_2 values are similar for each of fibre volume fraction.

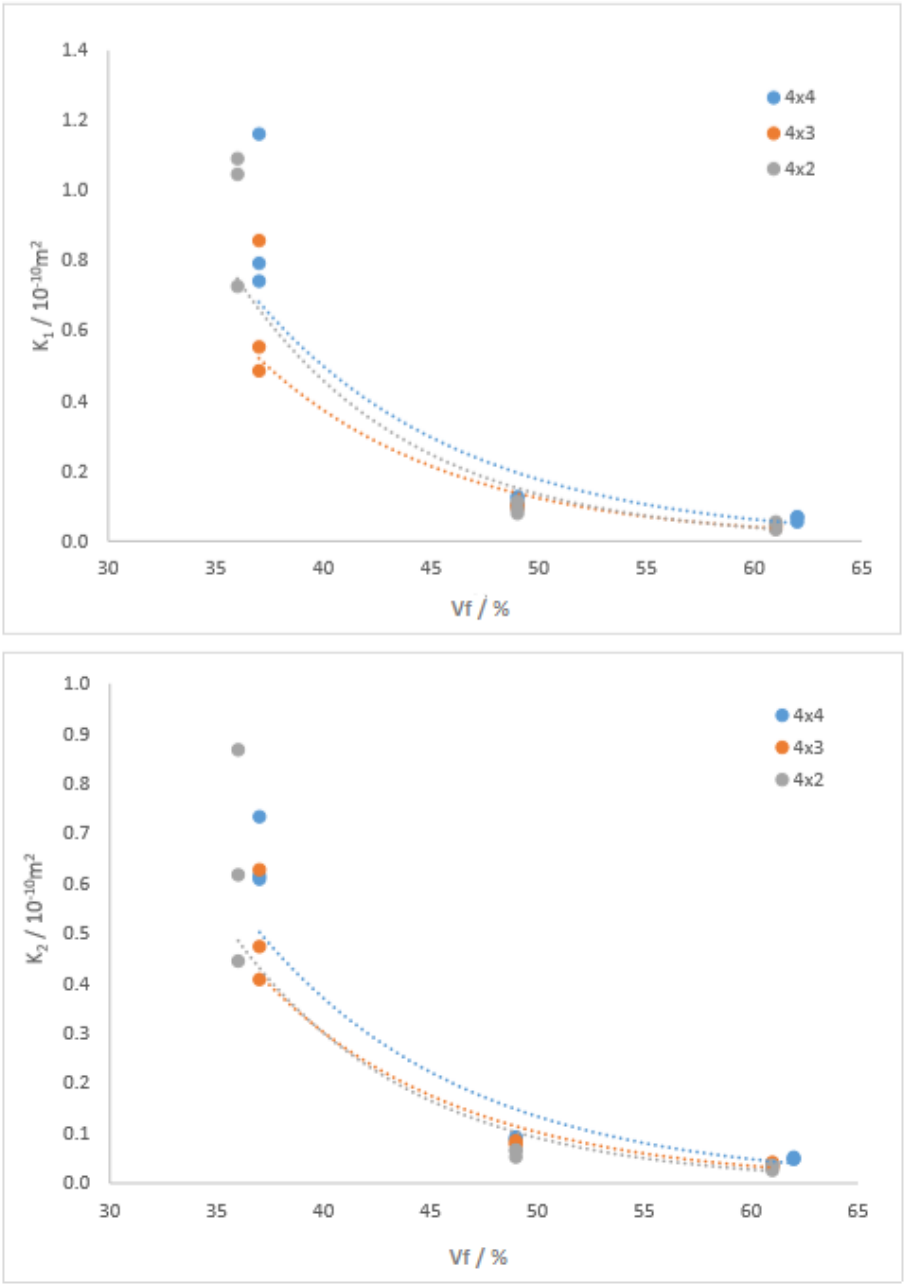


Figure 87 Experimentally determined data for principal permeability values, K_1 and K_2, as a function of the fibre volume fraction, V_f

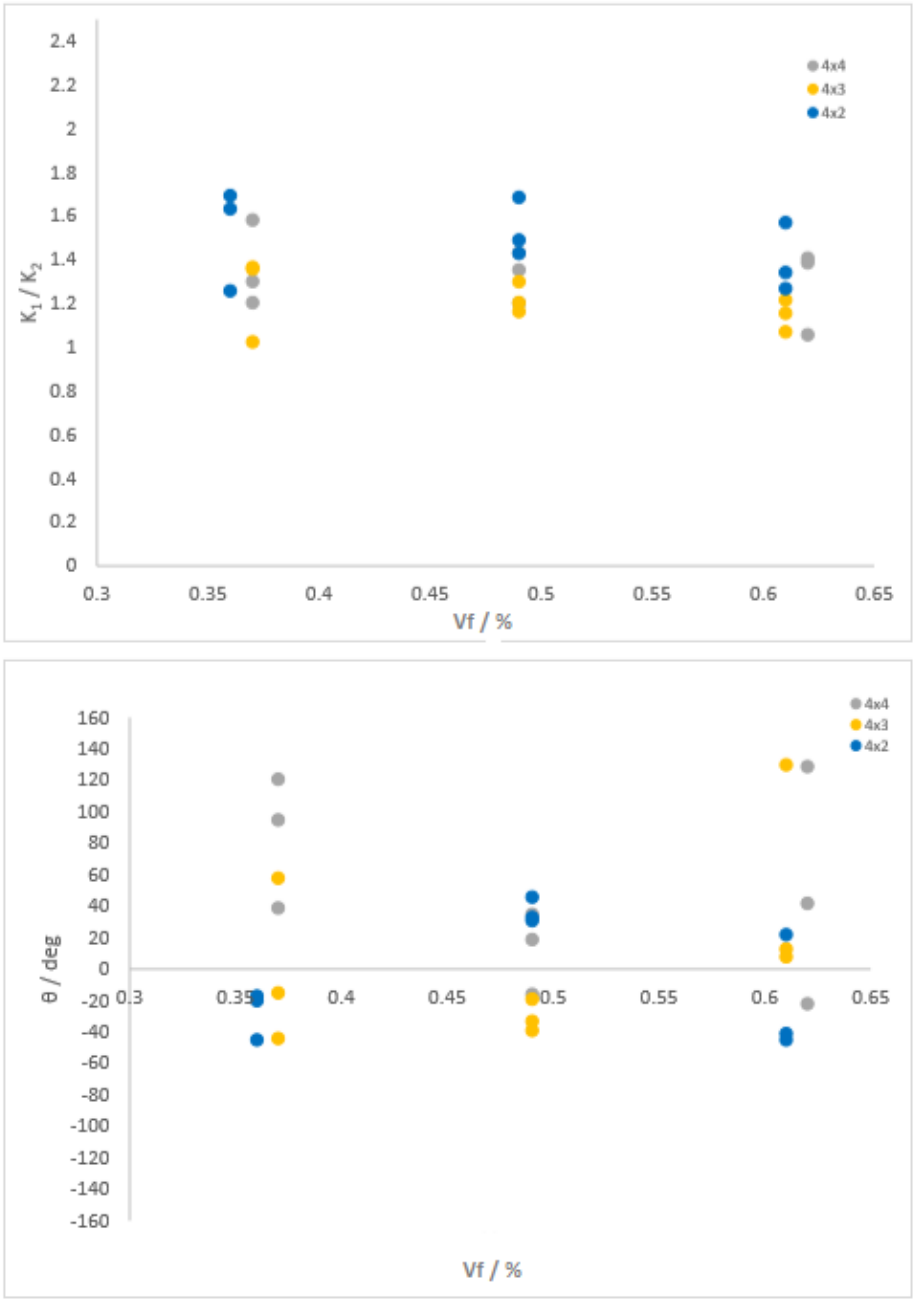


Figure 88 Experimentally determined data for ratio of anisotropy, K_1/K_2, and angle of flow (describing the orientation of the main flow direction) as a function of the fibre volume fraction, V_f

5.3.3.2 In-plane Shear of Scrim-based Biaxial Fabrics

The deformation resistance of scrim supported biaxial non-crimp fabrics have been assessed by using picture frame testing. The deformation resistance of non-crimp fabrics manufactured by means of the new automated fibre placement process is found to be significantly lower compared to that of conventional stitched fabrics due to the unique deformation mechanisms of sliding (mainly), rotation and compaction of the carbon fibre tows. The comparison between the 4x2 and 4x4 scrim supported fabrics in terms of shear are shown in figure 89. Both positive and negative shear behaviour is expected to be the same as the scrim yarns are located at 45^{o} relative to the fibre angle for both orientations. Moreover, in most studies it is agreed that the major issue when using the picture frame method is sample misalignment [91]. Even with most recent publications, a significant scatter of experimental values is observed indicating the difficulty in establishing a method that produces repeatable results [92, 93]. A robust method was developed in order to address this issue. By improving the design of existing picture frame test rigs, a new version was manufactured that offers higher accuracy than previous attempts.

It is shown that the density and location of the scrim yarns has a small influence on the deformation resistance of the materials. In comparison, varying the stitch thread parameters has a significant effect on conventional non-crimp fabrics. By altering any parameter of the stitch thread, the sliding mechanism that reduces the deformation resistance has an influence on the forming of non-crimps fabrics. The stitch thread conditions to minimise the deformation limits of non-crimp fabrics is well understood, for example the asymmetric shear behaviour of NCFs with pillar type stitch has been shown to be relative easy to control [89]. In a specific study it has been shown that a specific stitch thread pattern (tricot) has more asymmetric shear behaviour when the stitch length is longer [90]. However, the deformation mechanisms of the scrim supported fabric are different to conventional stitch fabrics. The bond strength between the scrim and the carbon fibre tow exhibit delamination during different stages of shear.

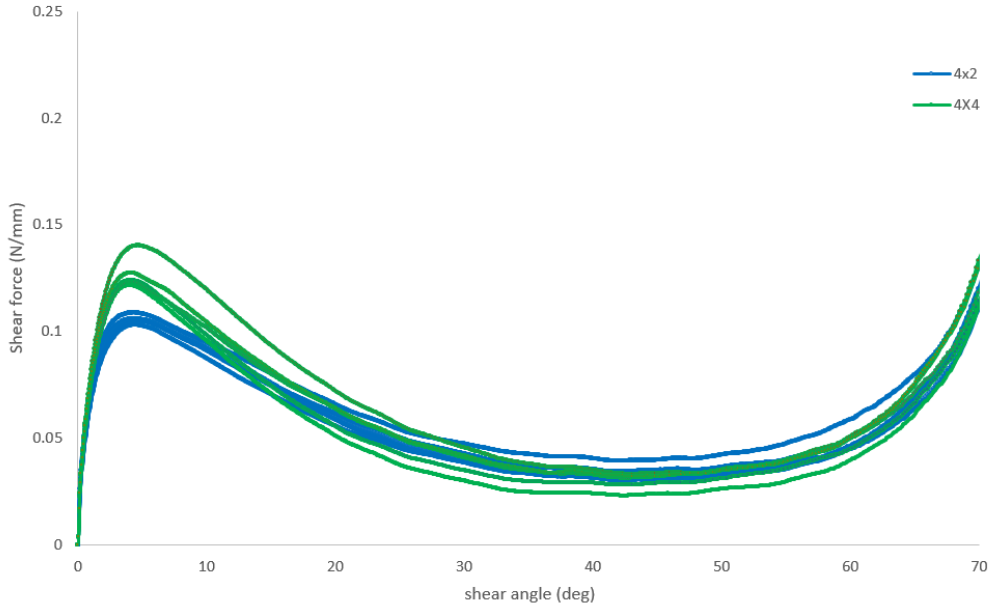


Figure 89 Shear force vs shear angle comparison between the 4x4 and the 4x2 types of scrim materials

5.3.3.3 Forming of Scrim-based Biaxial Fabrics

The main deformation mechanism in fabric reinforcements forming is shear and this is independent of the type of the fabric and the method followed to form the part on a geometry [94 – 96]. By using the Apodius system (digital imaging system), the deformation and the shear angle distribution for each preform was measured. Figures 90 through 93 show the analysis of the preforms of the fabric with high stitch thread tension while figures 94 through 97 the fabric with the low stitch thread tension is illustrated.



Figure 90 Manufactured preform 4x2

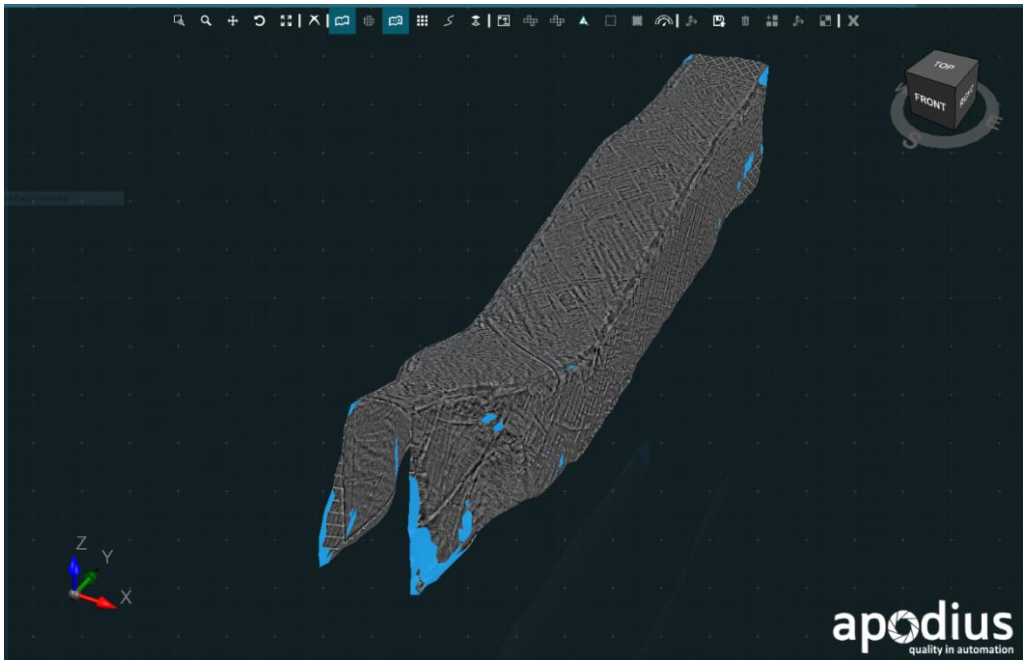


Figure 91 Scanning of preform 4x2 using the Apodious system

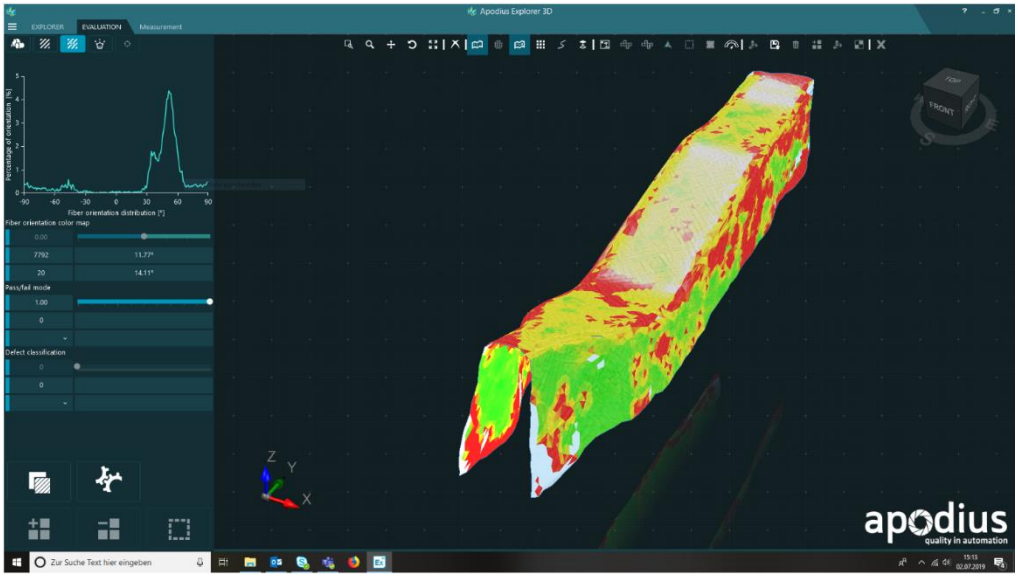


Figure 92 Analysis of the preform 4x2 using the Apodious software

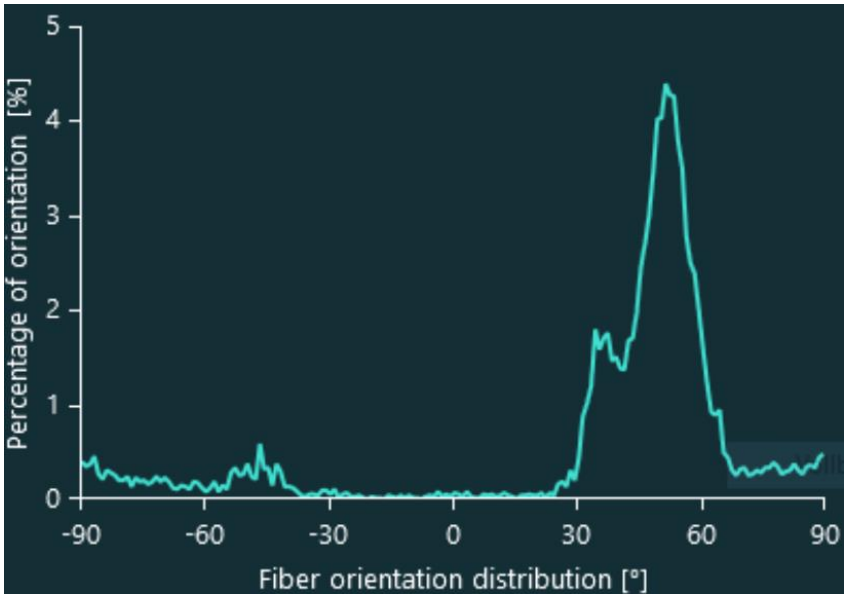


Figure 93 Fibre orientation distribution of the preform 4x2



Figure 94 Manufactured preform 4x4

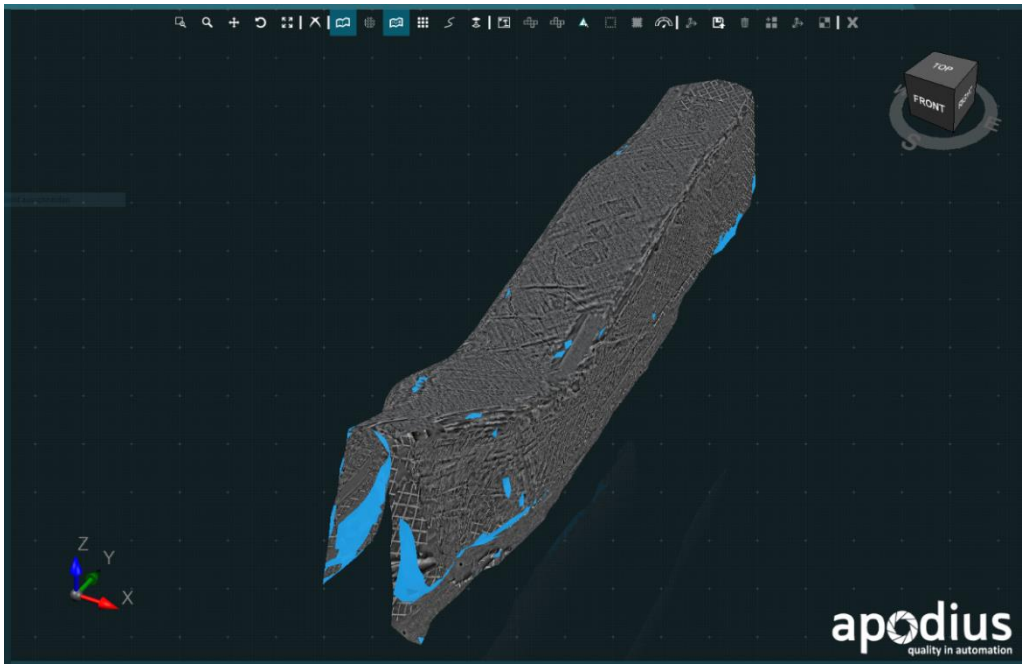


Figure 95 Scanning of preform 4x4 using the Apodious system

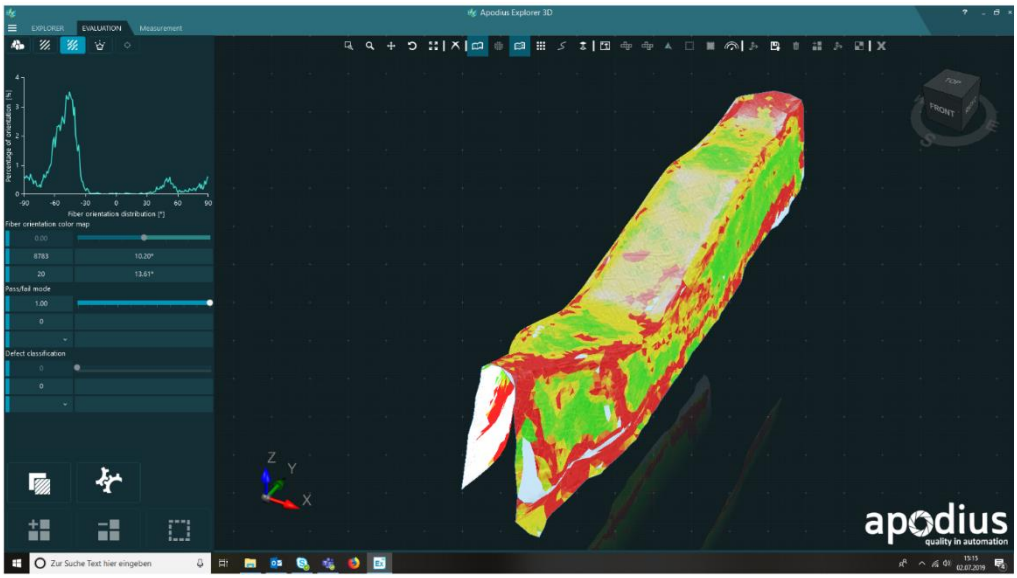


Figure 96 Analysis of the preform 4x4 using the Apodious software

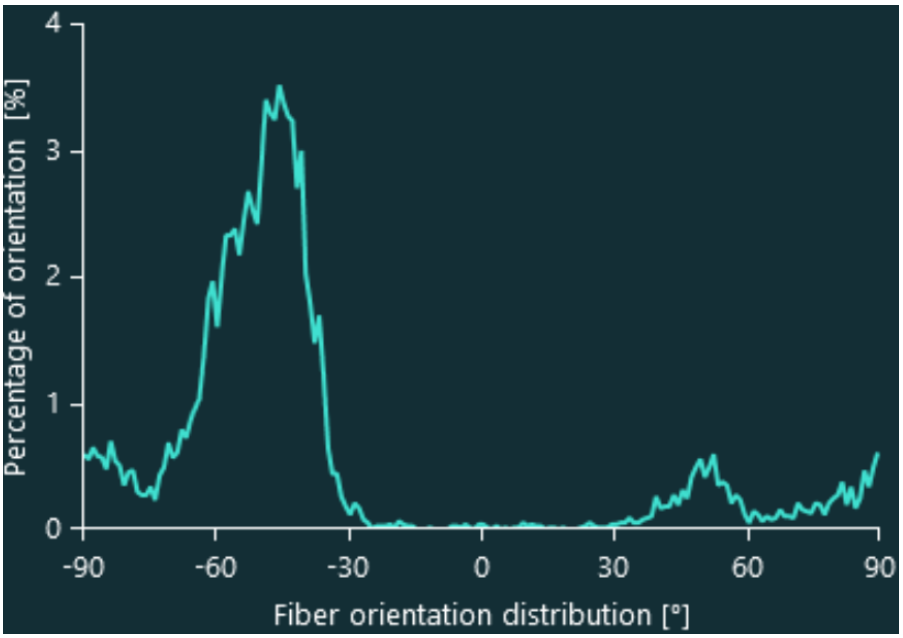


Figure 97 Fibre orientation destribution of the preform 4x4

When a textile is formed on a three dimensional geometry, a number of different deformation mechanisms occur with the most dominant the intra-ply shear. However, mechanisms such as crossover slip and un-crimping of the fabric, can affect the material deformation. Since only a specific number of fibre filaments are adhered to one side of the scrim material, their rotation is hindered during draping over the geometry. Although this phenomenon does not appear to affect the quality of the preform (and create defects such as gaps). Maximum shear occurs along the regions of double curvature and on the sides of the tool near these areas. Both fabrics exhibit similar behaviour during forming, where defects are minimal. Moreover, the fibre distribution for both the 4x2 and the 4x4 scrim materials is similar as expected when observing the in-plane shear results of the picture frame testing. The fibre angle distribution is between 30 and 60 degrees, with highest percentage at 45 degrees, as seen when using the digital imaging equipment. Results outside from this fibre angle region can be considered as interference that might occur either on how the system is used or the settings during the scanning process. Shear behaviour for both fabrics is similar, as it is observed in section 5.3.3.2, and coincide with the similar behaviour during forming and processing of the preforms with the Apodious system.

It has to be noted that although the distribution scale is in the negative zone, compared to the results of the 4x2 scrim, it should be considered as an absolute value. This is due to an error during testing were the top ply of the material was placed in reverse and thus the Apodius system registered negative values. While there is no difference between the positive and negative of the graph, the results are shown in negative as the placement of the fabric layer on the surface of the tool coincided with the negative registration of the tool. If the fabric layer was rotated at 180^{o}, the results would be in the negative zone. Some "spikes" in the graph showing results in the $+90^{o}$ zone are considered interference that might have occurred during the scanning process. The standard deviation can be calculated by the fibre angle distribution. In addition, for preform manufacturing no powder binder is required which eliminates an additional step to the composites manufacturing process compared when if a conventional stitched fabric was used to be used (figure 98).

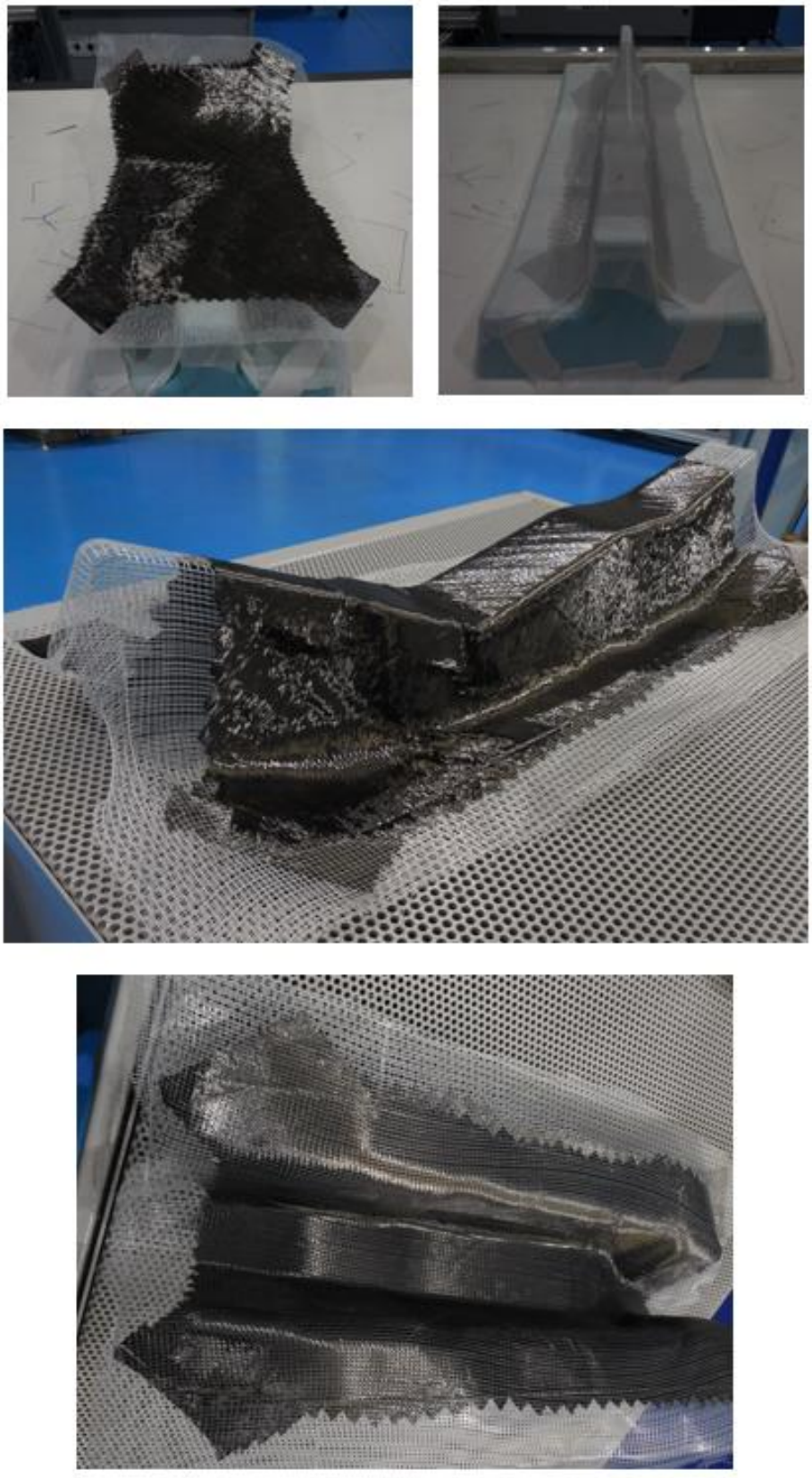


Figure 98 Preform manufacture using scrim material

5.4. Effects of Scrim Material Size (dtex)

Changing the dtex for triaxial scrim materials

Three different sizes of thread were chosen for this study: 74 dtex, 280 dtex and 1100 dtex with -30°/0/-30° scrim yarn orientations. The material parameters are listed in table 12. Although the scrim material with the 280 dtex has a higher number of warp yarns, conclusions can still be drawn from the experimental results. The trend for the K_2 permeability coincides with what is expected for the effect of larger value of dtex of the yarns in the scrim to be when placed on a flat surface (carbon fibre tows). An increase in permeability is observed for the larger diameter scrim yarns of the 1100dtex product. For the K_1 permeability values, there is no distinct difference between the permeability values for the 74 and 280 dtex values of the two scrim types. This can be attributed to the nesting effect to a degree, however the 1100 dtex scrim yarn has a significant influence to the K_1 permeability. The permeability measurement results are plotted and are shown in figure 99. The mean permeability of all points at a given fibre volume fraction is shown in figure 100.

Scrim code	core material	architecture	dtex
A200/20-74	polyester-filament-yarn	200 yarns - warp / 20 mm distance between the yarns - weft	74
A400/18-280	polyester-filament-yarn	400 yarns warp / 18 mm distance between the yarns - weft	280
A200/18-1100	polyester-filament-yarn	200 yarns warp / 18 mm distance between the yarns - weft	1100

Table 12 Materials parameters

Number of filaments in the scrim yarns:

74dtex – 24 filaments

280dtex - 100 filaments

1100dtex – 200 filaments

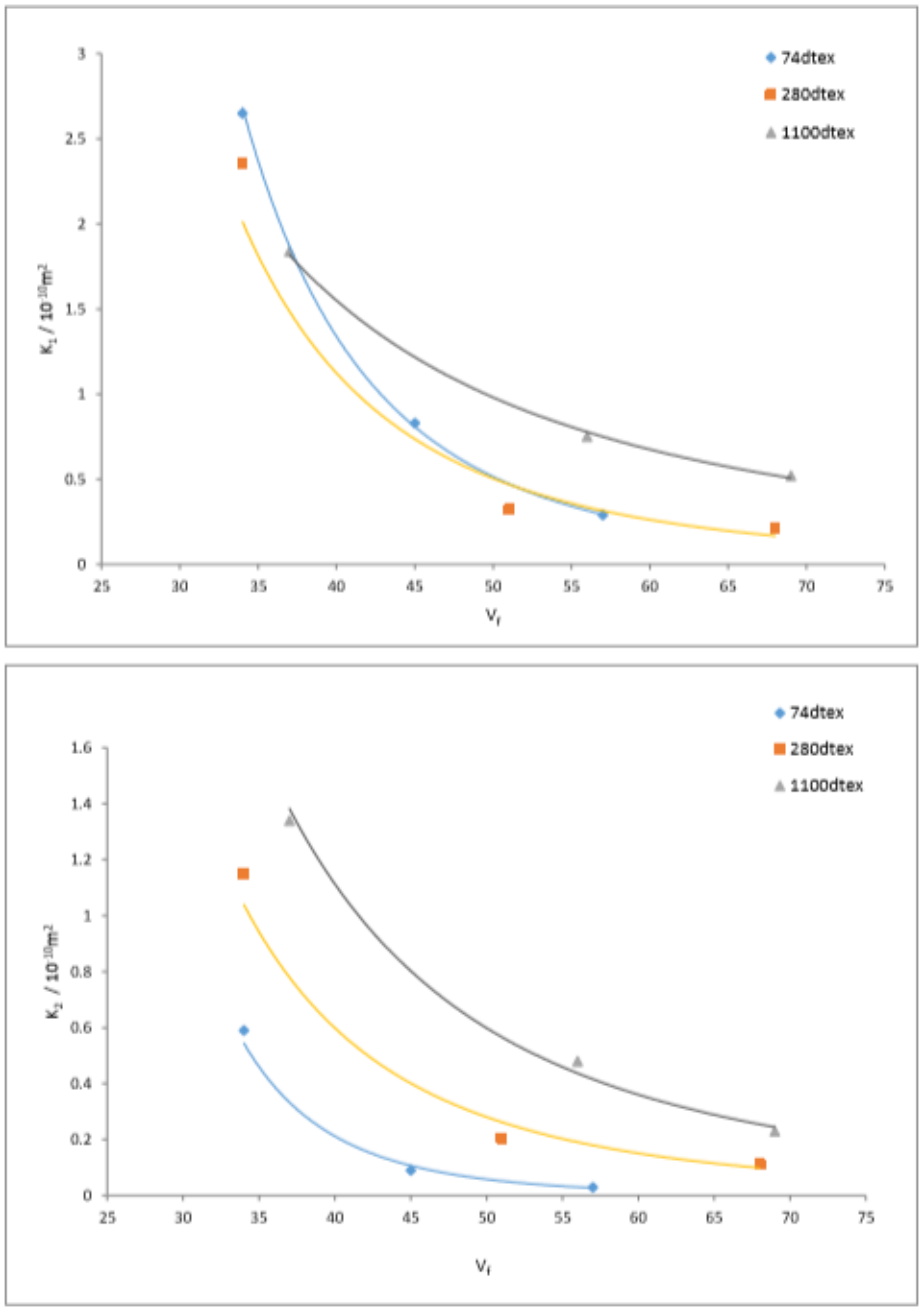


Figure 99: Experimentally determined data for principal permeability values, K1 and K2, as a function of the fibre volume fraction, Vf

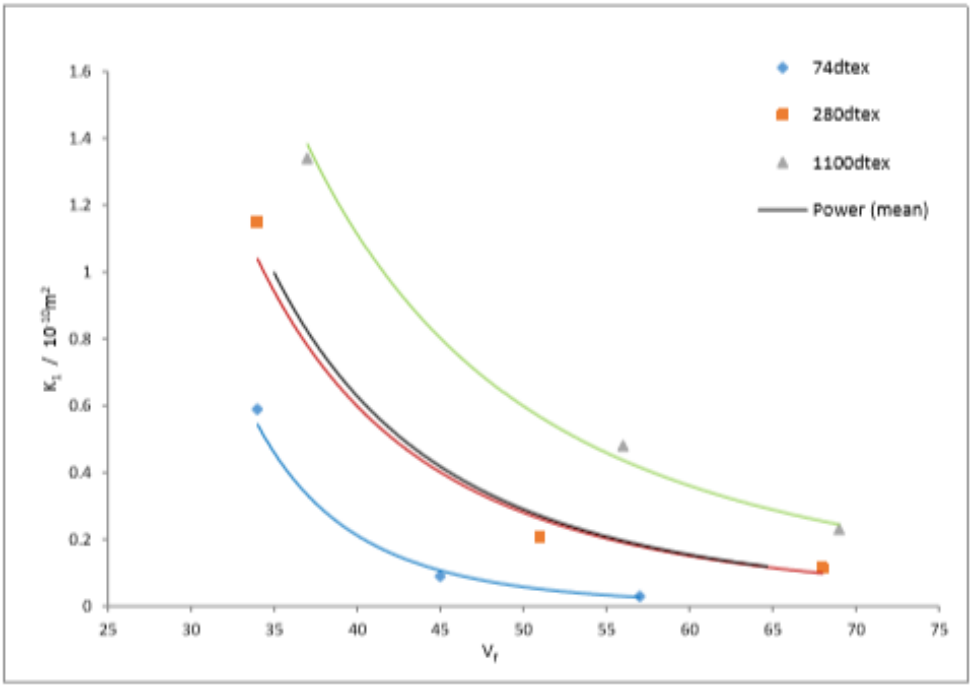


Figure 100: Calculated mean permeability

Mean permeability fitted curve:

$$y = 218066x^{-3.458} \qquad (7)$$

$$K_2 = m * FVF^{-3.458} \qquad (8)$$

Where m: constant

Proposing a relationship that would relate K_2 permeability with the different dtex of the scrim yarns:

$$K_2 = 50^2 * x * FVF^{-3.458} \qquad (9)$$

Where

x: number of filaments in yarn

A closer approximation (validation results are plotted and are shown in figure 101):

$$K_2 = 50^2 * x * FVF^{-3.5} \qquad (10)$$

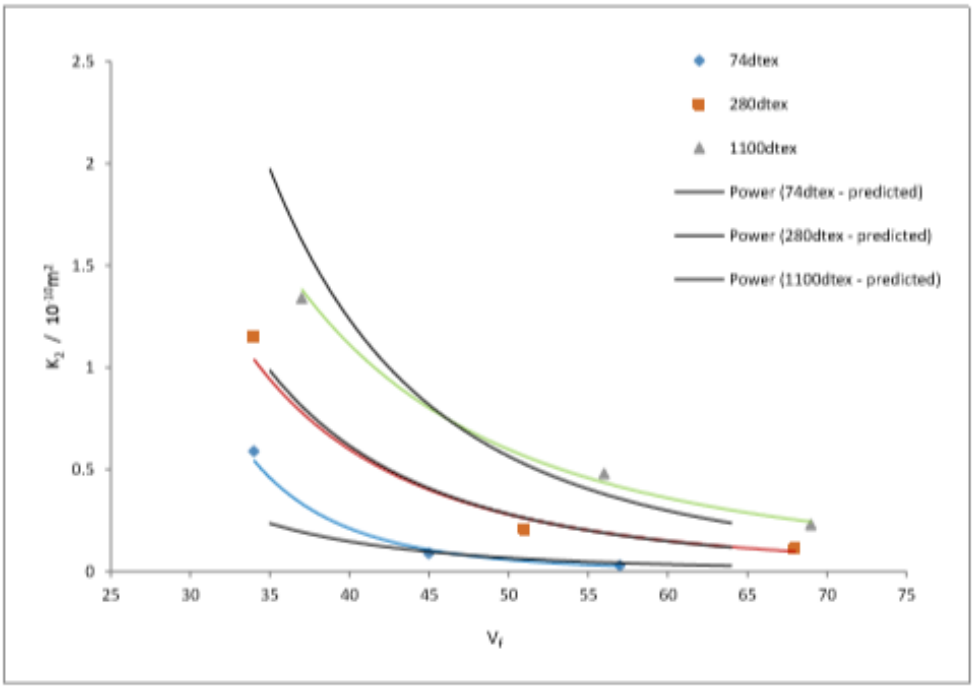


Figure 101: Predicted and calculated permeability

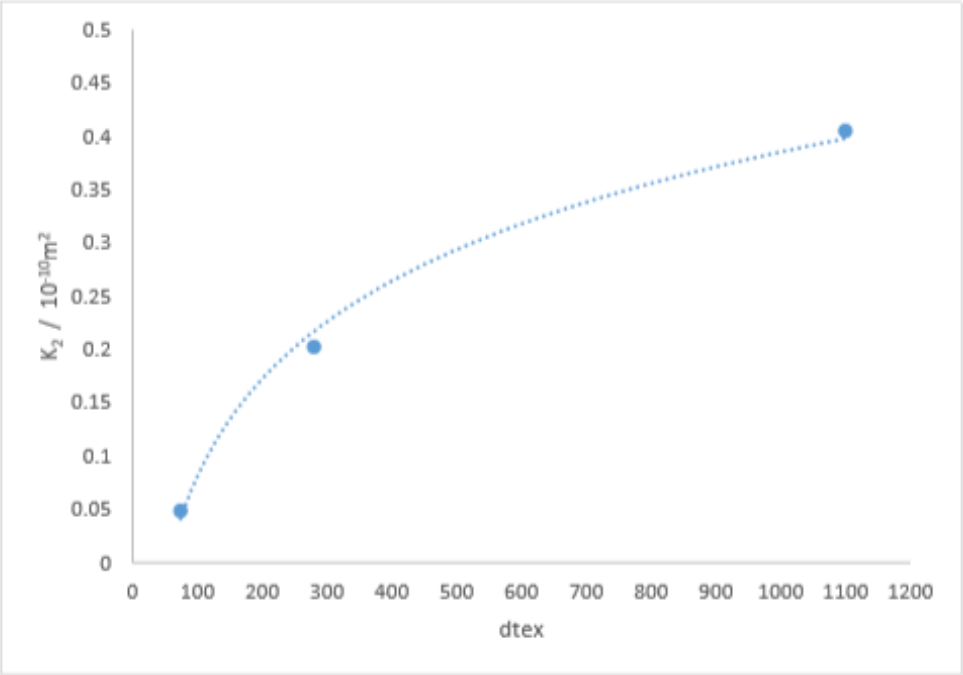


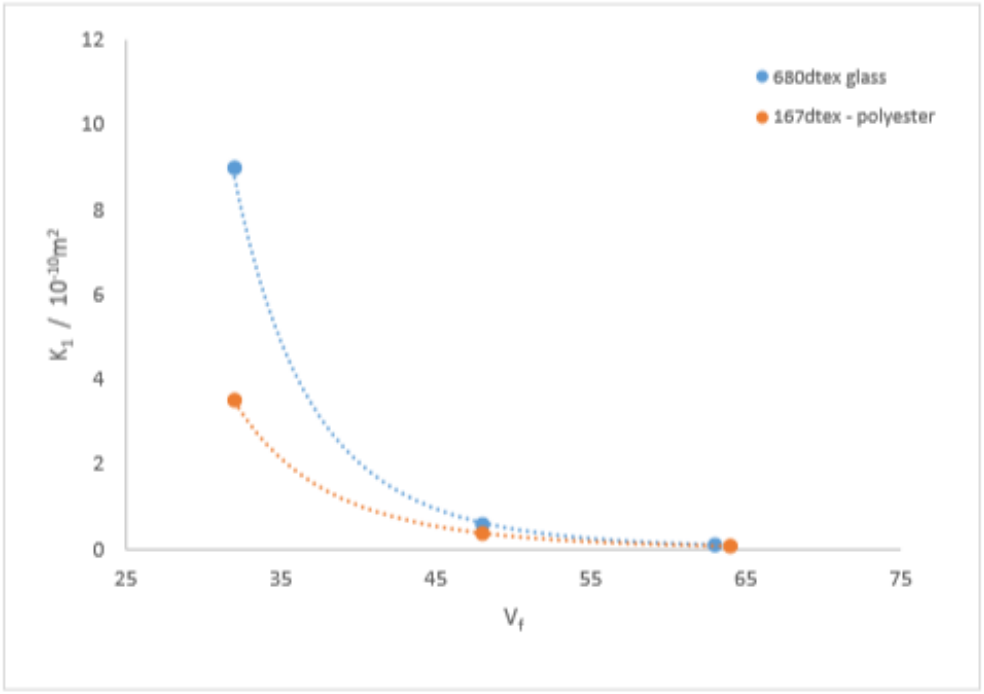
Figure 102: Correlation between scrim yarn dtex and permeability at 55% fibre volume fraction (typical target FVF for composite parts)

Changing the dtex for biaxial scrim materials

Two biaxial types of scrim materials are studied here. The thread density for the biaxial $0^o/90^o$ type scrims was varied between 0.8 yarns per 10 mm and 4 yarns per 10 mm in both scrim directions. The material parameters are listed in table 13. Due to the difficulties of production capabilities of scrim materials with different dtex values from manufacturers, a limited number of biaxial scrim materials with this parameter could be studied. Overall, an increase in permeability is observed when increasing the scrim yarns dtex as it was observed with the triaxial scrim materials in a previous chapter. In the warp direction (direction of the fibre), the scrim are expected to nest between the fibre filaments and thus have a small influence on K_1 permeability. The scrim yarns are expected to flatten and its filaments to spread during compaction which translates into an increase K_2 permeability the higher the dtex value of a scrim material. The results are shown in figure 103.

Scrim code	core material	dtex	architecture
TR005G	glass-filament-yarn	680dtex	2.5 yarns per 10mm - warp / 0.8 yarns per 10mm - weft
M4113SR22N	polyester-filament-yarn	167dtex - warp / 150dtex - weft	4 yarns per 10mm - warp / 3 yarns per 10mm - weft

Table 13 Materials parameters



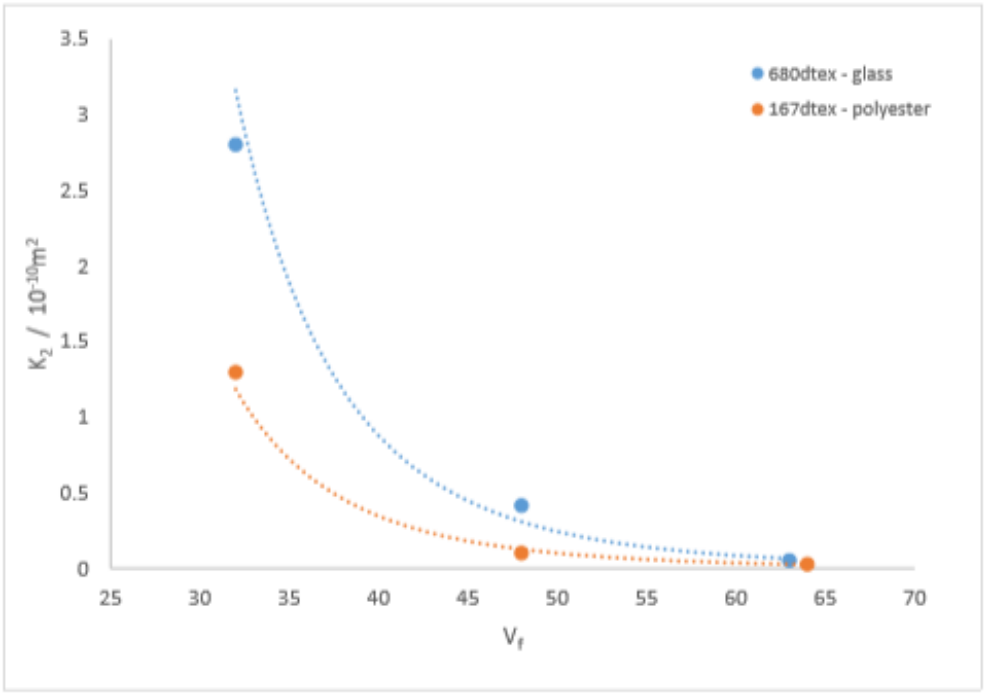


Figure 103: Experimentally determined data for principal permeability values, K1 and K2, as a function of the fibre volume fraction, Vf

6. Direct Dry Fibre Placement (DDFP)

The material development was part of a new automated fibre placement (AFP) process developed at Hexcel Leicester, project of which was part of a joined collaboration between companies and institutes [97]. The new AFP aimed at developing a process capable of depositing dry carbon fibre tows on a substrate to create the net shape structural fabric. Moreover, a secondary equipment development included a diaphragm forming rig able to take the fabric and using it to manufacture a preform and thus reducing cycle times, costs and waste.

The aim of the project:

"With the ever more stringent requirements on improved fuel efficiency and CO_2 emission reduction for road vehicles, a key enabling technology is the use of advanced composite materials to significantly reduce the mass of vehicles on the road. Life cycle analysis has shown that approximately 15% of total CO_2 emissions results from material and parts production, assembly and disposal. The remaining 85% of the CO_2 is emitted during operation and driving. The lighter the vehicle is, the less fuel is burnt and the lower are the CO_2 emissions. A 10% further reduction in vehicle mass improves fuel consumption by 7%, and every litre of fuel saved reduces CO_2 emissions by 2.6kg. Advanced carbon fibre composite materials have higher strength to weight ratios, better chemical and heat resistance and greater design flexibility when compared to conventional automotive construction materials. A consortium, led by an automotive OEM, with partners including a material supplier, high value manufacturing catapult centres and an academic institution, aim to develop technologies that will significantly reduce the cost of utilising these advanced materials in vehicle structures, a traditional barrier to date. Through a combination of reduced material wastage and automated pre-form manufacture, these technologies will have a significant impact on the cost of resin transfer moulded composite components. Not only will they be of benefit to the automotive industry, but also to other industrial sectors such as wind energy, sporting goods and aerospace." [97].

Follow up projects that span a multiyear commitment towards improving the process are listed in the references [98,99]. The concept and process are shown in figures 104. A patent was published and is also listed in the references [100]. The author's role for all the project was that of the leading composite materials scientist. The author was responsible for:

- All composite materials development
- Early development of second machine cell (diaphragm forming equipment) and providing proof of concept and additional support for the fibre deposition system

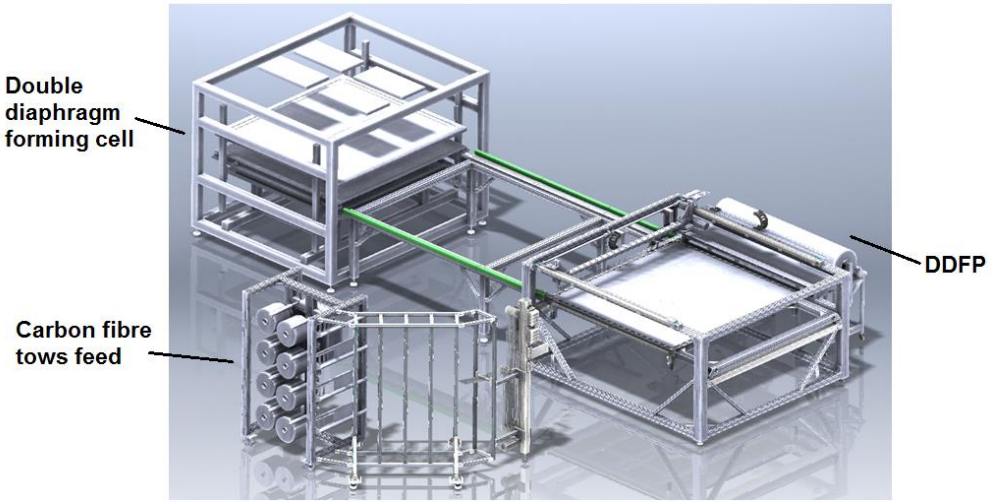


Figure 104 Direct Fibre Placement (DDFP) concept drawing

Control of fibre placement is very important for the mechanical performance of a manufactured composite. In order to optimize the load-carrying capabilities of a part, the fibre orientation, and the quality of the manufactured fabric is of the utmost importance. For this reason, hand-lay is still the preferred method of composite manufacture. However, this method is labour intensive, the repeatability level is low, and the production rates are slow. Other manufacturing methods such RTM can increase production cycles, however these also rely on manual operation. In order to faster produce parts with higher level of complexity, AFP (automated fibre placement) has been developed. This manufacturing method has the potential of producing near-net shape preforms of high quality without the use of stitch threads. The design and manufacturing process of the composite materials is discussed in a

subsequent chapter. The technology was used to manufacture the final set of the scrim supported fabrics. Currently, the desire shape for a composite part is cut from a fabric roll (either using scissors or an automated procedure) and the rest of the material is discarded. Using the new technology, the fibres can be deposited to the exact shape of the part and at the same time optimize the structural fabric's properties. The advantages of the process are illustrated in figure 105.

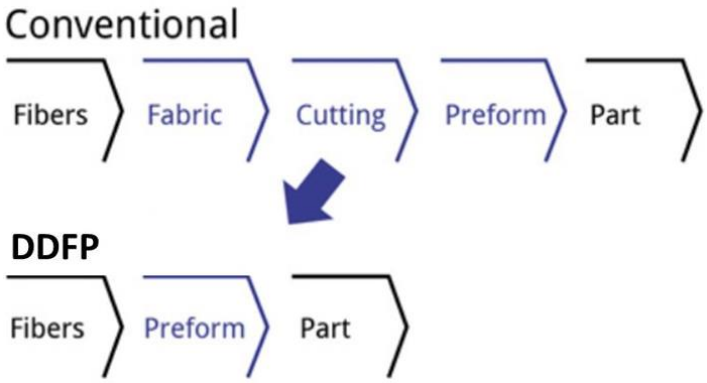


Figure 105 DDFP comparison with conventional fabric manufacture

Machine Concept:

A 2D net shape deposition system that would significant reduce waste compared to broadgood manufacture. The system utilises dry carbon fibre tows deposited on a substrate (scrim). The deposition table can quickly rotate to any angle to allow tows to be laid at the exact angle required by the final application. The manufactured fabrics can be transferred straight into a double diaphragm forming machine for pre-forming with no intermediate handing required. Early research included proof of concept for both deposition system and diaphragm forming cell. The fibre deposition system can be seen in figure 106 and the produced fabric in figure 107. In figure 108, the diaphragm forming cell procedure is shown, where a flat stack is placed between the two membranes and formed over a tool to produce the preform. The final part could potentially be manufactured with this process as well [98].

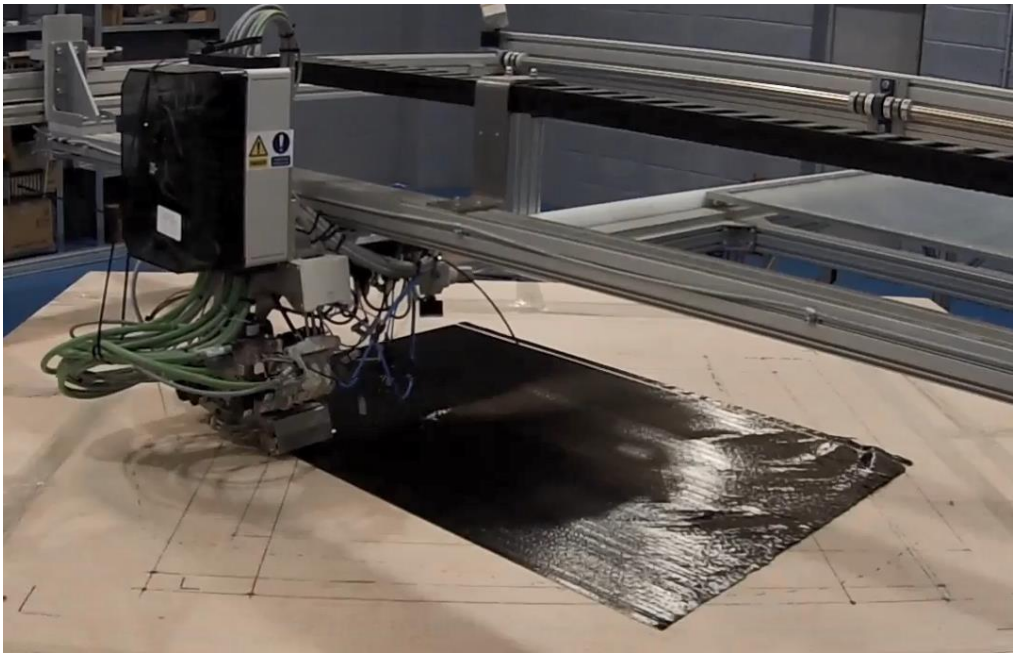


Figure 106 Manufacture of a fabric on the DDFP

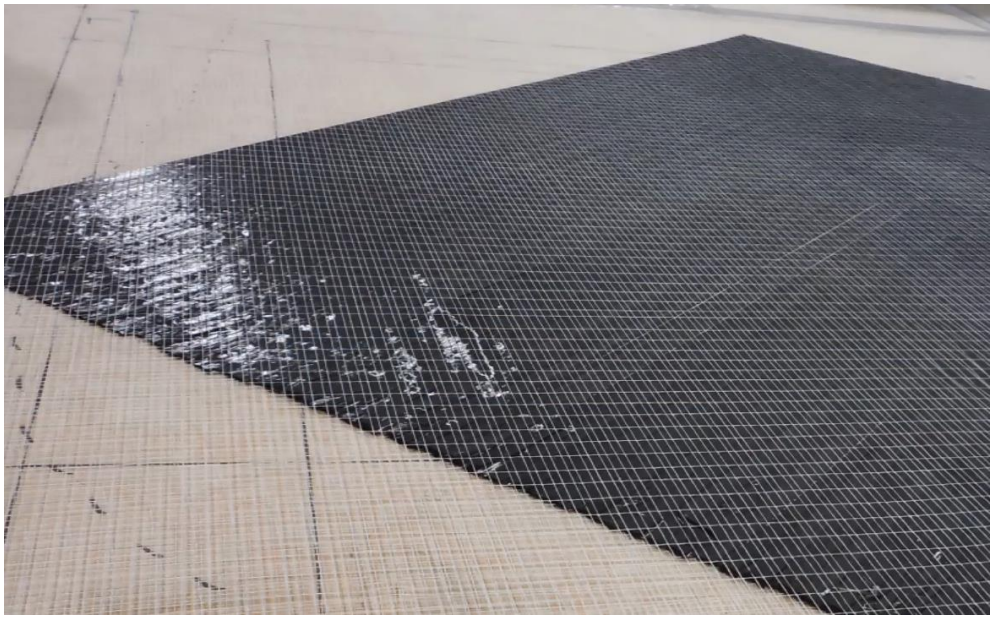


Figure 107 Scrim material used as substrate for fibre deposition

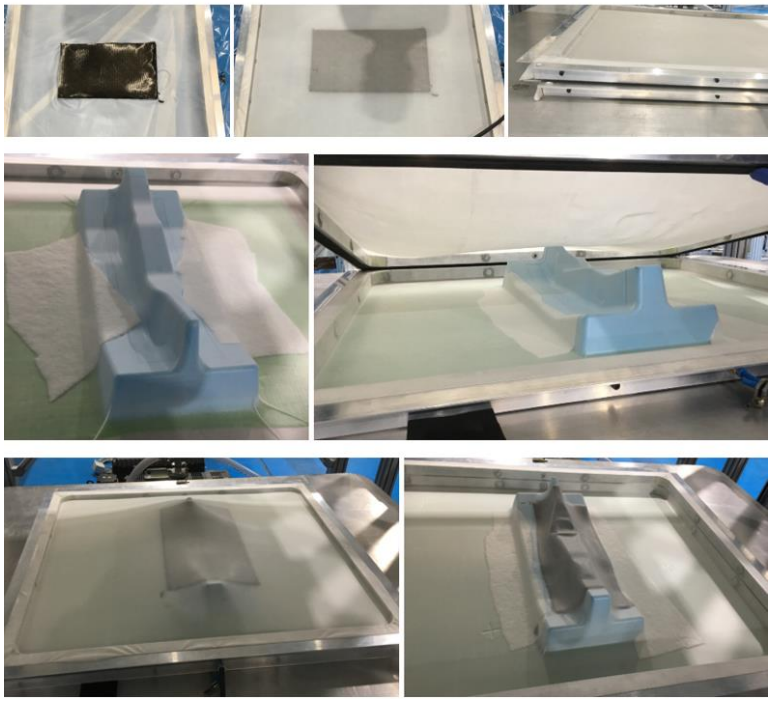


Figure 108 Double diaphragm forming cell

In both woven and the conventional non-crimp fabrics, the shapes of the desired manufactured components must be cut out of a fabric roll. The new type of material and manufacturing process allows for the desired shaped to be manufactured to the exact specification set by a company as well layers of materials deposited on specific areas (for example where the anticipated loads during a crash would be) and this is shown in figure 109.

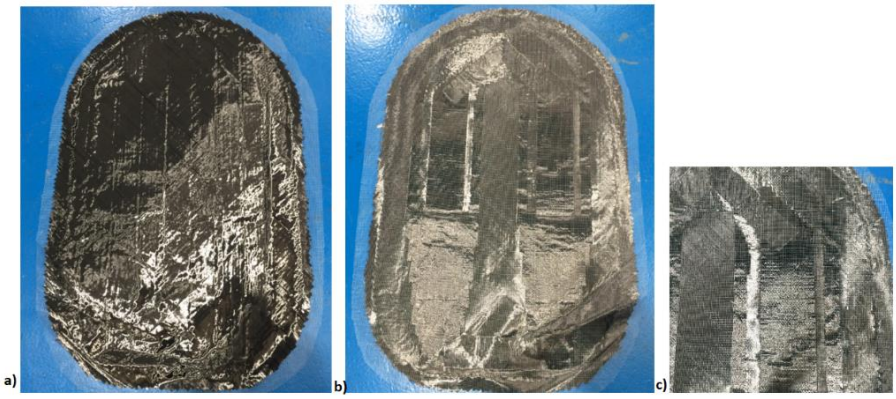


Figure 109 Net shape manufacture a)top view of fabric stack, b)bottom view of fabric stack, c)close up of fibre deposition capabilities on anticipated composite part loads

The scrim can also be placed at different orientations. Scrim materials with orientations otherwise impossible to source from scrim manufacturers can be used for the fibre deposition system (figure 110). This scrim arrangement translates to the scrim in the fabric corresponding to the element that resists deformation thus exhibiting shear resistance: changing the angle of the scrim to 0 º/90 º relative to the carbon fibre tows enables for a low shear resistance that improves the forming of the fabric. A comparison between the conventional fabric manufacturing process and the DDFP is illustrated in figure 111.

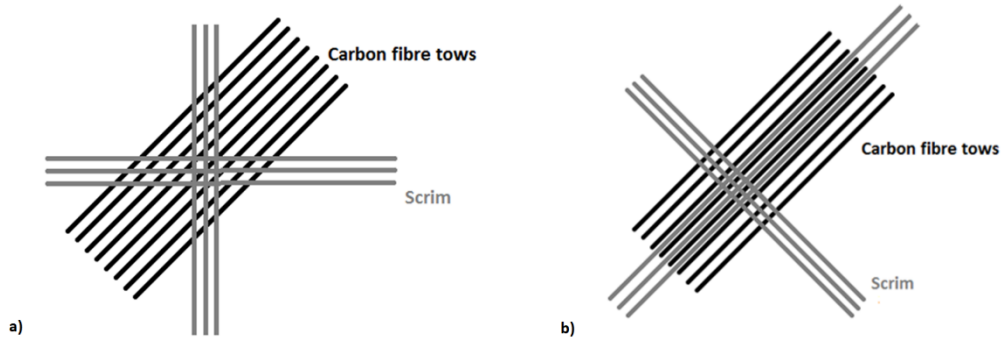


Figure 110 Placement of scrim at different orientations: Orientation of scrim at -45º/+45 º relative to the carbon fibre tows

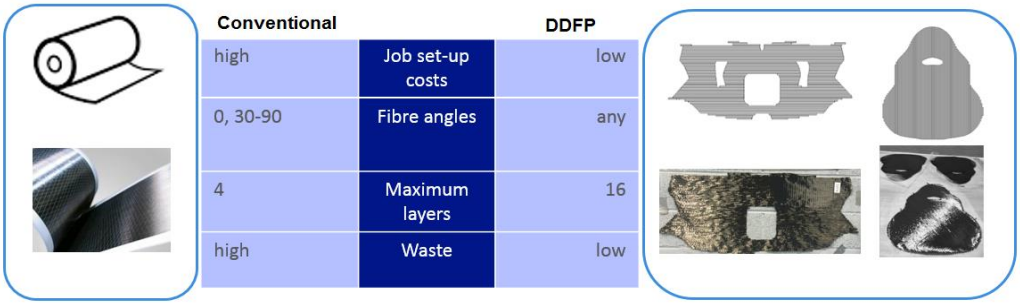


Figure 111 Comparison between conventional ncf and fabric manufactured by the newly developed DDFP process

The material format has a requirement for material stability in four distinct phases. Initially, the material must be stable enough to avoid significant deformation during the fibre deposition/adhesion. Then, during all subsequent handling operations before forming, the material must exhibit sufficient

handling stability. During forming to a 3D shape the material must exhibit stability up to the time of polymer injection. Finally, during polymer injection, the material must be capable of resisting the loading due to the polymer flow without excessive fibre wash. The stability required for each of the four phases depends on the magnitude and rate of applied loads and the ambient conditions.

Deposition stability is defined as the stability required during the manufacture of 2D net shape preforms using the AFP head. The applied load is the vertical (compaction) pressure provided by the deposition roller, the tension from the deposited tow and the thermal load carried by the carbon tow being deposited.

Handling stability is defined as the stability required during the movement of the 2D preform from its deposition position to the 3D forming cell. The cell has been developed to minimise the handling between deposition and forming, but there may be cases where shipping of 2D preforms is preferential over shipping 3D preforms, in which case the material should resist loads due to manual or automated pick & place, packing and transportation. Forming stability is defined as the stability required during the forming of the preform from 2D to 3D. The ambient temperature has a significant effect on the mechanism for fabric deformation during forming. The new material is intended to be processed at elevated temperature.

Injection stability is defined as the stability required during polymer injection within the RTM tool. The load on the fabric is created by the polymer flow. Tools can be designed with a clamping perimeter which nips the fabric around the edge of the part. This generates waste on demoulding as the clamped region is trimmed. Conventional fabrics are coated in a powder-binder which joins the fabric preform together in the tool and helps to prevent fibre wash. The temperature of the tool and polymer during injection should be carefully considered when engineering a preform for injection stability: If the preform stability is created by a thermoplastic bond, the injection temperature of the tool or polymer should not exceed the melting temperature of the binder. During deposition, higher stiffness yarns process more favourably than lower

stiffness yarns. The polyester yarns in the scrims tested have an elongation of about 20% which is suitable for the deposition of the scrim. A higher elongation in the yarn creates gaps in the fabric, as the AFP head “drags” the scrim as it deposits the carbon fibre tow. As the yarns spring back, crimp will be created in subsequent areas where the additional layers of scrim are deposited.

Moreover, the author’s role included conducting a study for replacing existing parts and conducting studies for future replacement of current machine parts with composite materials in order to reduce weight and thus to allow for faster machine movement (figure 112). Higher composite materials costs could be counterweighted by the installation of components such as smaller machine drives and rollers. The component is used for supporting the AFP head unit circuitry. From one edge of the structure the AFP head circuitry is placed along with the motors and deposition head. The other edge of the L-shaped section, the secondary equipment and cables are attached.

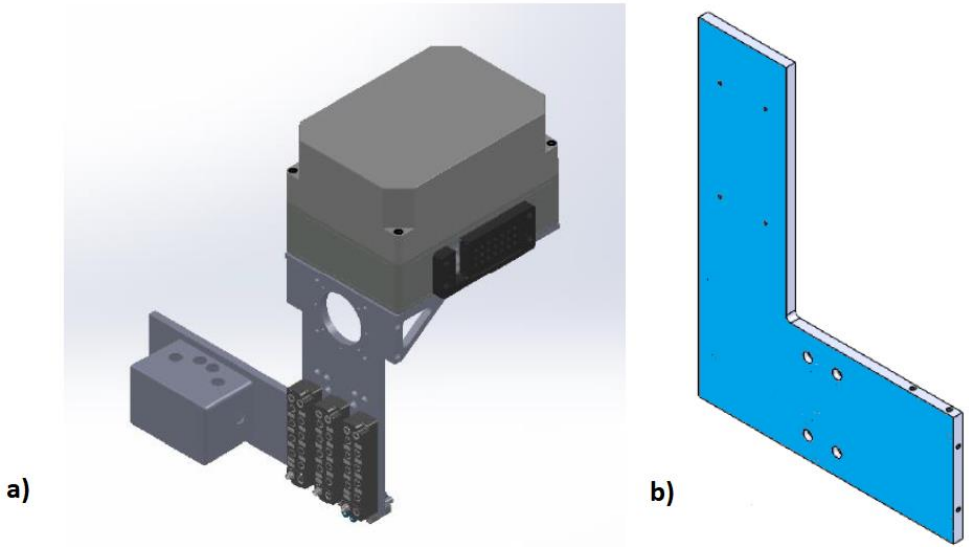


Figure 112 a)AFP head design and b)L-shaped part that can potentially be replaced in order to reduce overall parts weight

7. Conclusions

Materials with higher performance, higher quality and low cost, low waste and at a faster production rate are demanded constantly. A thorough understanding of the material behaviour and the effect on material processing is essential in order to meet composite parts production demands. The research presented here aimed, among other goals, to increase the knowledge on structural fabrics used in a number of different applications and industries. Non-crimp fabrics (NCFs) are the focus of this study. Plies of unidirectionally oriented fibre bundles, stitched together by warp or/and weft, depending on the type of layer, are typically manufactured using a knitting process.

A newly developed automated fibre placement method that produces net shaped part has been developed and discussed. The project aims to significantly reduce the overall costs of composites manufacture by reducing waste (currently 30% of the carbon fibre never makes it into the structure) to near zero, automating the pre-forming process and removing the additional processes. With the opportunity to utilise carbon fibre composite materials cost effectively in primary vehicle structures, the means to effectively achieve significant reductions in vehicle mass should be realised. This in turn will lead to significant reductions in fuel used throughout the life of the vehicle, and so reductions in CO_2 emissions. Published life cycle analyses identify the majority of CO_2 emissions are as a result of operation during the vehicles life, so carbon fibre composites are key to reducing these harmful emissions.

The main objective of the current research was to develop new types of fibre reinforcement architectures as well as new process that would improve manufacture. The main focus was to replace the support structure seen in conventional non-crimp fabrics (stitch) that causes inconsistencies during composite manufacture with a thermoplastic material (scrim) during the development of a new automated fibre placement process. The materials were characterized in terms of permeability and formability. In conventional stitched fabrics, the permeability is shown to be affected by large channels caused by the stitch thread that results in flow paths. Experimentally determined

permeabilities of the same type of fibre reinforcement can differ by a factor of 1.5, under the same initial conditions. Another aim of the study was to understand the material properties and be able to predict the permeability of a future fabric when changing the support structure's architecture.

The primary function of the scrim is to bond the carbon fibre tows together and to provide material/fabric stability. A secondary function is to provide channels through which the resin can flow during injection, in a similar way that the stitch thread aids flow through a conventional ncf, and also similar to that of a "flow mesh" layer when used to accelerate flow during a resin infusion process. Moreover, the scrim provides the means for preform manufacturing thus removing the need for powder binder and consequently reducing costs and cycle time. It was observed that when the scrim yarns are oriented off-axis relative to the carbon fibre tows, they remain on the surface of the tows creating flow channels. Contrarily, when the scrim yarns are aligned parallel to the carbon fibre tows they appear to have little effect on the permeability values as the yarns in the scrim nest between the carbon fibre filaments. Moreover, the larger the scrim yarn cross-sections, the larger the size of the adjacent channels, and the higher the resulted permeability values. This effect is also less pronounced if the scrim yarns are aligned with the tow direction as the scrim yarns nest between the fibre filaments. Increasing the number of yarns of the scrim will tend to increase the permeability of the manufactured fabrics.

Where typically the parallel permeability of NCFs would exceed the transverse permeability by one order of magnitude, the influence of the scrim yarns can minimize this difference. This behaviour can be explained by the architecture of the material. Due to the orientation of the scrim, the permeability of the principal axes of the material are rotated and placed at 90^{o} relative to the carbon fibres increasing flow. The scrim layers prevent the fibres from nesting and increase K_2, as in several studies it was observed that the major source of scatter in the permeability values is the nesting of the fibre filaments and the different history of material batches (different operators and materials supply/batch) and the different parameters of the fibre architecture.

Resistance to intra-ply shear was characterized using the picture frame testing. The fabric sample is clamped within an articulate frame, with two diagonally fixtures in the opposite corners where a mechanical testing equipment is displacing the edges. The results of load and extension are then converted to shear force vs shear angle. A new measurement rig was designed and manufactured in order to improve consistency and repeatability of the results. For conventional non-crimp fabrics, the initial resistance to deformation is relatively low and may be caused by friction at the crossover point of the tows. A significant rise in the resistance to shear deformation is observed once the neighbouring carbon fibre tows come into contact. Defects such as wrinkling and bridging are observed in this region.

The shear behaviour of the manufactured fabrics stitched fabrics was determined based on the stitch parameters of each fabric. It was observed that the stitch thread tension affects the shear behaviour significantly. The deformation process during the experimental testing was analysed. The fabric with the high stitch thread tension exhibits higher shear resistance. For the new type of fabrics with scrim, the deformation mechanism is not the same as the stitched fabrics. Experimental characterization was performed using the newly developed picture frame rig. The rig improves the repeatability of the testing, where previous iterations had the issue of fibre misalignment during sample placement. Results were obtained in terms of shear force at specific shear angles. The experimental results show that different types of scrim that were used for this study have minimal effect on the shear deformation of the fabric.

Single diaphragm forming was implemented in order to asses the different materials in the preforming stage. Digital imaging was used for the assessment of the preform parts, where the system scans the materials and measures the fibre orientations. All the fabrics with the different scrims displayed similar behaviour. The fibre angle distribution was between 30 and 60 degrees with the highest percentage of fibre angles located at 45 degrees. Physical examination of the parts concluded to the same observations. However, the stitched fabrics although exhibiting similar behaviour, and similar fibre angle distribution, physical observations showed that the fabric with the higher stitch

thread tension resulted in problematic areas to appear on the preform. This might be attributed to the digital scanning equipment, where small variations in the local structure of the material might not register using the existing settings on the equipment.

Future work:

- The scrim yarn material can affect flow if its cross-section shape changes during processing. The scrim yarns that are thermoplastic with a melting point below the deposition temperature will tend to soften and flatten. Those yarns that do not soften (but instead have a stable core with a low melt thermoplastic coating) will tend to maintain section geometry and hence may potentially enhance flow

- Influence of varying the scrim parameters on the mechanical performance of a manufactured composite: how the mechanical properties and different scrim architectures can be "balanced" in order to decide which attribute needs to be the focus of manufacture (i.e. if for example a higher permeable fabric is required for a composite part and there is lenience on the mechanical performance aspect of the component, then a denser scrim architecture can be selected as the preferred support structure for the fabric and thus select a scrim with higher permeability at the cost of reduced mechanical performance and vice versa

- For the existing version of the fibre reinforced architecture, the carbon fibre tows overlap by 2mm across their width in order to provide full fibre coverage. The introduction of gaps and their effect on permeability can be examined

8. References

1. Richard Loendersloot. The Structure–Permeability Relation of Textile Reinforcements. PhD–Thesis. University of Twente. Enschede. 2006.
2. Yehia Elmogahzy. Engineering Textiles: Integrating the Design and Manufacture of Textile Products. Woodhead Publishing Series in Textiles. 2009.
3. Hexcel Leicester documentation – available upon request.
4. N. Vernet, E. Ruiz, S. Advani, J.B. Alms, M. Aubert, M. Barburski, B. Barari, J.M. Beraud, D.C. Berg, N. Correia, M. Danzi, T. Delavière, M. Dickert, C. Di Fratta, A. Endruweit, P. Ermanni, G. Francucci, J.A. Garcil, A. George, C. Hahn, F. Klunker, S.V. Lomov, A. Long, B. Louis, J. Maldonado h, R. Meier, V. Michaud, H. Perrin, K. Pillai, E. Rodriguez, F. Trochu, S. Verheyden, M. Wietgrefe, W. Xiong, S. Zaremba, G. Ziegmann. Experimental determination of the permeability of engineering textiles: Composites Part A. 61. pp 172–184. 2014.
5. R.S. Parnas. Liquid Composite Molding. Hanser. 2000.
6. K. Hoes, D. Dinescu, H. Sol, M. Vanheule, R.S. Parnas, Y. Luo, I. Verpoest. New set-up for measurement of permeability properties of fibrous reinforcements for RTM. Composites Part A. 33. pp 959–969. 2002.
7. K. Hoes, D. Dinescu, H. Sol, R.S. Parnas, and S. V. Lomov. Study of nesting induced scatter of permeability values in layered reinforcement fabrics. Composites Part A. 35. pp 1407–1418. 2004.
8. A. Endruweit, A.C. Long, F. Robitaille, C.D. Rudd. Influence of stochastic fibre angle variations on the permeability of bi–directional textile fabrics. Composites Part A. 37. pp 122–132. 2006.
9. Karbhari V.M., Palmese G.R. Sizing related kinetic and flow considerations in the resin infusion composites. Journal of Materials Science. 32 pp. 5761-5774. 1997.

10. Steenkamer D.A., McKnight S.H., Wilkins D.J., Karbhari V.M. Experimental characterization of permeability and fiber wetting for liquid moulding. Journal of Materials Science. 30. pp 3207-3215. 1995.
11. H.G.S.J. Thuis. Measurement of permeability for different non-crimped fabrics. Technical Report FALCOM G4RD-CT-00694 - WP2.1.2. NLR. 2002.
12. T.S. Lundstrom, V. Frishfelds, and A. Jakovics. A statistical approach to permeability of clustered fibre reinforcements. Journal of Composite Materials. 38. pp 1137–1149. 2004.
13. J.R. Weitzenbock, R.A. Shenoi, P.A. Wilson. Radial flow permeability measurement. Part A: Composites Theory. 30. pp 781–796. 1999.
14. J.R. Weitzenbock, R.A. Shenoi, P.A. Wilson. Radial flow permeability measurement. Part B: Application Composites. 30. pp 797–813. 1999.
15. K. L. Adams, W. B. Russel, L. Rebenfeld. Radial Penetration of a visocus liquid into a planar anisotropic medium. Int. J. Multiphase Flow. 14. pp 203-215, 1988.
16. Kruckenberg, R. Paton (ed). Resin Transfer Moulding for Aerospace Structures. Netherlands. 1998.
17. May D. Aktas, A. Advani, S.G. Berg, D.C. Endruweit, A. Fauster, E. Lomov, S.V. Long, A. Mitschang, P. Abaimov, S. Abliz, D. Akhatov, I. Ali, M.A. Allen, T.D. Bickerton, S. Bodaghi, M. Caglar, B. Caglar, H. Chiminelli, A. Correia, N. Cosson, B. Danzi, M. Dittmann, J. Ermanni, P. Francucci, G. George, A. Grishaev, V. Hancioglu, M. Kabachi, M.A. Kind, K. Deléglise-Lagardère, M. Laspalas, M. Lebedev, O.V. Lizaranzu, M. Liotier, P.-J. Middendorf, P. Morán, J. Park, C.-H. Pipes, R.B. Pucci, M.F. Raynal, J. Rodriguez, E.S. Schledjewski, R. Schubnel, R. Sharp, N. Sims, G. Sozer, E.M. Sousa, P. Thomas, J. Umer, R. Wijaya, W. Willenbacher, B. Yong, A. Zaremba, S. Ziegmann, G. In-plane permeability characterization of engineering textiles based on radial flow experiments: a benchmark exercise. Composites Part A: Applied Science and Manufacturing, 121. 2019.
18. Harald Grossing, Ewald Fauster, Markus Weninger, Ralf Schledjewski. Influence of Textile Parameters on the In-Plane Permeability

Characteristics of Non-Crimped Fabric Preforms. 37. pp 1854–1863. 2016.

19. T.S. Lundstrom. The permeability of non-crimp stitched fabrics. Composites: Part A. 31. pp 1345–1353. 2000.
20. H. Talvensaari, E. Ladstatter, W. Billinger. Permeability of stitched preform packages. Composite Structures. 71. pp 371–37. 2005.
21. A Williems. Forming simulation of textile reinforced composite shell structures. Master thesis Belgium. 2008.
22. Gilbert Lebrun, Martin N. Bureau, Johanne Denault. Evaluation of bias-extension and picture-frame test methods for the measurement of intraply shear properties of PP/glass commingled fabrics. Composite Structures. 61. pp 341–352. 2003.
23. P. Harrison, M. J. Clifford, A. C. Long. Shear characterisation of woven textile composites. Composites Science and Technology. 64. pp 1453-1465. 2004.
24. Breuer U., Neitzel M., Ketzer V., Reinicke R. Deep drawing of fabric reinforced thermoplastics: Wrinkle formation and their reduction. Polymer Composites. 17. pp 643-647. 1996.
25. Prodromou A.G., Chen J. On the relationship between shear angle and wrinkling of textile composite preforms. Composites Part A. 28. pp 491-503. 1997.
26. Wang J., Page J.R., Paton R. Experimental investigation of the draping properties of reinforcement fabrics. Composites Science & Technology. 58. pp 229-237. 1998.
27. Sharma S.B., Sutcliffe M.P.F., Clifford M.J., Long A.C. Experimental investigation of tow deformation during draping of woven fabrics. Proc 4th International European Scientific Association for Material Forming Conference. Liège. Belgium. pp 107-110. 2001.
28. O.Rozant, P.E.Bourban, J.A.E.Manson. Drapability of dry textile fabrics for stampable thermoplastic preforms. Composites Part A. 31. pp 1167–1177. 2000.
29. P. Harrison, M.J. Clifford, A.C. Long. Shear characterisation of viscous woven textile composites: a comparison between picture frame and

bias extension experiments. Composites Science and Technology. 64. pp 1453–1465. 2004.

30. P. Boisse, N. Hamila, E. Vidal-Sallé, F. Dumont. Simulation of wrinkling during textile composite reinforcement forming. Influence of tensile, in-plane shear and bending stiffnesses. Composites Science and Technology. Elsevier. 71. pp 683. 2011.
31. J. Cao, R. Akkerman, P. Boisse, J. Chen, H.S. Cheng, E.F. de Graaf, J.L. Gorczyca, P. Harrison, G. Hivet, J. Launay, W. Lee, L. Liud, S.V. Lomov, A. Long, E. de Luycker, F. Morestin, J. Padvoiskis, X.Q. Peng, J. Sherwood, Tz. Stoilova, X.M. Tao, I. Verpoest, A. Willems, J. Wiggers, T.X. Yu, B. Zhu. Characterization of mechanical behavior of woven fabrics: Experimental methods and benchmark results. Composites: Part A. 39. pp 1037–1053. 2008.
32. Paulė Bekampiene. Jurgita Domskiene. Influence of Stitching Pattern on Deformation Behaviour of Woven Fabric during Forming. ISSN 1392–1320 Materials Science. 16. 2010.
33. Oleg Stolyarova , Till Quadfliegb, Thomas Griesb. Characterization of shear behavior of warp-knitted fabrics applied to composite reinforcement. The Journal of the Textile Institute. 108. pp 89–94. 2017.
34. Long Li, Yan Zhao, Ha-gia-nam Vuong, Yuan Chen, Jin Yang, Yuexin Duan. In-plane shear investigation of biaxial carbon non-crimp fabrics with experimental tests and finite element modelling. Materials and Design. 63. pp 757–765. 2014.
35. Helga Krieger1, Thomas Gries. Scott E. Stapleton. Shear and drape behavior of non-crimp fabrics based on stitching geometry. International Journal of Material Forming. 11. pp 593–605. 2018.
36. A. C. Long, B. J. Souter, F. Robitaille, C. D. Rudd. Effects of fibre architecture on reinforcement fabric deformation, Plastics, Rubber and Composites. 31. pp 87-97, 2002.
37. A.C. Long, B.J. Souter, F. Robitaille, C.D. Rudd. Effects of Fibre Architecture during preform manufactur**e.** Advanced Composites Letters. 8. pp 333-344. 1999.

38. Cao, J. Characterization of mechanical behavior of woven fabrics: Experimental methods and benchmark results. Composites Part A: Applied Science and Manufacturing. 39. pp 1037–1053. 2008.
39. Luby Steven, Bernardon Edward. Design of fabric preforms for double diaphragm forming. Conference on Fibrous Composites in Structural Design. pp 1171 – 1184. 1992.
40. Andrew Long, ed. Composite forming technologies. 1st ed. Cambridge. Woodhead Publishing. 2007.
41. John Summerscales, TJ Searle. Low pressure (vacuum infusion) techniques for moulding large composite structures in Proceedings of the Institution of Mechanical Engineers Part L - Journal of Materials: Design and Applications. 219. pp 45-58. 2005.
42. H.E.N. Bersee, S. Lindstedt, G. Niño, Adriaan Beukers. Diaphragm Forming of Thermoset Composites. 16th International Conference on Composite Materials. 2007.
43. Haorong Li. Forming of Advanced Thermoset Composites: Process Development and Study. PhD Thesis. 1998.
44. A Long, ed. Design and manufacture of textile Composites. 1st ed. Cambridge. Woodhead Publishing. 2005.
45. A. Endruweit, P. Ermanni. Influence of Fixation Structures on the In-Plane Permeability of Unidirectional Glass Fibre Tapes. Journal of composite materials. 36. 2002.
46. New approaches to modifying the impact toughness of RTM components**.** No90. JEC composites magazine. 2014.
47. NRL Pearce, FJ Guild, J Summerscales. Improving the resin transfer moulding process for fabric-reinforced composites by modification of the fabric architecture. 31. pp 1433-1441. 2000.
48. Adams KL, Rebenfeld L. In-plane flow of fluids in fabrics: structure/flow characterization. Textile Res J 57. pp 647-654. 1987.
49. Adams KL, Russel WB, Rebenfeld L. Radial penetration of a viscous liquid into a planar anisotropic porous medium. Int J Multiphase Flow 14. pp 203–215. 1998.
50. Chan AW, Hwang ST. Anisotropic in-plane permeability of fabric media. Polym Eng Sci. 31. pp 1233-1239. 2002.

51. Chan AW, Morgan RJ. Tow impregnation during resin transfer molding of bi-directional nonwoven fabrics. Polymer Composites. 14. pp 335-340. 1993.
52. Carter EJ, Fell AW, Summerscales J. A simplified model to calculate the permeability tensor of an anisotropic fibre bed. Compos Manuf. 6. pp 228–235. 1995.
53. Um MK, Lee SK. A study on the determination of in-plane permeability of fiber preforms. Polym Compos. 20 pp. 771–779. 1992.
54. Tygavac - manufacturer of vacuum bagging and composite tooling materials for prepreg/autoclave, resin infusion, and wet lay-up processes: https://www.tygavac.co.uk/
55. Fenner Precision - precision-engineered elastomeric solutions: http://www.fennerprecision.com/
56. Ube – manufacturer of products including chemicals, plastics, cement and moulding machines: https://www.ube.com
57. Upilex - chemicals and plastics manufacturer: www.upilex.jp
58. J-Flex - elastomer solutions provider: https://j-flex.co.uk/
59. Mosites supplier of rubber sheet and custom rubber goods: https://www.mositesrubber.com/
60. Solvay – chemicals manufacturer: https://www.solvay.com/ (former Cytek)
61. Airtech - manufacturer of vacuum bagging and composite tooling materials for prepreg/autoclave, resin infusion, and wet lay-up processes up: https://www.airtechintl.com/
62. Steinback – Provider of forming solutions, conveying solutions, thermal and acoustic insulation, gaskets and stamped parts, bags and film packaging and technical ceramics**:** https://www.steinbach-ag.de
63. Zoltek – carbon fibre manufacturer: https://zoltek.com/
64. Toray – carbon fibre manufacturer: http;//www.Toray.com
65. Apodious – measurement solutions for the composites industry: https://apodius.de/
66. Bafatex – scrim manufacturer: http;//www.Bafatex.com/
67. Adfors – scrim manufacturer: http://www.adfors.com/

68. James Dewhurst – scrim manufacturer: http://www.jamesdewhurst.com/
69. Porcher – scrim manufacturer: http://www.porcher-ind.com/
70. Hexcel – chemicals and fibre reinforcements manufacturer: http;//www.Hexcel.com (former Formax)
71. Kirson – scrim manufacturer: http://www.kirson.de/
72. EMS Grilon – yarn manufacturer: http://www.emsgrivory.com
73. EY Technologies – yarn manufacturer: http://www.eytechnologies.com/
74. EMS Grilon – yarn manufacturer: http://www.emsgriltech.com
75. Php fibre – yarn manufacturer: https://php-fibers.com
76. Evelina Bergengren. Filip Sköld. An investigation on thin film adhesion measurement methods. http://lup.lub.lu.se/student-papers/record/8883564
77. Peel tests overview: https://www.sciencedirect.com/topics/engineering/peel-test
78. IR lamp supplier: https://reitelite.co.uk/product/infrared-heater-lamps/
79. Endruweit, P. McGregor, A.C. Long, M.S. Johnson. Influence of the fabric architecture on the variations in experimentally determined in-plane permeability values. Composites Science and Technology 66. pp 1778–1792. 2006.
80. G. Bechtold. L. Ye. K. Friedrich. Influence of stochastic of fibre distribution on permeabilities of fibre bundles. Volume 63, Issue 14. pp 2069-2079. 2003.
81. M. Nordlund, T. S. Lundström. Effect of Multi-Scale Porosity in Local Permeability.Modelling of Non-Crimp Fabrics. Transp Porous Med 73 pp 109–124. 2008.
82. Richard Loendersloot. The structure – permeability relation of textile reinforcements. 2006.
83. Lomov, S.V., Verpoest, I., Barburski, M., Laperre, J.: Carbon composites based on multiaxial multiply stitched preforms. Part 2. KES-F characterisation of the deformability of the preforms at low loads. Compos. A: Appl. Sci. Manuf. 34 pp 359–370. 2003.

84. Pan R, Liang Z, Zhang C, Wang B. Statistical characterization of fiber permeability for composite manufacturing. Polym Compos. 21 pp 996–1006. 2000.
85. Grujicic, M., Chittajallu, K.M., Walsh, S. Effect of shear, compaction and nesting on permeability of the orthogonal plain-weave fabric preforms. Mater. Chem. Phys. 86 pp 358–369. 2004.
86. Senoguz, M.T., Dungan, F.D., Sastry, A.M., Klamo, J.T.: Simulations and experiments on low-pressure permeation of fabrics: Part II. The variable gap model and prediction of permeability. J. Compos. Mater. 35 pp 1285–1322. 2001.
87. Dungan, F.D., Senoguz, M.T., Sastry, A.M., Faillaci, D.A.: Simulations and experiments on low-pressure permeation of fabrics: Part I-3D modeling of unbalanced fabric. J. Compos. Mater. 35 pp 1250–1284. 2001.
88. Hoes, K., Dinescu, D., Sol, H., Parnas, R.S., Lomov, S.: Study of nesting induced scatter of permeability values in layered reinforcement fabrics. Compos. A: Appl. Sci. Manuf. 35 pp 1407–1418. 2004.
89. Draghboudi Samir, Hamid Satha. Determination of the in-plane shear rigidity modulus of a carbon non-crimp fabric from bias-extension data test. Journal of Composite Materials 48 pp 2729-2736. 2014.
90. Wiggers, Joram. Analysis of textile deformation during preforming for liquid composite moulding. PhD thesis, University of Nottingham. 2007.
91. A. C. Long, B. J. Souter, F. Robitaille & C. D. Rudd. Effects of fibre architecture on reinforcement fabric deformation, Plastics, Rubber and Composites, 31 pp 87-97. 2002.
92. Rothe S., Wendt E., Krzywinski S., Halász M., Bakonyi P., Tamás P., Bojtos A. Investigation of Shear-Induced Deformation of Reinforcing Textiles by Optical Measurement Devices. Materials. *12*. 1029. 2019.
93. Chen Shuai. Fabric forming simulation and process optimisation for composites. PhD thesis, University of Nottingham. 2016.
94. Long AC, ed. Composites forming technologies. 1st ed. Cambridge. Woodhead Publishing. 2007.

95. Lomov SV. Non-crimp fabric composites: manufacturing, properties and applications. Cambridge. Woodhead. 2011.
96. Advani S, Hsiao KT. Manufacturing techniques for Polymer Matrix Composites (PMCs). Cambridge. Woodhead. 2012.
97. Affordable Lightweighting Through Pre-form Automation (ALPA): https://gtr.ukri.org/projects?ref=101879
98. Affordable Composites for Lightweight Vehicles:https://gtr.ukri.org/projects?ref=132231
99. Building a Volume Supply Chain for affordable lightweight composite Structures: https://gtr.ukri.org/projects?ref=102632
100. Thomas James. Arthur Swarbrick. Ian Hayto. Karanatsis Dimitris. Ian Jones. Tim Jones. Christopher Beard. Apparatus for and method of fibre placement for the formation of fibre preforms. WO2018187719 (A1). 2018 - https://worldwide.espacenet.com/publicationDetails/biblio?CC=WO&NR=2018197719A1&KC=A1&FT=D&ND=3&date=20181101&DB=&locale=en_EP#